

USGS RESEARCH ON ENERGY RESOURCES, 1992

PROGRAM AND ABSTRACTS

EIGHTH V.E. MCKELVEY FORUM ON MINERAL AND ENERGY RESOURCES

U.S. GEOLOGICAL SURVEY CIRCULAR 1074



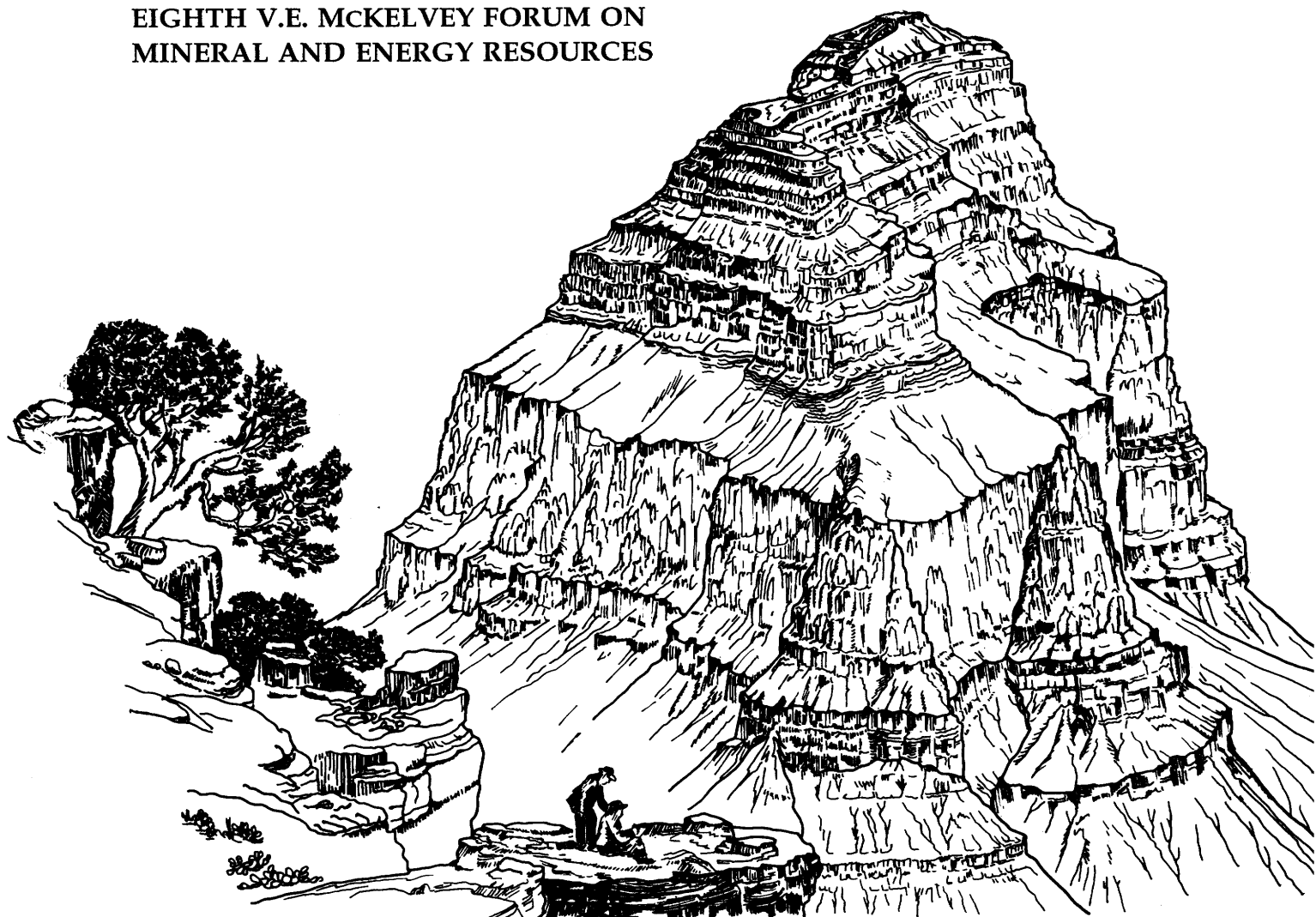
Cover.—“The Panorama from Point Sublime in the Kaibab,” by William H. Holmes, from Sheet XV of Atlas to accompany the Monograph on the Tertiary history of the Grand Cañon District, by Clarence E. Dutton (U.S. Geological Survey Monograph 2, 1882). Redrawn by Rob Wells.

USGS RESEARCH ON ENERGY RESOURCES, 1992

PROGRAM AND ABSTRACTS

Edited by L.M.H. CARTER

**EIGHTH V.E. MCKELVEY FORUM ON
MINERAL AND ENERGY RESOURCES**



U.S. GEOLOGICAL SURVEY CIRCULAR 1074

U.S. DEPARTMENT OF THE INTERIOR
MANUEL LUJAN, JR., Secretary

U.S. GEOLOGICAL SURVEY
Dallas L. Peck, Director



Any use of trade, product, or firm names in this publication is for descriptive purposes only and does not imply endorsement by the U.S. Government.

UNITED STATES GOVERNMENT PRINTING OFFICE: 1992

Organizing Committee for the 1992 McKelvey Forum:

Chair: Christine E. Turner

Co-chairs: Neil S. Fishman, Edward A. Johnson

Program:

Thomas S. Ahlbrandt

Anny B. Coury

Thomas D. Fouch

John A. Grow

Robert B. Halley

Joseph R. Hatch

Samuel Y. Johnson

Bonnie McGregor

James K. Otton

James W. Schmoker

Stanley P. Schweinfurth

Christine E. Turner

Publicity:

Helen L. Britton

Sally J. Dyson

Neil S. Fishman

Vito F. Nuccio

Budget:

Patricia E. O'Connell

Logistics:

Sigrid Asher-Bolinder

Bonnie L. Crysdale

Russell F. Dubiel

Mitchell E. Henry

Edward A. Johnson

Kathleen K. Krohn

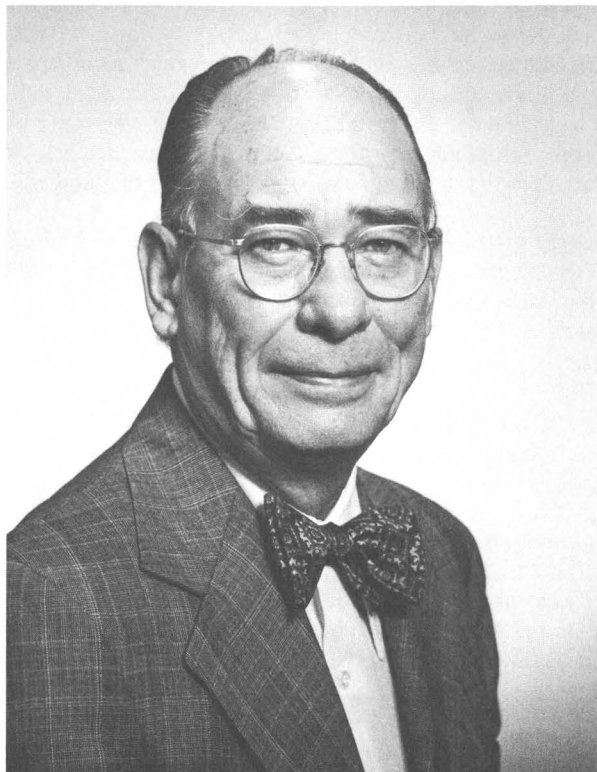
Drafting:

George M. Garcia

Carol S. Holtgrewe

Thomas Kostick

Free on application to the Books and Open-File Reports Section, U.S. Geological Survey, Denver Federal Center, Box 25425, Denver, CO 80225



A society's wealth depends on the use it makes of raw materials,
energy, and especially ingenuity.

—V.E. McKelvey

FOREWORD

Dallas L. Peck, U.S. Geological Survey

The extended abstracts in this volume are summaries of papers presented orally and as posters at the Eighth Annual V.E. McKelvey Forum on Energy and Mineral Resources. The McKelvey Forum serves as an opportunity for communication between the U.S. Geological Survey (USGS) and the earth-science and energy and mineral communities by presenting the results, recent progress, and pertinent data of current USGS research in formal lectures and posters. The poster sessions and the more informal meetings during the forum provide many opportunities for concerned persons to meet individually with our scientists. I hope that the 1992 McKelvey Forum will help make our programs even more responsive to the needs of these communities, particularly to the fossil-energy industry, and that the interaction and cooperation begun here will continue to expand.

The forum is named for former Director Vincent E. McKelvey in recognition of his lifelong dedication to the study of mineral and energy resources as research scientist, Chief Geologist, and Director of the USGS. The forum is an annual event that alternates in subject matter between mineral and energy resources; this year the emphasis is on energy. Although the format and topics addressed change somewhat from year to year, the primary purpose of the forum remains the same: to encourage direct communication between USGS scientists, the representatives of other earth-science and mineral and energy organizations, and interested individuals.

Energy programs of the USGS include investigations related to oil and gas, coal, geothermal resources, uranium, thorium, and oil shale. Our studies encompass the entire National domain. Presentations in this year's forum include recent research in basin evolution, reservoir characterization and computer applications in the energy fields. A growing number of citizens of this country are becoming increasingly aware of the importance of effective, efficient utilization of our Nation's energy endowment. Research results presented at this forum will contribute directly to that goal, and we are excited by the opportunity to present them to you and to start discussions with our colleagues in industry and academia.

We welcome your suggestions concerning future energy research directions and projects and also for improving the McKelvey Forum.



Dallas L. Peck, Director
U.S. Geological Survey

Eighth V.E. McKelvey Forum on Mineral and Energy Resources

HOUSTON, TEXAS, FEBRUARY 17-20, 1992

PROGRAM OF LECTURES AND DISCUSSIONS

MONDAY, FEBRUARY 17, 1992

7:00–9:00 p.m. **Registration/Ice Breaker (Cash Bar)**
Atrium, Wyndham Greenspoint Hotel

TECHNICAL PROGRAM

In the Atrium, immediately outside Raphael Ballrooms A and B, each speaker will be available during the first coffee break following his/her talk for informal discussions. Tables and chairs will be available for this purpose. Come share your thoughts and bring your questions.

TUESDAY, FEBRUARY 18, 1992

7:00 a.m. **Registration**

OPENING SESSION

Gary W. Hill and Donald L. Gautier, presiding

8:30 a.m.	Welcome and Opening Remarks <i>Dallas L. Peck, Director, U.S. Geological Survey</i>
	Welcome from Interior Secretary Manuel Lujan, Jr. <i>John M. Sayre, Assistant Secretary for Water and Science, U.S. Department of the Interior</i>
8:40	Introduction <i>William L. Fisher, Director and State Geologist, Bureau of Economic Geology, Texas</i>
8:50	KEYNOTE ADDRESS: Role of water in petroleum formation <i>Michael D. Lewan</i>

TECHNICAL SESSION

Gary W. Hill and Donald L. Gautier, presiding

9:40	Field growth in the Gulf of Mexico—A progress report <i>Lawrence J. Drew and Gary L. Lore</i>
10:00	Highlights of the McKelvey poster presentations <i>Christine E. Turner and William G. Miller</i>
10:15	COFFEE BREAK AND POSTER SESSION
10:40	Climate controls on Carboniferous cyclic sedimentation and organic productivity <i>C. Blaine Cecil</i>

PROGRAM OF LECTURES AND DISCUSSIONS (CONTINUED)

11:00	Bridging the gap between third- and fifth-order cycles in carbonate sequences—The western margin of the Great Bahama Bank <i>Robert B. Halley and R. Jude Wilber</i>
11:20	Sequence stratigraphy in the search for hydrocarbons in nonmarine strata <i>Peter J. McCabe</i>
11:40	Reservoirs and source rocks of the Upper Jurassic Norphlet Formation, Mississippi and Alabama <i>C.J. Schenk and J.W. Schmoker</i>
12:00 noon	Adjournment of session; lunch

TECHNICAL SESSION

Thomas S. Ahlbrandt and David J. Taylor, presiding

1:30	Oil and gas—Where in the world, and why <i>C.D. Masters</i>
1:50	Collisional tectonics and the global generation of oil and gas <i>David G. Howell</i>
2:10	Oil field growth in the United States—How much is left in the barrel? <i>D.H. Root and E.D. Attanasi</i>
2:30	Alaskan North Slope geothermics, geodynamics, and hydrology—Implications for oil and gas <i>Kenneth J. Bird, David G. Howell, Mark J. Johnsson, and Leslie B. Magoon</i>
2:50	Huge indigenous oil in mature source rocks—Beyond elephants? <i>Leigh Price</i>
3:10	Major frontier exploration plays in petroleum basins of the U.S.S.R. <i>Gregory F. Ulmishek</i>
3:30	Adjournment of technical session
3:50–6:00	POSTER SESSION AND RECEPTION

TUESDAY EVENING, FEBRUARY 18, 1992

7:30 p.m.	USGS DIRECTOR'S LECTURE: Fractal nature of hydrocarbon accumulations and price—Implications for resource assessment, exploration and development strategies, and economic forecasting <i>Christopher C. Barton</i>
8:30–10:00	POSTER SESSION (Cash Bar)

WEDNESDAY, FEBRUARY 19, 1992

TECHNICAL SESSION

Bonnie A. McGregor and Joseph R. Hatch, presiding

8:30 a.m.	Redefining Hutton's unconformity—Geology in a digital world <i>William G. Miller</i>
8:50	Architectural analysis of eolian sandstones—The Lower Jurassic Nugget Sandstone of northeastern Utah <i>Fred Peterson and C.J. Schenk</i>

PROGRAM OF LECTURES AND DISCUSSIONS (CONTINUED)

9:10 Turbidity-current processes and turbidite elements—What you get is not what you see *William R. Normark*

9:30 Ground-truthing the distal Mississippi fan with SeaMARC images and cores—What happens at the end of the pipe *D.C. Twichell, W.C. Schwab, C.H. Nelson, H.J. Lee, N.H. Kenyon, T.F. O'Brien, and W. Danforth*

9:50 COFFEE BREAK AND POSTER SESSION

10:20 Diagenesis in a bottle—Experimental strategies for studying thermal maturity in clays and organic matter *Gene Whitney and Michael D. Lewan*

10:40 Some geologic controls of coalbed gas generation, accumulation, and production, Western United States *Dudley D. Rice, Jerry L. Clayton, Romeo M. Flores, Ben E. Law, and Ronald W. Stanton*

11:00 Geologically oriented overview of horizontal drilling in the United States *James W. Schmoker*

11:20 Gas hydrates in deep ocean sediments offshore southeastern United States—A future resource? *William P. Dillon, Richard F. Mast, Kristen Fehlhaber, and Myung W. Lee*

11:40 Unconventional resources—Are they in our future? *Thomas S. Ahlbrandt*

12:00 noon McKELVEY FORUM LUNCHEON—Wedgwood Room
Remarks by FRANK A. BRACKEN, *Deputy Secretary, U.S. Department of the Interior*: A perspective on national energy policy
FEATURING: An hour with *John Wesley Powell*
—Live on Stage

TECHNICAL SESSION

Walter E. Dean and Harold J. Gluskoter, presiding

2:00 Origin of fluid pressure, fracture generation, and the movement of fluids in the Uinta Basin, Utah *J.D. Bredehoeft, J.B. Wesley, and T.D. Fouch*

2:20 Origin of the Santa Maria basin, California *Richard G. Stanley, Samuel Y. Johnson, Ronald B. Cole, Mark A. Mason, Carl C. Swisher III, Mary Lou Cotton Thornton, Mark V. Filewicz, David R. Vork, Michele L. Tuttle, and John D. Obradovich*

2:40 Petroleum geology research in the Santa Maria province, California *Caroline M. Isaacs*

3:00 COFFEE BREAK AND POSTER SESSION

3:30 Basin evolution in the foreland of thin- and thick-skinned thrust terranes—Example from the Sylhet trough, Bangladesh *Samuel Y. Johnson and A.M.N. Alam*

PROGRAM OF LECTURES AND DISCUSSIONS (CONTINUED)

3:50 The regional context of Railroad Valley oil-fields—An integrated geological and geophysical transect, east-central Nevada *Christopher J. Potter, John A. Grow, Karen Lund, and William J. Perry, Jr.*

4:10 Thermochronologic constraints on relation between extensional geometry of the northern Grant Range and oil occurrences in Railroad Valley, east-central Nevada *Karen Lund, L. Sue Beard, L.W. Snee, and William J. Perry, Jr.*

4:30 Gulf Coast lignite quality—The needs of the 90's *Robert B. Finkelman, W.R. Kaiser, Susan J. Tewalt, and James A. Luppens*

4:50 Conclusion of technical lecture sessions

THURSDAY, FEBRUARY 20, 1992

8:00 a.m. SHORT COURSE: Recent advances in plate tectonics and continental crustal evolution *Warren B. Hamilton* (Raphael Ballrooms A and B)

4:30 p.m. Conclusion of McKelvey Forum 1992

V.E. McKELVEY FORUM—POSTER SESSIONS

The posters will be available for viewing from 8:00 a.m. to 4:30 p.m. Tuesday and Wednesday in Raphael Ballrooms C and D. Authors will be present in their booths during coffee breaks and during the main poster session on Tuesday afternoon from 3:50 to 6:00 p.m., at which time complimentary food and beverages will be available. Also, authors will be present on Tuesday evening from 8:30 to 10:00 p.m., immediately following the Director's Lecture; a cash bar will be set up at this time. The following list of posters is arranged alphabetically by author.

Petroleum geology and exploration potential of the Pripyat Basin, U.S.S.R.

Mahlon M. Ball, Jerry L. Clayton, Gregory F. Ulmishek, Paul G. Lillis, Gordon L. Dolton, Ted A. Daws, Richard F. Mast, Augusta Warden, Michael Keller, Vladamir Bogino, and Zinovy Poznaikovitch

Petroleum reservoir evaluation by borehole gravity survey

Larry A. Beyer

Interactive volume modeling of coal and associated depositional systems, Eocene Brunner Coal Measures, Buller coal field, New Zealand

Laura R.H. Biewick, Margaret S. Ellis, Dorsey Blake, Romeo M. Flores, Richard Sykes, and Carol L. Molnia

Sagavanirktok Formation—A new look with seismic data in the Prudhoe Bay-Kuparuk River region, Alaskan North Slope

Kenneth J. Bird and Timothy S. Collett

Gravity and aeromagnetic interpretation of structure in Railroad Valley and the Grant Range, east-central Nevada

H. Richard Blank and John A. Grow

Tectonostratigraphy and Neogene extensional tectonism on part of the California continental border-land—A seismic-reflection perspective

R.G. Bohannon and E.L. Geist

Normal faulting in collisional foredeeps—Implications for basin analysis

Dwight C. Bradley and W.S.F. Kidd

Coal availability studies—An update

M. Devereux Carter, Nancy K. Gardner, James C. Cobb, Roy S. Sites, and Nick Fedorko, III

Natural gas hydrates—A proven resource

Timothy S. Collett

Tar sands and heavy oils—Resources, recovery, and realism

B.L. Crysdale, C.J. Schenk, and R.F. Meyer

Evidence for petroleum-assisted speleogenesis, Lechuguilla Cave, Carlsbad Caverns National Park, New Mexico

K.I. Cunningham and K.I. Takahashi

Cretaceous resources, events, and rhythms—Continental Scientific Drilling Transect of the Western Interior seaway

Walter E. Dean and Michael A. Arthur

POSTER SESSIONS (CONTINUED)

Undiscovered oil and gas resources of Federal lands and waters
G.L. Dolton, R.F. Mast, and R.A. Crovelli

Fluvial architecture and reservoir heterogeneity—Triassic and Tertiary examples from the Colorado Plateau
Russell F. Dubiel, Steven C. Good, and Christopher J. Schenk

Origin of the Challenger Knoll oil, Gulf of Mexico
N. Terence Edgar and Jerry L. Clayton

Estimation of gas hydrate concentrations using seismic methods
Kristen Fehlhaber, William P. Dillon, and Myung W. Lee

Synsedimentary authigenic illite and implications for geothermometry in sedimentary basins
Neil S. Fishman and Christine E. Turner

High-resolution paleoclimate reconstruction from Alaskan ice-core records
J.J. Fitzpatrick, T.K. Hinkley, G.P. Landis, R.O. Rye, and G. Holdsworth

Tectonic and climatic changes expressed as sedimentary and geochemical cycles in Paleogene lake systems, Utah and Colorado—Implications for petroleum source and reservoir rocks
Thomas D. Fouch and Janet K. Pitman

Late Cretaceous and early Tertiary evolution of the Uinta and Piceance basins (northeastern Utah and northwestern Colorado) and associated development of hydrocarbons
K.J. Franczyk, T.D. Fouch, R.C. Johnson, C.M. Molenaar, and W.A. Cobban

Hydrocarbon source-rock evaluation of Desmoinesian (Middle Pennsylvanian) coals from southeastern Iowa, Missouri, southeastern Kansas, and northeastern Oklahoma
Joseph R. Hatch

Anadarko basin reservoir and non-reservoir sandstones—A comparison of porosity trends
Timothy C. Hester and James W. Schmoker

Testing new coal models—The 1991 Kaiparowits Plateau Drilling Project
R.D. Hettinger and P.J. McCabe

$\delta^{13}\text{C}$ of terrestrial and marine organic matter in Cretaceous rocks of the Western Interior of North America
Charles W. Holmes, John M'Gonigle, and Brent Dalrymple

Seismic reflection studies of Lake Baikal, U.S.S.R.
D.R. Hutchinson, A.J. Golmstok, T.C. Moore, M.W. Lee, C.A. Scholz, and K.D. Klitgord

The ARC/INFO Geographic Information System applied to geologic investigations of the Norphlet Formation, Alabama and Mississippi
C. William Keighin and C.J. Schenk

The Santa Maria Province Project, California
Margaret A. Keller, Caroline M. Isaacs, and Richard G. Stanley

POSTER SESSIONS (CONTINUED)

Fracturing and reservoir development in the Katakutuk Dolomite, Arctic National Wildlife Refuge, Alaska

John S. Kelley, Chester T. Wrucke, and Augustus K. Armstrong

Major controls on accumulation of Upper Cretaceous coals in North America

M.A. Kirschbaum, L.N.R. Roberts, and P.J. McCabe

Evolution of the Illinois Basin

Dennis R. Kolata, W. John Nelson, Janis D. Treworgy, Stephen T. Whitaker, Michael L. Sargent, Lloyd C. Furer, and M.C. Noger

GIS visualization of coal stratigraphic and geochemical information

Kathleen K. Krohn, Carol L. Molnia, Susan J. Tewalt, and William G. Miller

Alteration of lignin during biodegradation in peats and the early stages of coalification

Harry E. Lerch, William H. Orem, and Timothy A. Moore

Development of the Ellesmerian continental margin and the Brookian orogeny, Alaska—A DNAG perspective

Thomas E. Moore, Wesley K. Wallace, Kenneth J. Bird, Susan M. Karl, and C. Gil Mull

Controls on gas generation and production, tight sandstone reservoirs, Uinta Basin, Utah

Vito F. Nuccio, James W. Schmoker, and Thomas D. Fouch

The desktop core library, a CD-ROM approach

Michael P. Panetta, Frances E. Gay, and Russell A. Ambroziak

Petrography and Rock-Eval studies of organic matter in Precambrian rocks, U.S.A. and U.S.S.R.

Mark Pawlewicz and James G. Palacas

Relation of natural fractures to composition and cyclicity in chalk of the Niobrara Formation, Berthoud field, Colorado

Richard M. Pollastro

USGS Core Research Center—A million feet of geologic history

Diana L. Richards and Thomas C. Michalski

Research thrusts of the current five-year USGS Evolution of Sedimentary Basins program—Illinois, Paradox, Eastern Great, and SWAN basins

J.L. Ridgley, A.C. Huffman, Jr., H.E. Cook, C.J. Potter, S.Y. Johnson, and W.E. Dean

Isostatic residual gravity mapping of Wyoming

S.L. Robbins and J.A. Grow

Paleocene paleogeography, tectonics, and coal distribution in the Rocky Mountain region—An overview

S.B. Roberts, M.S. Ellis, R.M. Flores, D.J. Nichols, W.J. Perry, Jr., and G.D. Stricker

Reservoir heterogeneities in the Morrison Formation in southern Utah—A Prudhoe Bay analog

John W. Robinson and Peter J. McCabe

Geochemistry and origin of oil in Cambrian and Ordovician reservoirs, Ohio

Robert T. Ryder, Robert C. Buruss, and Joseph R. Hatch

POSTER SESSIONS (CONTINUED)

Algodones depositional system—Modern analog for the Upper Jurassic Norphlet Formation, Mississippi and Alabama

C.J. Schenk

Tectonic and climatic controls on the sedimentary record of the early Mesozoic Newark Supergroup rift basins, Eastern North America

Joseph P. Smoot

Interactive computer display of petroleum exploration and undiscovered resource potential of the United States

Kenneth I. Takahashi, Debra K. Higley, and Richard F. Mast

NERSL—National Energy Research Seismic Library

David J. Taylor and Frederick N. Zihlman

Preliminary 1:100,000-scale geologic map of Santa Maria 30' × 60' quadrangle, central coastal

California—Progress toward a digital compilation

Marilyn E. Tennyson

Multifaceted studies of a lacustrine source rock—The Paleogene Green River Formation, Colorado, Utah, and Wyoming

Michele L. Tuttle, Walter E. Dean, Mark Stanton, James Collister, Wendy Harrison, Thomas D. Fouch, Janet Pitman, Trond Hanesand, and Nils Telhaes

The Coal Resource Evaluation and Assessment Project (COALREAP) in Pakistan—Energy for the future

Peter D. Warwick, John R. SanFilipo, Roger E. Thomas, and James E. Fassett

Late Paleocene and early Eocene terrestrial and marine environments, Lakhra coal field, Sindh Province, Pakistan

Christopher Wnuk, Elisabeth M. Brouwers, and Norman Frederiksen

Energy research on Indian lands

R.S. Zech, H.H. Arndt, L.H. Biewick, J.K. Hardie, R.C. Johnson, J.L. Ridgley, Courtney Williamson, and Robyn Wright-Dunbar

Eighth V.E. McKelvey Forum on Mineral and Energy Resources

USGS Research on Energy Resources, 1992 Program and Abstracts

Edited by L.M.H. Carter

Unconventional Resources— Are They in Our Future?

Thomas S. Ahlbrandt

Unconventional hydrocarbon resources are so designated because economic, technologic, or regulatory constraints do not allow their development. For example, in a 1978 FERC (Federal Energy Regulatory Commission) study, marsh gas collected beneath large plastic tents was only recoverable at \$130/MCF (thousand cubic feet) and the study authors correctly concluded that it was not a viable methane resource at that time. Many unconventional resources have the advantage of large in-place volumes which, although in many cases widely disseminated, are intriguing because they represent reduced risk of dry holes during development.

As constraining technologic or regulatory parameters will be modified, unconventional resources will increasingly become economic and may further displace conventional resources. Heavy oils have already displaced light oils domestically in several significant areas. Presently, 73 percent of all U.S. enhanced oil recovery and about 70 percent of California's oil production are heavy oil. Heavy oil fields already represent about 15 percent of the total number of giant fields (> 500 MMBO (million barrels of oil)) and in the U.S. include such giant fields as Smackover, San Ardo, Hawkins, Huntington Beach, Wilmington, South Belridge, Coalinga, Kern River, and Midway-Sunset. Heavy oil from Venezuela is expected to produce 500,000 BOPD (barrels of oil per day) by 1995 from the degraded remnants of perhaps the world's largest oil accumulation, estimated to be 1.6 trillion BO (barrels of oil) in place at

this time, of which 250 BBO is recoverable and viable in the \$9–\$12 per barrel range. The original accumulation is estimated to have been 8 trillion BO in place. Very large bitumen or natural asphalt resources, such as the Canadian Athabasca, Peace River, and Cold Lake Cretaceous and Devonian reservoirs, are thought to be viable in the \$15–\$20 per barrel range.

Unconventional natural gas resources are also becoming increasingly viable. Coalbed methane, which accounts for about 25 percent of potential natural gas resources in the U.S., will displace nearly a trillion cubic feet (TCF) of gas from conventional resources in the near term and perhaps several TCF by the turn of the century. Similarly, production of gas from low-permeability resources may displace some production of conventional gas as increasingly smaller conventional accumulations are developed. Coalbed methane and tight gas, both abundant in the Rocky Mountain and Appalachian regions, will likely experience significant production increases. Optimistic scenarios suggest that tight gas and coalbed methane resources may provide more domestic natural gas production than conventional resources by the year 2010. Horizontal drilling technology will most likely unlock the large currently uneconomic gas resources in tight reservoirs. Technologies like this will most certainly change the status of what are presently considered unconventional resources.

Beyond the turn of the century, more speculative gas resources, particularly gas hydrates or even gas from oil shale, may become increasingly significant contributors. Geopressured gas-bearing brines, although clearly a large resource base, will most likely be used primarily for thermally enhanced oil recovery efforts and only secondarily as hydraulic, thermal or natural gas energy sources. If the concerns for global warming and a cleaner atmosphere are considered, then greater use of natural gas is anticipated and perhaps will provide

additional incentives to develop unconventional gas resources. Clearly, for future hydrocarbon supplies, resources considered to be unconventional today, particularly gas resources, will increasingly displace conventional resources as economic, technologic, and regulatory barriers are modified.

Petroleum Geology and Exploration Potential of the Pripyat Basin, U.S.S.R.

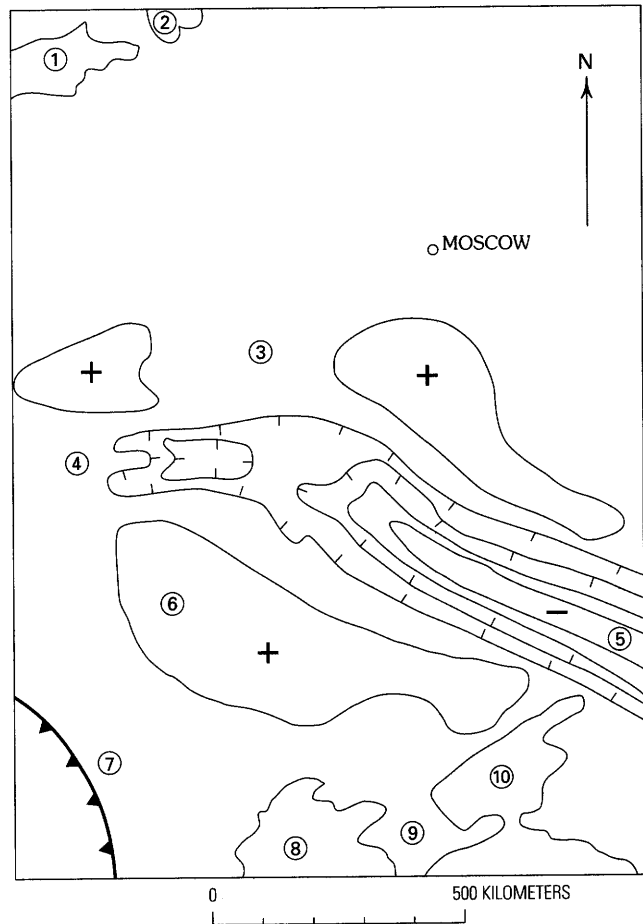
Mahlon M. Ball, Jerry L. Clayton,
Gregory F. Ulmishek, Paul G. Lillis,
Gordon L. Dolton, Ted A. Daws,
Richard F. Mast, Augusta Warden,
Michael Keller, Vladimir Bogino,
and Zinovy Poznaikovitch

This study is an initial step in applying U.S. Geological Survey oil and gas assessment techniques to basins within the U.S.S.R. in order to compare methods used by U.S. and Soviet scientists. The goal of both groups of government earth scientists is to improve the ability to assess undiscovered recoverable oil and gas resources.

The Pripyat basin is the extreme northwest end of the middle Paleozoic, Dnieper-Donets aulacogen that separates the Ukrainian shield from the rest of the Russian craton (fig. 1). Gravity, magnetic, and seismic refraction measurements show that its basement structure is typical of intracontinental rifts and that basement consists of east-west-trending tilted blocks bounded by listric normal faults believed to intersect mantle rocks, at a depth of approximately 40 km, above an elevated asthenospheric ridge.

The sedimentary sequence within the Pripyat basin is as much as 6 km thick and is subdivided into five units: (1) The lowest, pre-rift unit consists of basal terrigenous clastics overlain by thin Middle Devonian quartz sands, shales, carbonates, and anhydrites. This lowermost unit grades upward into (2), a lower salt interval of Frasnian Age. The lower salt contains some interbedded carbonate. Above the lower salt, (3) a carbonate unit containing some black shale is referred to as the intersalt carbonate. (4) The upper salt, a relatively pure halite, caps the intersalt carbonate. Faults tend to die out upward in the upper salt interval, and salt flowage is mostly restricted to this interval. The upper salt is overlain by (5) terrigenous clastics ranging in age from youngest Devonian to Quaternary. Only the basal sands of unit 1 are pre-rift sediments. The remaining units are syn-rift deposits with the exception of the post-rift unit 5.

Principal source rocks are black-shale facies in the intersalt carbonate formation. This same formation contains about two-thirds of the hydrocarbon reserves.



EXPLANATION

- ① Gulf of Finland
- ② Lake Ladoga
- ③ Russian craton
- ④ Pripyat basin
- ⑤ Dnieper-Donets basin
- ⑥ Ukrainian shield
- ⑦ Carpathian fold-thrust belt
- ⑧ Black Sea
- ⑨ Crimea
- ⑩ Gulf of Azov
- Regional high
- Regional low

Figure 1 (Ball and others). Regional index map of Pripyat basin, U.S.S.R. Solid contour encloses regional geophysical high; hachured contour encloses regional low.

The remaining reserves are in carbonate and clastic rocks beneath the lower salt. Faulted structural traps control all fields. Stratigraphic pinchouts, lower Famennian (intersalt) reefs, and roll-over closures on downthrown blocks are potential exploration targets.

Pyrolysis assay of 284 samples reveals the presence of potential source rocks (mostly in shales in the intersalt carbonate unit 3) containing as much as 3 weight percent

organic carbon (types II and III kerogen). The rocks are generally marginally mature to mature (0.6–0.9 vitrinite reflectance equivalent) with respect to petroleum generation. Thermally immature oils (vitrinite reflectance equivalent of about 0.5 percent) occur in clastic and carbonate rocks in the central rift. Oil is only produced in the northern part of the basin and exhibits a range of thermal maturity levels, generally more mature than those toward the south. No systematic relationship exists between reservoir depth and degree of thermal alteration of the oils. We are currently conducting detailed studies of biological markers contained in the oils to determine whether multiple source rocks have expelled oil in the basin, or whether the oils were expelled from a single source rock over a range of maturities (burial depths).

Fractal Nature of Hydrocarbon Accumulations and Price—Implications for Resource Assessment, Exploration and Development Strategies, and Economic Forecasting

Christopher C. Barton

Fractal geometry is a branch of mathematics that redefines how we may quantitatively describe and model complex patterns and distributions. It can be applied to three complex patterns and distributions of importance to the petroleum industry: (1) the size-frequency distribution of petroleum accumulations and its consequences on assessments of the volume of undiscovered petroleum resources, (2) the spatial clustering of petroleum accumulations and its consequences on exploration and development strategies, and (3) the fluctuation of oil price and the use of fractal statistics to quantify price behavior.

Hydrocarbon accumulations vary in size over scales spanning many orders of magnitude. A proper mathematical description of this variation is sought in order to assess the volume of hydrocarbons contained in undiscovered accumulations. Size-frequency data sets extending over six orders of magnitude, from small fields in a play to giant fields of the world, have proven to be fractal; and any given population of hydrocarbon accumulations consists of the sum of many fractal subpopulations in nested hierarchical levels without a characteristic size scale. The volume of the undiscovered accumulations is calculated for several data sets using a convergence constraint which requires only that the volume of hydrocarbons in a given data set be finite, thus constraining the value of the exponent in the power-law distribution to be less than one. Data sets that include too

large an area or too diverse a set of subpopulations fail to meet the convergence requirement. This failure commonly follows from combining fractal subpopulations with different upper field-size limits indicating that predictions of the undiscovered resources on continental and world scales should be made for collections of smaller, geologically homogeneous populations which may then be aggregated.

The spatial clustering of hydrocarbon accumulations also varies over length scales spanning many orders of magnitude. A fractal description of this clustering provides a mathematical characterization that can be used to optimize exploration and development strategies. The spatial clustering of hydrocarbon accumulations in 40×40 mile square portions of two stratified reservoirs, the J sandstone of the Denver basin and the Muddy Sandstone of the Powder River basin, is found to be fractal. Thus, the accumulations cluster at all scales tested, with the fractal dimension (D) 1.49 and 1.43, respectively, over length scales ranging from 1 to 10 miles. The fractal nature of the spatial clustering of hydrocarbon accumulations in a given reservoir has significant consequences on the selection of appropriate exploration and development strategies.

The fluctuation of oil price as a function of time also exhibits fractal structure with a chaotic attractor underlying price behavior. This result reveals a mathematical structure of the oil market which could provide a new basis for economic forecasting of oil price.

C.C. Barton can be reached at the USGS, (303) 236-1280.

Petroleum Reservoir Evaluation by Borehole Gravity Survey

Larry A. Beyer

Borehole gravity surveys of petroleum reservoirs, which can provide unique bulk-density, porosity, and pore-fluid density information, have been made intermittently for more than 25 years and have gradually received greater industrial acceptance. However, today's requirements for improved description and monitoring of petroleum reservoirs argue for even broader use of borehole gravity surveys. Broader use and acceptance of borehole gravimetry require that its capabilities and limitations be fully understood and carefully applied to each case study; a logic flowchart that incorporates geologic, well-log, and reservoir information with the capabilities and limitations of borehole gravimetry can aid this decision-making process. Broader acceptance also comes about through successful demonstrations of improved reservoir description that, for example,

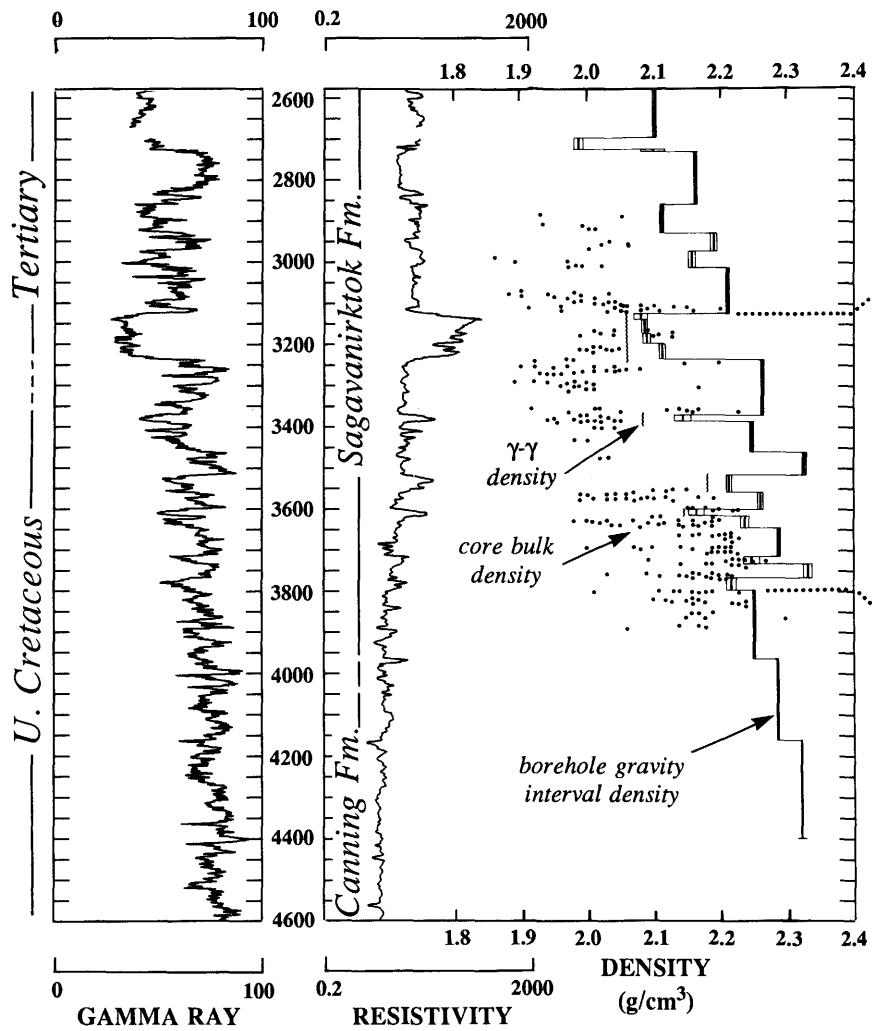
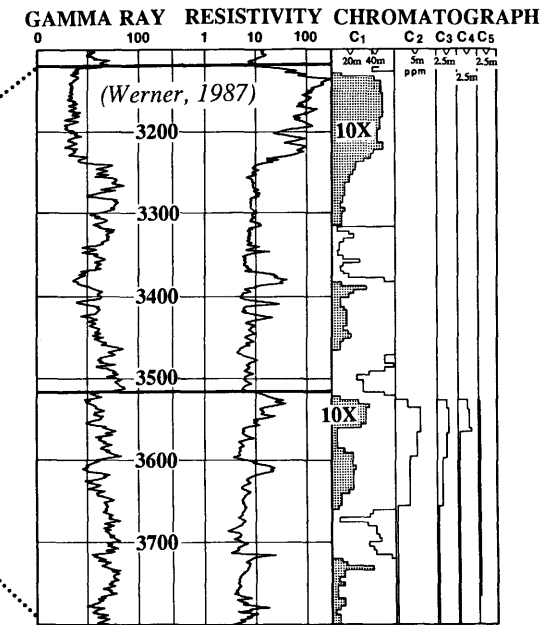


Figure 1 (Beyer). Interval density profile based on borehole gravity survey through the lower part of the Sagavanirktok Formation (Cretaceous and Tertiary), West Sak 17 well, Kuparuk River oil field, Alaska. The unproduced oil-bearing sandstones of the lower part of the Sagavanirktok Formation are poorly consolidated fluvial to deltaic deposits, locally referred to (by M.R. Werner in a 1987 study) as the "Ugnu and West Sak sands." API gravities of oil in these sandstones generally range from 12° to 20°. Gamma ray and resistivity logs (left) and portion of gas chromatograph log (right) also are shown. Bulk densities



of conventional core samples of sandstone from three nearby wells and the interval-averaged gamma-gamma densities for four sandstone intervals from the formation density log of the West Sak 17 well also are plotted with the gravity-based density profile. Core densities, based on fresh-water saturation, are calculated from laboratory measurements of porosity provided by the Kuparuk field operator. Core porosities and calculated densities are not adjusted for overburden stress and reservoir pressures.

delineate new productive intervals, define original or secondary gas zones, or more accurately assess porosity for improved reserve calculations and production.

Borehole gravity measurements, because of their greater lateral sensing distance than those of conventional log methods, frequently improve evaluation of (1) carbonate reservoirs that are characterized by large-scale porosity and (2) poorly consolidated reservoirs or other reservoirs where borehole rugosity and formation invasion perturb shallow-sensing log methods. Borehole gravity measurements also are unaffected in a practical sense by metallic casing or cement behind casing. Because of their high precision and relatively high accuracy, borehole gravity measurements may allow detection of vertical variations or temporal changes of pore-fluid density in reservoirs with moderate to high porosity.

Selected results of borehole gravity studies by the U.S. Geological Survey and industry in California, Alaska, Rocky Mountains, Gulf Coast, Michigan basin, and Middle East illustrate (1) improved description of carbonate and poorly consolidated clastic reservoirs, (2) through-casing evaluations of older or bypassed (potential) reservoirs, (3) discovery of otherwise undetected reservoirs, and (4) evaluation of vertical and temporal pore-fluid density variations in reservoirs, such as gas cap detection and monitoring. More accurate assessment of reservoir density (and therefore porosity) by borehole gravity survey is shown in figure 1, which compares core, gamma-gamma, and borehole gravity densities. In this study, the larger volume of these poorly consolidated reservoir rocks investigated by the borehole gravity measurements indicates the effectiveness of borehole gravity-based reservoir density (and porosity) over both core and gamma-gamma log data.

Interactive Volume Modeling of Coal and Associated Depositional Systems, Eocene Brunner Coal Measures, Buller Coal Field, New Zealand

Laura R.H. Biewick, Margaret S. Ellis, Dorsey Blake, Romeo M. Flores, Richard Sykes, and Carol L. Molnia

Three-dimensional (3-D) computer modeling of lithofacies in the Eocene Brunner Coal Measures in the Buller coal field, South Island, New Zealand, enhances visualization of the evolution of depositional patterns associated with peat accumulation. Interactive displays show 3-D vertical and lateral variations of lithofacies augmenting detailed paleoenvironmental interpretations of the Brunner Coal Measures by Flores and Sykes.

The Buller coal field, which extends about 20 mi (32 km) along the West Coast of South Island, includes the sandstone-dominated, fining-upward Brunner Coal Measures. Conglomerates, sandstone grits, and subordinate siltstones and mudstones in the lower part of the Brunner Coal Measures were deposited on an undulating peneplain surface developed on Paleozoic and Cretaceous basement rocks. Above this lower interval is a middle interval consisting of coal in the Main Seam or splits of the Main Seam and detrital sediments in partings between the splits. The middle interval is overlain by interbedded sandstones, siltstones, and mudstones and minor coals of the upper interval, which laterally interfingers with marine mudstones of the Eocene Kaiata Formation.

For this study we focused on the lower interval between the basement and the base of the Main Seam or lowest split, and on the middle interval extending from the base of the Main Seam or lowest split to the top of the Main Seam or highest split. Continuous-core data from the New Zealand Geological Survey, which included lithologic information from 1,108 exploratory drill holes, were used in this study. Data distribution is uneven: drill holes are clustered densely in areas of greater economic interest, such as the northeast-trending belt immediately west of the Mt. William fault, whereas large areas contain no data (for example, the north-central part of the coal field in the watershed of the Ngakawau River). Interactive Surface Modeling (ISM) and Interactive Volume Modeling (IVM) software of Dynamic Graphics, Inc., were used to analyze this data set. An important aspect of IVM modeling is the ability to cut into and rotate the display for detailed study in any direction.

We created displays showing present-day sea level as datum and displays showing approximated paleosurfaces using the base of the Main Seam as datum. Some of the displays show the percentage of coarse-grained (conglomerate and (or) sandstone), or fine-grained (mudstone and siltstone) detritus with respect to the thickness of the lower interval. Other 3-D displays exhibit the percentage of coal or partings with respect to the thickness of the middle interval. Gridding the percentage (p) of each lithology within an interval required adding control points to the data set. Each drill-hole data point has a surface location (x,y), an elevation (z), and a percentage value (p) to be contoured. To produce an accurate 3-D representation showing the percentage of a lithology, the p value has to be constant at the drill-hole location throughout the interval thickness, not just represented at the top of the interval. To establish this constancy, control points at each drill-hole location were added with the same x,y , and p values, but with different z values spaced at 10-ft (3-m) intervals covering the

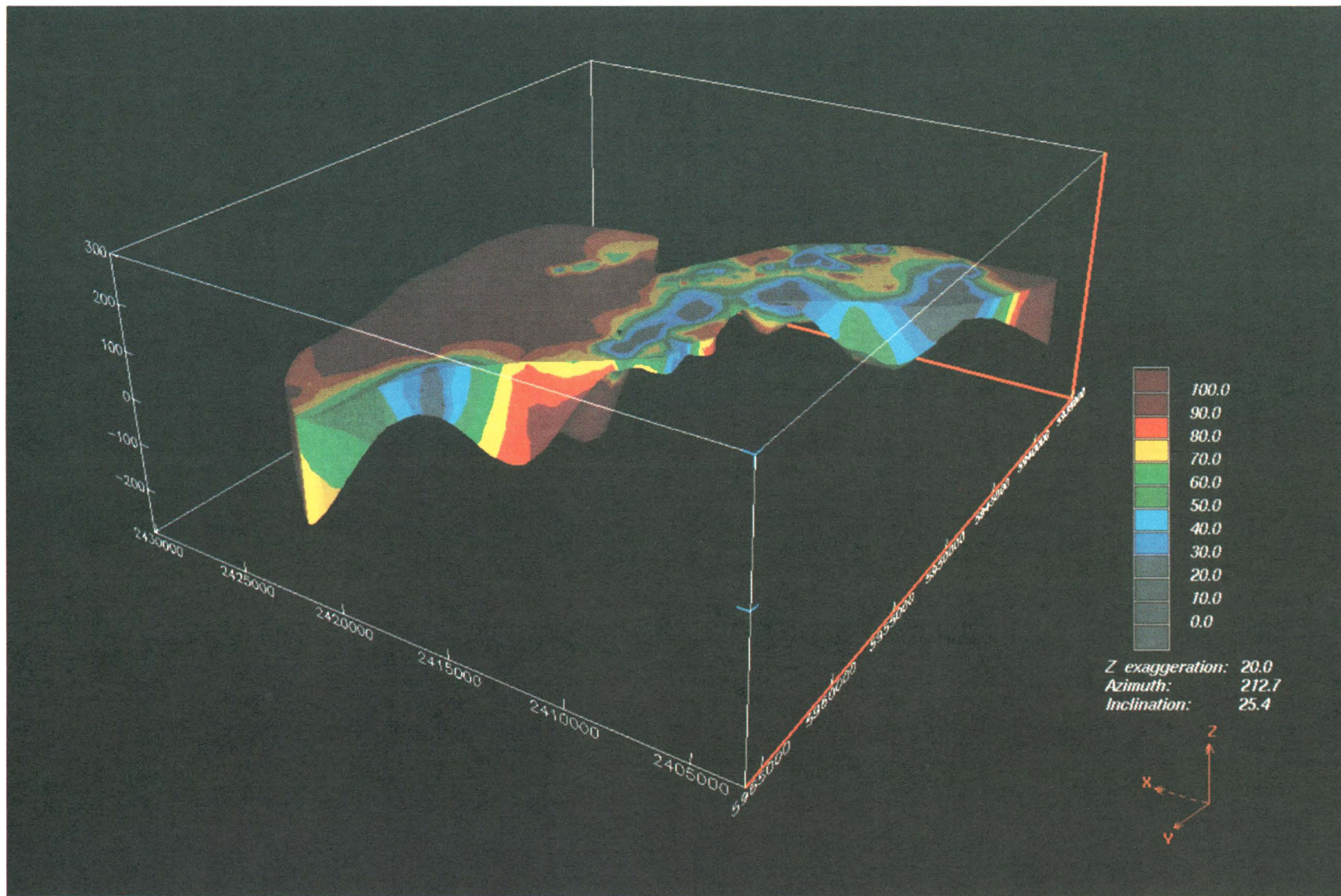


Figure 1 (Biewick and others). Display showing the percent of coarse-grained detrital sediments (conglomerate and (or) sandstone) in the lower interval of the Brunner Coal Measures, New Zealand. Datum is the base of the Main Seam. North is in the direction of the y-axis.

thickness of the interval. The resultant grids extrapolated p only between the drill holes, creating representative displays contoured in 3-D.

One of the displays that were created with the base of the Main Seam as datum is shown in figure 1. General northeast-southwest trends in lithofacies may have been influenced by known syndepositional faults and a topographically controlled paleovalley. In the lower interval, areas with high percentages of coarse-grained material indicate gravel and sand buildup in channels infilling the paleovalley. The figure also shows a northeast-southwest-trending drainage and variable 3-D geometry of internal grain-size distribution. Interactive manipulation of the display (for example, slicing into the model on the z axis) reveals an extrapolated projection of changes in the sediment-load buildup and drainage pattern(s) through time. Similarly, displays created for the middle interval indicate generalized patterns of coal distribution and of peat accumulation through time when sliced along the z axis.

The displays graphically and interactively illustrate lithologic trends that support and augment the interpretation of areal distributions of depositional systems and paleoenvironments by Flores and Sykes. According to their interpretation, the lower interval represents deposits of trunk and tributary braided streams and the coal-bearing interval represents deposits of raised mires that developed on abandoned braidbelts.

Interpretation of specific paleoenvironments requires detailed examination of sedimentologic and stratigraphic data. This computer study enabled the collation of a massive stratigraphic data base to show generalized lithofacies trends. Interactive 3-D computer modeling has proved to be an effective tool for analyzing and displaying the vertical and lateral relationships of lithofacies and paleoenvironmental distribution useful in the construction of predictive depositional models.

Sagavanirktok Formation— A New Look with Seismic Data in the Prudhoe Bay–Kuparuk River Region, Alaskan North Slope

Kenneth J. Bird and Timothy S. Collett

The Upper Cretaceous and Tertiary deltaic Sagavanirktok Formation constitutes the latest stage of filling of the Alaskan North Slope's Colville basin and a treasure trove of energy resources. These resources include an estimated 40–60 billion barrels (in place) of low-gravity oil, 37–44 trillion cubic feet of natural gas in hydrate form, and more than 600 billion metric tons of low-rank coal. Most oil and gas deposits in the

Sagavanirktok occur at shallow depths (<1,000 m) in a relatively restricted area overlying the giant oil and gas fields, Prudhoe Bay and Kuparuk River. The first commercial oil production from the Sagavanirktok Formation was initiated in the Milne Point field in 1990 by the Continental Oil Company; however, at this time most Sagavanirktok oil and gas deposits are classified as unconventional resources.

Access to approximately 200 km of multichannel seismic data in the Prudhoe Bay–Kuparuk River region, courtesy of the Exxon Company, provides new insight into the structural and stratigraphic framework of this area. These are the first modern seismic data available to us in this region; they represent a significant addition to our study of gas hydrates in the Sagavanirktok Formation, a project partially funded by the U.S. Department of Energy. Preliminary analysis of the seismic data confirms the northeast-trending regional dip and northward-expanding thickness of the Sagavanirktok Formation. The clinoform style of progradation, well demonstrated to the west in the National Petroleum Reserve in Alaska, continues through the Prudhoe Bay–Kuparuk River region: the Sagavanirktok representing the topset and the coeval Canning Formation representing the foreset and bottomset parts of the clinoform sequence. Bundles of strong reflections in the topset strata delineate the main coal-bearing intervals. Local high-amplitude reflectors in the bottomset strata may indicate turbidite sand accumulations within prodelta mudstone of the Canning Formation. In the region of the Prudhoe Bay oil field, prominent flat-lying reflections, which occur discontinuously at about 0.7 s (two-way travel time), cut across northeasterly dipping reflectors that mark the regional dip of the Sagavanirktok Formation. Preliminary analysis reveals that these flat-lying reflections occur at a depth of about 950 m, approximately coincident with the calculated base of the hydrate stability zone in this area. In the marine environment, prominent reflections coincident with the base of the hydrate stability zone are well known (bottom simulating reflectors, BSR's) and are postulated to be the result of free gas trapped below a hydrate seal. The reflectors observed on the seismic section over the Prudhoe Bay oil field appear to be the onshore equivalent of a BSR.

As production from the Prudhoe Bay and other North Slope oil fields declines, the enormous hydrocarbon resources of the Sagavanirktok Formation will become increasingly important. Exploration for new hydrocarbon resources will require appreciation of subtle structural-stratigraphic traps and other traps unique to the Arctic region, such as gas hydrates. Production of these hydrocarbon resources presents a major challenge and will require innovative approaches and new thinking.

Alaskan North Slope Geothermics, Geodynamics, and Hydrology—Implications for Oil and Gas

Kenneth J. Bird, David G. Howell,
Mark J. Johnsson, and Leslie B. Magoon

Alaskan North Slope petroleum studies by the U.S. Geological Survey (USGS) are focused on the practically unexplored fold-and-thrust belt of the Brooks Range, a region estimated to have considerable resource potential. Questions being addressed include the quality, quantity, and distribution of reservoir- and source-rocks and the timing of trap formation relative to generation and migration of oil and gas. The answers to these questions will have an important bearing on this region's petroleum potential and, therefore, on resource assessment and exploration strategies.

The North Slope is one of the most prolific petroleum provinces in the United States. It currently supplies one-quarter of our daily domestic oil production (≈ 2 million barrels/day), has productive and nonproductive conventional oil accumulations and nonproductive heavy oil accumulations that originally contained nearly 70 billion barrels of oil (BBO) in place, and has large in-place volumes of principally associated natural gas (≈ 40 trillion cubic feet of gas, TCFG) that are presently uneconomic. In the 1987 national assessment of undiscovered recoverable conventional oil and gas resources, the USGS estimated that, at the mean, nearly one-quarter of our Nation's remaining undiscovered conventional oil resources (≈ 13 BBO) and one-seventh of its undiscovered natural gas resources (≈ 54 TCFG) lie beneath the North Slope and adjacent State offshore waters.

A peculiar feature of discovered North Slope oil and gas accumulations is their geographic concentration in a relatively small area on the foreland—more than 95 percent are located within 60 km of Prudhoe Bay. Yet the considerable volume of undiscovered oil and gas is estimated to be much more widely distributed—about 60 percent in the fold-and-thrust belt region and 40 percent in the foreland region. The fold-and-thrust belt region is estimated to contain undiscovered resources amounting to ≈ 6 BBO (mean; range 1–18 BBO) and ≈ 32 TCFG (mean; range, 7–86 TCFG). The basis for these estimates is the existence of hundreds of undrilled structures, the presence of clastic and carbonate reservoir rocks, abundant source rocks, seemingly favorable maturity patterns, oil and gas indications in wells and outcrop, and seven small to medium-sized oil and gas fields (six gas, one oil).

Our current studies are analyzing regional patterns of thermal maturity (based on vitrinite reflectance and

conodont color indices) and integrating surface and subsurface geology along a series of five planned transects oriented perpendicular to the fold-and-thrust belt and spaced, on the average, at 200-km intervals. We have completed thermal maturity mapping of the surface and subsurface of the North Slope and two seasons of field work on our first transect, located along the Dalton Highway.

Our findings to late 1991 show that nearly 12 km of uplift has occurred in the central Brooks Range, where reflectance isograds are cut by major thrust faults, indicating that maximum burial postdated at least early phases of thrusting. In the foothills, warping of reflectance isograds indicates that some folding (and faulting?) continued subsequent to thermal imprinting, an observation which suggests that oil and gas exploration in the fold-and-thrust belt may be a matter of looking for re-migrated hydrocarbons. Regional patterns on the surface show that thermal maturity decreases northward from the Brooks Range to the coastline; minimal maturity values are found east of Prudhoe Bay. In the central North Slope (between about long 149° and 158° W.), thermally immature rocks extend nearly to the front of the Brooks Range, whereas to the east and west thermally mature rocks are exposed. We interpret this to indicate regional differential uplift along the strike of the Brooks Range orogen, with greater uplift in the west and east than in the center. This central area should be prospective for oil for longer distances to the south than to adjacent areas west and east.

A related USGS study in the National Petroleum Reserve in Alaska has found that geothermal gradients and heat flow are higher on the north (foreland) side of the basin and lower in the foothills (fold and thrust) belt of the Brooks Range. This thermal pattern is consistent with forced convection by a topography-driven groundwater flow system that would effectively cool the topographically higher fold-and-thrust belt and warm the topographically lower foreland region. Similarities between present-day thermal gradients and vitrinite reflectance profiles suggest that the postulated groundwater flow system probably has been a feature of the fold-and-thrust belt throughout its 150-m.y. history and may have provided a driving mechanism for petroleum migration.

Gravity and Aeromagnetic Interpretation of Structure in Railroad Valley and the Grant Range, East-Central Nevada

H. Richard Blank and John A. Grow

Potential-field anomalies in Railroad Valley and adjacent areas, used in conjunction with geologic,

seismic, and drilling data, contribute uniquely to an understanding of upper crustal structure of this complex region and thereby help to constrain hypotheses for the generation and localization of its hydrocarbon deposits. Railroad Valley extends nearly 175 km in a generally north-south direction and has a maximum width of some 25 km. The associated Bouguer gravity anomaly field, reflecting mainly the density contrast between pre-Tertiary bedrock and late Cenozoic valley fill, delineates a buried axial trough much narrower than the full width of the valley. The trough is characterized by colinear deeps 30–50 km long that are separated by transverse rises. It is probably no coincidence that all six of the producing oil fields in Railroad Valley are situated on the margins of the deepest gravity low, which is located in Butterfield Marsh, west of the northern Grant Range. This low has a residual amplitude of -43 mGal. Exploration drilling has established that the thickness of valley fill (Tertiary and Quaternary deposits, including Tertiary volcanics) here exceeds 4.2 km. At such depths the prevailing geothermal gradient may be sufficient to convert organic material to oil, and high-angle faults on the margins of the deep could have facilitated upward migration to suitable traps and reservoirs. The density contrast corresponding to a 43-mGal anomaly produced by 4–5 km of valley fill is much less than the 0.40–0.45 g/cm³ predicted for fill relative to Paleozoic carbonates, a discrepancy attributed to an abundance of high-density carbonate material in the Tertiary and Quaternary section. This conclusion is supported by data from down-hole sonic and lithologic logs. Megacrysts of Paleozoic carbonate rock are locally present and in some places have been detected by high-precision commercial gravity surveys.

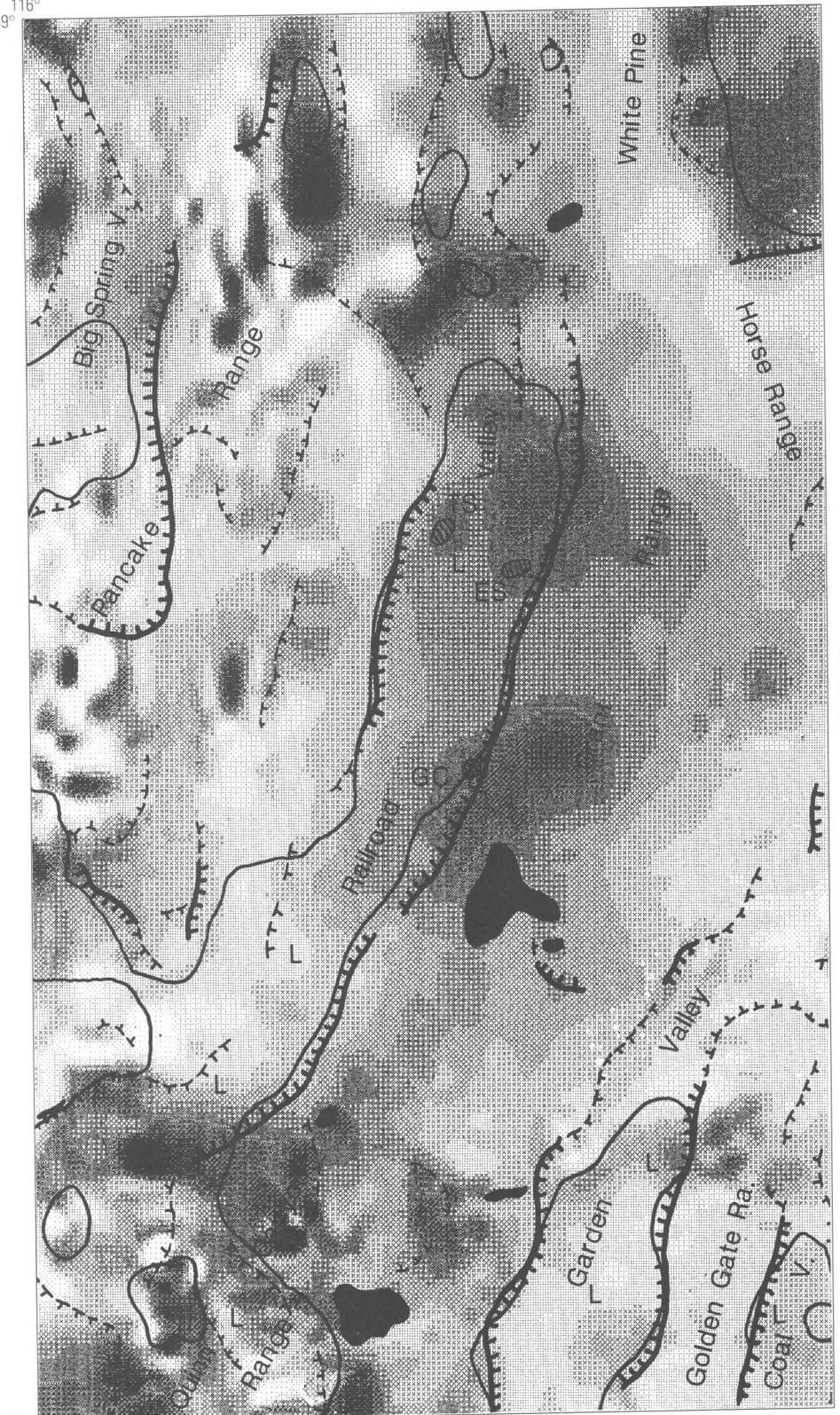
The anomaly has horizontal gradients along its eastern flank of as much as 11 mGal/km, whereas those on the western flank are about half as strong. This asymmetry results from a bedrock surface in the form of a half-graben with its floor tilted down to the east, in agreement with seismic reflection data. The eastern marginal gradient continues as a well-constrained gravity feature for 65–70 km along the range front, approximately between lat $38^{\circ}45'$ N. and $38^{\circ}15'$ N. The locus of *maximum* gradients (fig. 1) is a line 2–10 km west (basinward) of the nearest bedrock outcrops. This line roughly coincides with a line of springs and ground-water seepage, and marks the trace of the main boundary fault (range-front fault) on the west side of the Grant Range. East of Butterfield Marsh, and also just north of the Quinn Canyon Range, where the gradient is steepest, the fault or fault zone is probably a high-angle structure, but in the intervening segment (from the Grant Canyon oil field for about 15 km south), dips as low as 20° have been interpreted from seismic data. Both flatter dips and deeper burial of the density discontinuity could cause the

diminished gravity gradients. Down-hole logs show the rocks immediately east of the gradient maximum at Grant Canyon to be predominantly high-velocity, high-density Paleozoic carbonate sand/gravel and breccia (identified as valley fill) below the uppermost 400 m or so of section. A transverse seismic profile in this area reveals east-dipping reflectors abutting an underlying, gently west dipping reflector interpreted as a low-angle normal fault. Thus at Grant Canyon the range-front fault apparently truncates a section that includes detached and rotated allochthonous Paleozoic strata (either megacrysts in valley fill or forming the hanging wall of a low-angle normal fault).

The loci of gravity horizontal-gradient maxima in figure 1 are superimposed on a gray-scale map of the residual total-intensity aeromagnetic anomaly field (IGRF removed). The main aeromagnetic feature of interest is a broad positive anomaly that encompasses the north half of Railroad Valley and most of the Grant Range. The axis of this anomaly is roughly parallel to that of the negative gravity anomaly associated with Railroad Valley: both extend north-south across the area of figure 1 and are convex eastward. No offset of the aeromagnetic feature is observed where it is transected by the range-front fault, and the estimated depth to the top of the magnetic source is commensurate with a reasonable depth extent for the density discontinuity. Therefore the range-front fault is probably listric with respect to, or terminates at, a low-angle structure at or near the surface of the magnetic body. This structure may be the low-angle normal fault interpreted from seismic data at Grant Canyon. Mississippian Chainman Shale, a source rock for the hydrocarbons, may locally have been the horizon of detachment. Whether the low-angle fault passes beneath the Grant Range at depth or connects with a low-angle fault exposed on the west side of the Grant Range is not likely to be resolved from the potential-field data.

In the absence of strongly magnetic Paleozoic strata, the possible sources of the broad aeromagnetic anomaly are limited to Precambrian crystalline basement and Phanerozoic intrusives. Shorter-wavelength highs superimposed on the broad anomaly are attributable to structural relief and (or) variable magnetization of either rock. Our preferred interpretation for the source body is a Phanerozoic granitic (chiefly quartz monzonitic) batholith. Granitic plutons are exposed in the southwestern White Pine Range, in the southwestern and central Grant Range, and in the northern Quinn Canyon Range, all localities that are close to the axis of the broad anomaly; and quartz monzonite has been penetrated in several drill holes in Railroad Valley. Potassium-argon ages for biotite of these plutons range from 36 to 23 Ma. However, a 70-Ma minimum age of crystallization was determined for the Troy pluton in the Grant Range on the basis of whole-rock Rb:Sr analysis; and it now seems

116° 39° 115°15'



38° 116° 39° 115°15'

0 10 20 30 KILOMETERS
0 10 20 30 MILES

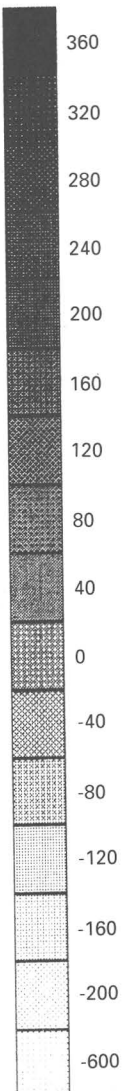


Figure 1 (Blank and Grow) (facing page). Gray-scale map of residual aeromagnetic total-intensity anomaly field of Railroad Valley, Grant Range, and vicinity, east-central Nevada. Data of several surveys have been merged, draped to 1,000 ft (305 m) above terrain and reduced to the pole. Selected gravity anomaly features are also shown: (1) loci of horizontal-gradient maxima of the Bouguer anomaly field (heavy barbed lines where intense, indicating steep, near-surface density discontinuities; light barbed lines where less intense, indicating less steep dips, more deeply buried density discontinuities, gradational density contrasts, or a combination of these); (2) areas of Airy isostatic residual anomaly lower than -20 mGal (outlined by solid lines); and (3) isostatic residual anomaly minima lower than -30 mGal (labeled "L"). Standard parameters have been used for the gravity reductions. Hatched areas in Railroad Valley are oil fields (TS, Trap Spring; ES, Eagle Springs; GC, Grant Canyon). Solid black areas denote exposed silicic intrusive rock, chiefly granitoid.

likely that the plutons are part of a composite body, initially emplaced in Cretaceous time but becoming a locus of renewed heating and possibly magmatism in the Tertiary.

The inferred batholith must have had a major role in the tectonic evolution of the Railroad Valley–Grant Range region. Initial emplacement occurred during a late stage of synkinematic regional metamorphism recorded in lower Paleozoic rocks of the Grant Range. Renewed magmatism in Oligocene–Miocene time may have contributed to arching of the range, as well as to high heat flow in Railroad Valley. In addition, a structural parallelism indicates that the presence of the batholith probably influenced the configuration of youthful extensional structures such as the Railroad Valley graben.

Tectonostratigraphy and Neogene Extensional Tectonism on Part of the California Continental Borderland—A Seismic-Reflection Perspective

R.G. Bohannon and E.L. Geist

Tectonostratigraphic terranes and extensional structures are being studied on part of the California Continental Borderland using seismic-reflection data primarily from USGS line 120, which traverses the tectonic grain of the province south of San Clemente Island. After applying prestack multiple suppression and migration, we can present the data on line 120 in depth section. Ancillary data from two crossing lines and several nearby parallel lines, in standard stack sections, are also useful. We can enhance details of fault structures

by locally portraying the amplitude data in color. Stratigraphic control comes from onshore outcrops east of the end of the line at Oceanside and north of the line at San Clemente Island, and from well data on southern Cortes Bank.

Line 120 crosses four tectonostratigraphic terranes. The offshore segment of the Santa Ana terrane near Oceanside has well-developed reflectors imaging a thick Cretaceous to Miocene section that dips gently westward above basement. Several large listric normal faults with intermediate to low eastward dips truncate the sedimentary section against schistose rocks of the adjacent Catalina terrane beneath the Neogene sediments in the Gulf of Santa Catalina. Reflective horizons are thin and discontinuous across the Catalina terrane where Miocene sedimentary and volcanic rocks lie directly on Catalina Schist (Mesozoic). Southwest of San Clemente Island the Nicolas terrane can be easily distinguished from the Catalina by a thick, well-developed, gently deformed reflective sequence of Cretaceous to upper Miocene strata present beneath southern San Nicolas basin and Cortes Bank. The boundary between the latter terranes is at an east-dipping normal fault that lies along the southwest side of the West Cortes Basin. In the Patton terrane, reflective strata are confined to small Neogene basins that developed in low-grade, acoustically chaotic metamorphic rocks.

Numerous basins, primarily half-grabens, formed during the late Miocene to Holocene in the Nicolas, Catalina, and Santa Ana terranes along line 120. The southern Patton terrane has an irregular bathymetry, but basins are poorly developed or absent. East-northeast- and west-southwest-facing half-grabens are bounded by normal faults that have intermediate to gentle dips. Some of the fault planes produce reflectors, but most are marked by terminations in stratal reflectors. Listric and planar fault geometries are both present.

Normal Faulting in Collisional Foredeeps—Implications for Basin Analysis

Dwight C. Bradley and W.S.F. Kidd

We report the results of structural and stratigraphic analysis of three foredeeps cut by syncollisional normal faults (Ordovician Taconic foredeep, Carboniferous Arkoma basin, and present-day Timor-Aru trough), and we use these examples to generalize about extensional processes in environments of lithospheric flexure. Normal faults on the cratonic flanks of collisional foredeeps (those formed during arc–passive-margin

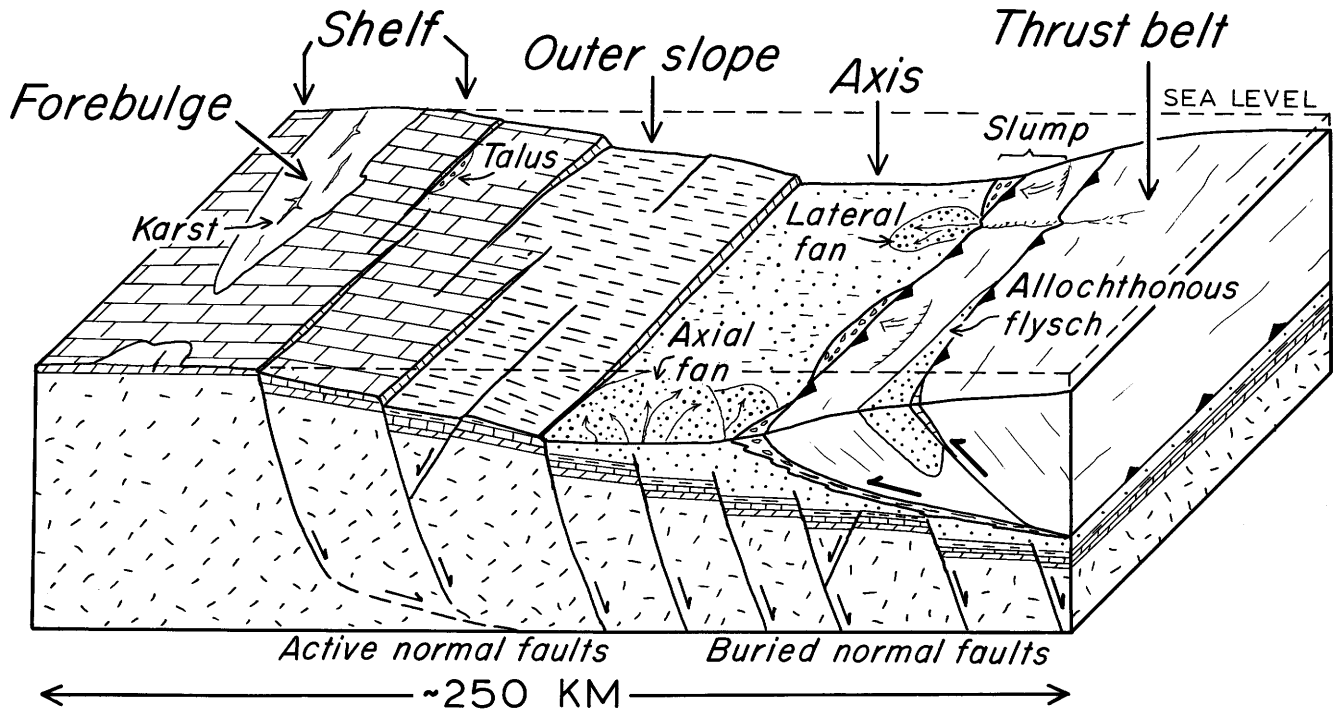


Figure 1 (Bradley and Kidd). Schematic block diagram of Taconic collisional foredeep in New York, showing distribution of facies belts and extensional and contractional deformation regimes shortly before plate convergence ended. Timor-Aru trough and Arkoma basin are similar. Fault

dashed where inferred; barbs show direction of movement on faults; sawteeth on overthrust block. Patterns show rock types as follows: random dashes, Precambrian basement; bricks, carbonate rocks of passive-margin platform; parallel dashes, shale; stipple, graywacke and shale.

collision, as opposed to Andean-type foreland basins) are analogous to normal faults in deep-sea trenches, except that the faulted lithosphere is continental rather than oceanic. (See expanded discussion in a 1991 study of Bradley and Kidd.) Normal faulting occurs within an overall setting of plate convergence when the subducting lithosphere is flexed beyond its elastic limit. Because the top of the lithosphere extends while the lower lithosphere contracts, the dynamics of extension in this setting differ fundamentally from those of rifting induced by divergent plate motion.

The normal faults we studied typically occur as far as 100 km toward the foreland from the thrust front and parallel with it, have throws of as much as about 1 km, are spaced 5–10 km apart, and account for regional near-surface extension typically of a few percent, locally 10–15 percent. Most faults have down-to-basin displacement, together offsetting the underthrust plate like a descending escalator (fig. 1). Fault blocks are rotated with respect to the enveloping surface of the faulted plate, which implies that a detachment exists at depth to accommodate block rotation. In the Taconic foreland of New York, we estimate that steep normal faults ruptured the crust to a depth of 15–20 km, ending at a subhorizontal detachment. Dip-slip displacement on these normal faults was sufficient to produce water

depths in the Arkoma basin and Taconic foredeep comparable to those in the Timor-Aru trough. Accordingly, we suggest that normal faulting can be the primary mode of subsidence of the upper lithosphere in normal-faulted foredeeps.

In each example, stratigraphic relations prove that normal faulting was largely syncollisional. In the Taconic foredeep of Newfoundland, the onset of normal faulting was synchronous with development of an unconformity attributed to migration of a forebulge across the passive-margin platform in advance of the convergent plate boundary (data from a 1991 study by I. Knight and others). Along strike in New York, normal faulting began after passage of the Taconic forebulge, during drowning of the carbonate platform beneath prograding foredeep clastics (fig. 1). In the Timor-Aru trough, normal faults are absent along the forebulge, but active faults cut the cratonic flank, where platform drowning is occurring today. In both the Arkoma basin (1986 study of D.W. Houseknecht) and the Taconic foredeep of New York (1991 study of Bradley and Kidd), the zone of active normal faulting migrated cratonward through time; normal faulting evidently ceased at any given location before arrival of the thrust front. The association of Mississippi-Valley-type Pb-Zn deposits (for example, in the northern Arkoma basin and the Taconic foredeep of

Newfoundland) and hydrocarbon fields (for example, in Oman and Venezuela) with flexure-induced normal faults suggests that these structures can influence the regional-scale migration paths of basinal fluids (brines and hydrocarbons).

Origin of Fluid Pressure, Fracture Generation, and the Movement of Fluids in the Uinta Basin, Utah

J.D. Bredehoeft, J.B. Wesley, and T.D. Fouch

The Altamont-Bluebell oil field in the deep Uinta Basin has reservoir pressures that approach lithostatic. One hypothesis to explain the high fluid pressures is that Type I kerogen has been converted to oil, a mechanism that decreases the density of the hydrocarbons during the change in phase. This phase change can result in increasing the pore fluid pressure. To test this hypothesis, a three-dimensional simulation of fluid flow within the Uinta Basin was performed.

The kinetics of oil generation from oil shale (conversion of Type I kerogen) was investigated by several research groups. To a first approximation the reaction is a function of temperature. The temperature in a geologic environment is a function of the depth of burial and the geothermal gradient. The maximum depth of burial may have occurred as long as 10 million years in the past. A 3 °C/km change in the geothermal gradient is sufficient to change the rate of oil generation by an order of magnitude. The maintenance of high pressures at Altamont depends upon the permeability of the sediments. There is a linear relationship between the geothermal gradient and the reservoir permeability that is necessary to maintain the high fluid pressures.

Natural hydrofractures are simulated by increasing the permeability tenfold where the reservoir fluid pressure exceeds the least principal stress. Simulated hydrofracs are restricted to the productive area of the field.

The analysis demonstrates that oil generation can account for the high fluid pressure, and other fluid-related phenomena in the Uinta Basin.

Coal Availability Studies—An Update

M. Devereux Carter, Nancy K. Gardner, James C. Cobb, Roy S. Sites, and Nick Fedorko, III

In 1987, a cooperative program between the U.S. Geological Survey and the State geological agencies of

Kentucky, Virginia, and West Virginia was initiated in the Central Appalachian Region to (1) identify the major constraints to current coal mining that could inhibit the availability of coal resources and (2) estimate the amount of coal resources that may actually be available for development.

This program has been tested in twelve 7.5' quadrangles (five in Kentucky, four in West Virginia, and three in Virginia) to determine if the identified constraints to mining in the region would significantly affect the availability of coal for development. The 12 study areas were selected to be representative of their general localities so that the results might be extrapolated to the surrounding regions of shared characteristics.

Restrictions that could keep the coal resource from being mined fall into two general categories: land use (primarily human-caused) and technologic (mainly geologic). Land-use restrictions applicable to the study areas to 1991 are power lines, pipelines, cemeteries, oil and gas wells, towns, major streams, public roads, railroads, airports, national and State parks, and a forest preserve. Technologic restrictions include coal beds considered too thin or too deep to mine, buffer zones around active or abandoned mines, mined and minable coal beds too close above or below one another, oil and gas wells penetrating underground-minable coal beds, and such geologic factors as washouts, faults, disturbed areas, and impurities within the coal beds.

Within the 12 areas studied so far, only one-half the original coal resource is estimated to be available for mining. Coal mined and lost-in-mining accounts for 15 percent of the reduction of the original resource, whereas land-use restrictions compose 3 percent, and technological restrictions 32 percent. More than 3.5 billion tons are estimated to be unavailable because of restrictions to mining within the 12 study areas.

Statistical analysis on sulfur data further indicates that only approximately one-half of the coal resources in these areas could be expected to meet current new-source performance standards of 1.2 pounds SO₂ per million Btu input.

Economic considerations, such as mining costs, available transportation, both land and coal ownership, proximity to markets, and size of mining unit, and the application of recovery factors are beyond the scope of this study by USGS and State geological surveys. The U.S. Bureau of Mines (USBM) is conducting follow-on studies applying economic and recovery factors to determine the estimated amount of recoverable coal within the same quadrangle study areas. The USBM studies will result in an estimate of coal that is actually producible—a much smaller amount than the available resource.

As expected, the results of the first 12 studies are inconclusive in terms of delineating regional trends. Studies in about 20 strategically placed 7.5' quadrangles may be necessary to adequately represent the entire Central Appalachian Region. Statistical analysis will begin in 1992, including extrapolation into the surrounding region.

During 1991, coal availability studies were expanded into the Northern Appalachian Region in Ohio and West Virginia. Studies in Pennsylvania and Tennessee will commence in 1992.

Climate Controls on Carboniferous Cyclic Sedimentation and Organic Productivity

C. Blaine Cecil

Cyclic sedimentation is generally attributed to tectonic and (or) eustatic controls. The stratigraphy of chemical and siliciclastic sedimentary rocks cannot, however, be explained on the basis of these physical processes alone. As an example, the Pennsylvanian System of the United States contains transgressive-regressive cycles (cyclothsems) that appear to be eustatically driven; also, basins were tectonically active as subsidence was necessary to provide accommodation space. In the Western Interior, Eastern Interior, and Appalachian basins, stratigraphic repetition of siliciclastic rocks and marine and nonmarine rocks that contain a strong chemical signature, such as coal beds, paleosols, black shales, and limestone, is indicative of paleoclimatic cycles as well as base-level change brought about by tectonics and (or) eustasy. Such climate cycles, induced by changes in rainfall patterns within catchment basins, are recorded in stratigraphic sequences by (1) changes in paleosediment flux; (2) formation of laterally extensive paleosols, whose individual characteristics range from modern Aridisols (arid-climate soils) to Vertisols (seasonal-climate soils) to Oxisols (ever-wet-climate soils); and (3) paleobotanical changes already long attributed to changes in paleoclimate. Furthermore, in the Appalachian basin, laterally extensive coal beds and the characteristics of coeval upland paleosols are consistent with pluvial periods, whereas the driest parts of climate cycles are recorded in nonmarine sequences by lacustrine limestone beds that can be traced laterally into highly calcareous paleosols that approach Aridisols in their structure, chemistry, and mineralogy.

On a continental scale, zonal-circulation paleoclimates are also recorded in addition to paleoclimate cycles. The paleogeography of North America during the Pennsylvanian was such that the Eastern United States was equatorial relative to the Midcontinent and Western United States. The resulting paleoclimate gradient from

the Appalachian basin to the Western United States (wetter to drier, respectively) is indicated by the development of coal beds in the Appalachian basin while evaporites were being deposited in the Paradox basin contemporaneously with alluvial fans and eolianites in the Rocky Mountain region.

Marine black shales, rich in organic matter, are important stratigraphic markers and are economically important as major hydrocarbon source beds and sources of metals. Such shales may also owe their origin to paleoclimate. Most models for the origin of black shales suggest that organic matter in these shales was preserved by anoxic bottom waters that resulted from (1) density stratification in silled basins, (2) deep-water conditions, or (3) high organic productivity in response to upwelling ocean currents as a control on the formation of shale rich in organic matter. However, organic productivity in tropical epeiric seas may also be related to climate cycles. Under dry climatic regimes, water loss from evaporation in epeiric seas is replaced by inflow of open marine water, a condition favorable for shallow-marine carbonates. In contrast, high rainfall during pluvial periods could slow or reverse inflow and provide a low density cap. The latter situation favors (1) influx of terrestrially derived materials including fine-grained siliciclastic sediment, nutrients and dissolved metals, and terrestrial organic matter; (2) increased marine biological productivity and deposition because of nutrient influx; and (3) cessation of carbonate deposition and the onset of black shale deposition. Such alternating wet and dry conditions during the Pleistocene and Holocene are known controls on the stratigraphic distribution of sapropels in the eastern Mediterranean Sea, and similar cycles have been suggested as a stratigraphic control for coal-bearing sequences of the Pennsylvanian System in the Eastern United States. Climate cycles, therefore, may also have influenced the origin of Paleozoic marine sequences, including their organic matter composition and the metal content of Carboniferous black shale.

Although climate is a well-known control on sediment flux, including organic productivity, it is often assumed to be constant in tectonic and (or) eustatic models of stratigraphy and sedimentation. Carboniferous cyclic stratigraphy, however, appears to be a function of climatically driven changes in sediment flux as well as tectonic and eustatic changes in base level.

Natural Gas Hydrates— A Proven Resource

Timothy S. Collett

Large volumes of hydrocarbon gas can occur in sediments in the form of gas hydrates. These substances

are solids, composed of rigid cages of water molecules that trap molecules of gas. Cold surface temperatures at high latitudes are conducive to the development of onshore permafrost and gas hydrate in the subsurface. The combined information from Arctic gas-hydrate studies shows that in permafrost regions, gas hydrates may exist at subsurface depths ranging from ≈ 400 to $\approx 6,000$ ft. Because large quantities of gas hydrates are widespread in permafrost regions, they may be a potential energy resource. Worldwide estimates of the amount of gas within continental gas hydrates range from 500 to 1,200,000 trillion cubic feet.

One of the primary objectives of the U.S. Geological Survey/U.S.S.R. Ministry of Geology (VNIGNI) cooperative research agreement is the assessment of the resource potential of the known Arctic gas-hydrate accumulations. The gas hydrates in the Soviet Messoyakha field, located in the West Siberian basin, and those of the Prudhoe Bay-Kuparuk River area in northern Alaska are the most studied gas-hydrate accumulations in the world and the focus of our cooperative research efforts. The production history of the Messoyakha field has demonstrated that gas hydrates are an immediate producible source of natural gas and that production can be started and maintained by conventional methods. Geologic similarities between the Messoyakha and Prudhoe Bay-Kuparuk River gas-hydrate accumulations further suggest that the Alaskan gas hydrates may also be a producible source of natural gas.

The Messoyakha field, discovered in 1968, was the first producing field in the northern part of the West Siberian basin. Gas yields from the upper part of the Messoyakha reservoir were unusually low, and analyses of production data suggested the presence of natural-occurring gas hydrates. Subsequent analyses of available temperature data and well logs confirmed the presence of gas hydrates in the upper part of the Messoyakha reservoir, thus separating the Messoyakha field into an upper, gas-hydrate, and lower, free-gas accumulation. Long-term production from the gas-hydrate part of the Messoyakha field has been achieved by a simple depressurization scheme. As production began in 1969, the reservoir pressures followed predicted values. However, by 1971 the measured reservoir pressures began to deviate from predicted values, a deviation which has been attributed to the liberation of free-gas from dissociating gas hydrates. Soviet researchers have estimated that about 36 percent (≈ 183 billion cubic feet) of the gas withdrawn from the Messoyakha field has come from the gas hydrates.

Both the Messoyakha and Prudhoe Bay-Kuparuk River gas-hydrate accumulations occur in similar sequences of interbedded Cretaceous and Tertiary sandstone and siltstone reservoir rocks. Geochemical

analyses suggest that the gas hydrates of the Messoyakha and Prudhoe Bay-Kuparuk River fields are almost identical in composition, and they have been interpreted to contain a mixture of thermogenic methane that migrated from deep, mature sources and in-place, microbial methane. These similarities suggest that the origins of the two accumulations may be similar. The presence of a significant volume of free-gas trapped below both the Messoyakha and Prudhoe Bay-Kuparuk River gas-hydrate occurrences is very important to the consideration of potential production characteristics of gas hydrates in Alaska. Utilization of the gas-hydrate depressurization method of production requires that a portion of the accumulation be in a free-gas state. Therefore, the presence of free-gas below the Prudhoe Bay-Kuparuk River gas hydrates suggests that the depressurization production scheme utilized in the Messoyakha field may work in northern Alaska.

The most striking difference between the Messoyakha and Prudhoe Bay gas-hydrate/free-gas occurrences is the size of the accumulations. The total mapped area of the gas-hydrate occurrences in the Prudhoe Bay-Kuparuk River area is ≈ 650 mi², whereas the Messoyakha field covers an area of only ≈ 90 mi². This difference in field size accounts for the vast difference in the estimated gas volumes in the Messoyakha (2.8 trillion cubic feet) versus Prudhoe Bay-Kuparuk River (44 trillion cubic feet) gas-hydrate accumulations, which suggests that the ultimate production capacity of the Prudhoe Bay-Kuparuk River gas-hydrate occurrences may be much greater than the historical production from the Messoyakha field.

Tar Sands and Heavy Oils— Resources, Recovery, and Realism

B.L. Crysdale, C.J. Schenk, and R.F. Meyer

Resources.—Bitumen (tar-sand) and heavy-oil deposits represent a significant energy resource in the United States. The total bitumen resource for the United States is estimated to be 57 billion bbl. Utah has the largest resource, an estimated 29 billion bbl, followed by California with 9 billion bbl, Alabama with 6 billion, Texas with 5 billion, and Kentucky with 3 billion.

California leads the United States in the amount of heavy-oil resources in place, with 42 billion bbl, followed by Alaska with 25 billion bbl (although some estimates put Alaska's heavy-oil resources as high as 50 billion bbl). Wyoming has 5 billion bbl, and Texas, Arkansas, and Louisiana each have 2 billion, for a total U.S. heavy-oil resource estimate of 80–100 billion bbl.

Recovery.—Bitumens ($<10^\circ$ API gravity) and heavy oil (10° – 20° API gravity) have high viscosities (100–10,000 cP (centipoises) for heavy oil; $>10,000$ cP for bitumens) and cannot be recovered using conventional methods. The current technology for recovering these hydrocarbons involves thermal stimulation of reservoirs (generally steaming) to provide heat to the oil, which reduces the viscosity and allows the oil to be mobilized and thus recovered. Few tar sands, if any, are currently being exploited in the United States, except for road-surfacing material.

Of the estimated 80–100 billion bbl of heavy-oil resources in place in the United States, approximately one-half is not economically recoverable using current technologies. The difficulty in recovering heavy oil is exemplified by the Santa Rosa Sandstone in northeast New Mexico, estimated to contain 95 million barrels of 15° API gravity oil. Two steamflood projects were initiated, but only 365 barrels were ever produced.

Realism.—Nearly all of today's economically recoverable heavy oil is in California, and is being utilized now. Seventy percent of California's present daily oil production is heavy oil. Production of light oil peaked in California in 1954, and more heavy oil than light oil has been produced there since 1972. Recovering Alaska's heavy oil is problematic due to transportation and environmental problems.

Unless the economic market changes dramatically, the future of tar sands as a viable resource is marginal at best. However, new techniques or refinement of present ones that make the recovery of high-viscosity oils possible, such as fireflood or emulsion technology, may unlock some of the presently unavailable oil.

Evidence for Petroleum-Assisted Speleogenesis, Lechuguilla Cave, Carlsbad Caverns National Park, New Mexico

K.I. Cunningham and K.I. Takahashi

Limited sulfur isotope, mineralogic, and cave morphogenetic data suggest that speleogenesis (cavern development) in the Guadalupe Mountains of New Mexico and Texas was the result of solution via sulfuric acid derived from H_2S gas. The cave-bearing reef complex is adjacent to many oil and gas fields, and numerous gas migration routes into the reef complex are plausible. Cave gypsum and elemental sulfur isotopic values as light as -25.8 parts per mil (referenced to the Canyon Diablo Troilite) link these cave deposits to H_2S -bearing gas deposits. Uncommon cave deposits of pH-dependent minerals like 10 Å halloysite (endellite)

indicate strongly acidic (pH = 1–2) conditions consistent with the sulfuric acid hypothesis. Blind passages, passages dying with depth, and long (300–1,000 meters) horizontal passage extents have also been cited as evidence that the majority of solution occurred at a lowering water table where H_2S and atmospheric oxygen mixed to produce sulfuric acid. Whether or not the main acid-producing reaction occurred at the water table, in the mixing zone between fresh water and brines, or deeper in the system is debatable, and important to carbonate dissolution mechanisms. With the 1986 discovery and subsequent aggressive exploration of Lechuguilla Cave, we have recently been provided with additional data from a uniquely preserved 100+ kilometer long cave and the only Guadalupian cave to penetrate to the apparent water table.

Most caves in the Guadalupe Mountains, including Carlsbad Cavern, have been extensively invaded by seep water, resulting in the appreciable loss of massive and speleothemic gypsum. Sulfuric-acid-stage elemental sulfur is very rare: one small deposit is documented at Cottonwood Cave where oxidation has apparently slowed due to limited air exchange or other unknown factors. In contrast, Lechuguilla may contain more preserved gypsum and sulfuric-acid-stage sulfur than all other known caves in the Guadalupe combined: a laterally extensive siltstone caprock has apparently diverted most recent water away from the cave, such that occurrences of flowstone and other calcitic speleothems are highly contained and localized. Massive, chemically precipitated gypsum deposits and fragile, secondary speleothems begin near the entrance and extend to within 175 meters of the water table, an overall vertical distance of nearly 290 meters. The gypsum deposits are up to 10 meters thick in large rooms, occasionally fill passages, and sometimes occur on steep slopes and balconies on the sides of vertical shafts. Replacement textures have been noted in some blocks, but most accumulations appear to be the result of chemical precipitation or oxidation of early-formed sulfur masses. Elemental sulfur occurs as multi-ton, massive, vuggy, or encrusting deposits at diverse vertical levels in the cave. The remarkable preservation of the deposits (in contrast with other Guadalupe caves) suggests that oxygen availability in Lechuguilla has been very limited after drainage. The sulfur is slowly oxidizing to gypsum and liberating CO_2 and SO_2 into the humid cave atmosphere. This mixture ascends convectively to the higher sections of the cave where modern solution of the carbonate bedrock occurs. Sulfur and gypsum isotopic compositions are light: average $\delta^{34}S$ values for the main Lechuguilla sulfur deposits are -23.29 , and -25.55 for selenite from the Chandelier Ballroom. That inclusions in the sulfur contain a gas phase and both saline and fresh water strongly suggests that the deposits formed in the fresh

water–saline water mixing zone at temperatures < 50 °C. The morphology of Lechuguilla passageways further supports a model where upwardly circulating H₂S-rich saline water in joints and fractures encounters fresh, oxygen-rich water, resulting in greater-than-normal vertical solution above these leak points (vertical mazes). Zones of intensely dissolved and occasionally mineralized reef limestone (“todo corrodo” zones) are often associated with the bottom of these vertical mazes and are linked to underlying fissures that penetrate downward to the current water table. The structural attitude of these deep fissures is commonly dipping toward the back-reef beds (not into the basin) and may reflect a preferred ascending flow component in the system.

This information is presented at the 1992 Mc-Kelvey Forum in an expanded visual form as a sequence of text, charts, and photographic images running on an Apple Macintosh IIfx computer.

Cretaceous Resources, Events, and Rhythms—Continental Scientific Drilling Transect of the Western Interior Seaway

Walter E. Dean and Michael A. Arthur

Some of Earth's largest existing phosphorite deposits and hydrocarbon reserves were produced through combinations of processes of tectonism, volcanism, atmospheric and ocean chemistry, climate, eustasy, and sediment supply during Cretaceous time. In addition, major reserves of coal, kaolinite, bauxite, bentonite, and manganese lie in Cretaceous rocks. To predict and understand the availability and distribution of these resources requires models based on a comprehensive knowledge of the Cretaceous world. Because the Cretaceous Period was long (approx. 136–66 Ma) and left extremely widespread continental and marine strata in outcrop, subcrop, and ocean basins, its rock record provides important opportunities for understanding global processes and their variation.

The Cretaceous Western Interior seaway was a northwest arm of the Tethys Ocean that extended from the present Gulf of Mexico to the Arctic Ocean, during its maximum transgressions. Owing to its restricted geographic location and latitudinal extent, the seaway was in a strategic position to record changes in climate, sea level, and ocean circulation. Consequently, the strata deposited in the seaway monitor global climatic change during the Cretaceous; they present complex problems of paleoclimate, paleoceanography, and sediment flux; they exhibit well-developed solar-terrestrial orbital (Milankovitch) cycles; and they crop out in striking transgressive-regressive cyclic sequences.

As part of this comprehensive project, scientists of the USGS and several academic institutions proposed a multidisciplinary study of Lower and Upper Cretaceous marine carbonate and terrigenous clastic rocks in cores from four holes or groups of holes in a transect from western Kansas to eastern Utah across the former seaway. Drilling and related activities form part of the U.S. Continental Scientific Drilling Program, coordinated by the USGS, National Science Foundation, and Department of Energy. The study will focus on, from oldest to youngest, the Upper Cretaceous Graneros Shale, Greenhorn Limestone, Carlile Shale, Niobrara Formation, and lower part of the Pierre Shale. The rocks range from pelagic carbonates that contain organic-carbon-rich marine source rocks at the east end of the transect to nearshore coal-bearing units at the west end. Drill core will provide unweathered samples and the continuous smooth sequences required for studies in inorganic, organic and stable-isotopic geochemistry, mineralogy, and biostratigraphy, as well as thermal maturation and the migration of hydrocarbons along a burial gradient in organic-carbon-rich strata. Existing cores will be used where available, but some new holes will need to be drilled; the first phase of new drilling began in June 1991.

The USGS Core Research Center in Denver has several cores from western Kansas and northeastern Colorado that will meet the objectives of study of the east (most pelagic marine) end of the transect; no new drilling is planned for this end of the transect. The USGS obtained three cores from the west end of the transect (Phase 1 of new drilling), in the Kaiparowits basin near Escalante, Utah, in June 1991. Two of these cores contain coal-bearing sequences of the middle Turonian to lower Campanian Straight Cliffs Formation, of which the John Henry Member is nearly the same age as the Niobrara Formation in eastern Colorado. The third core contains all of the marine Tropic Shale that is the approximate age equivalent (Cenomanian and Turonian) of the Greenhorn Limestone and Graneros Shale in eastern Colorado and western Kansas. Geophysical logs have been obtained for all three holes.

The USGS Core Research Center also holds two cores of rocks equivalent in age in part to the Niobrara Formation and Pierre Shale, from the Mesaverde Group of the northern San Juan Basin on the Southern Ute Indian Reservation. The underlying Mancos Shale, which is the approximate age equivalent to the Graneros Shale, Greenhorn Limestone, and Carlile Shale, is scheduled for coring in the northern San Juan Basin near Durango, Colo., during Phase 2 of drilling in 1992. Another core hole to be drilled during Phase 2, in the vicinity of Florence and Cañon City, Colo., is to be located on the Brush Hollow anticline east of the Florence oil field, the oldest oil field in the United States. One aim of this drill

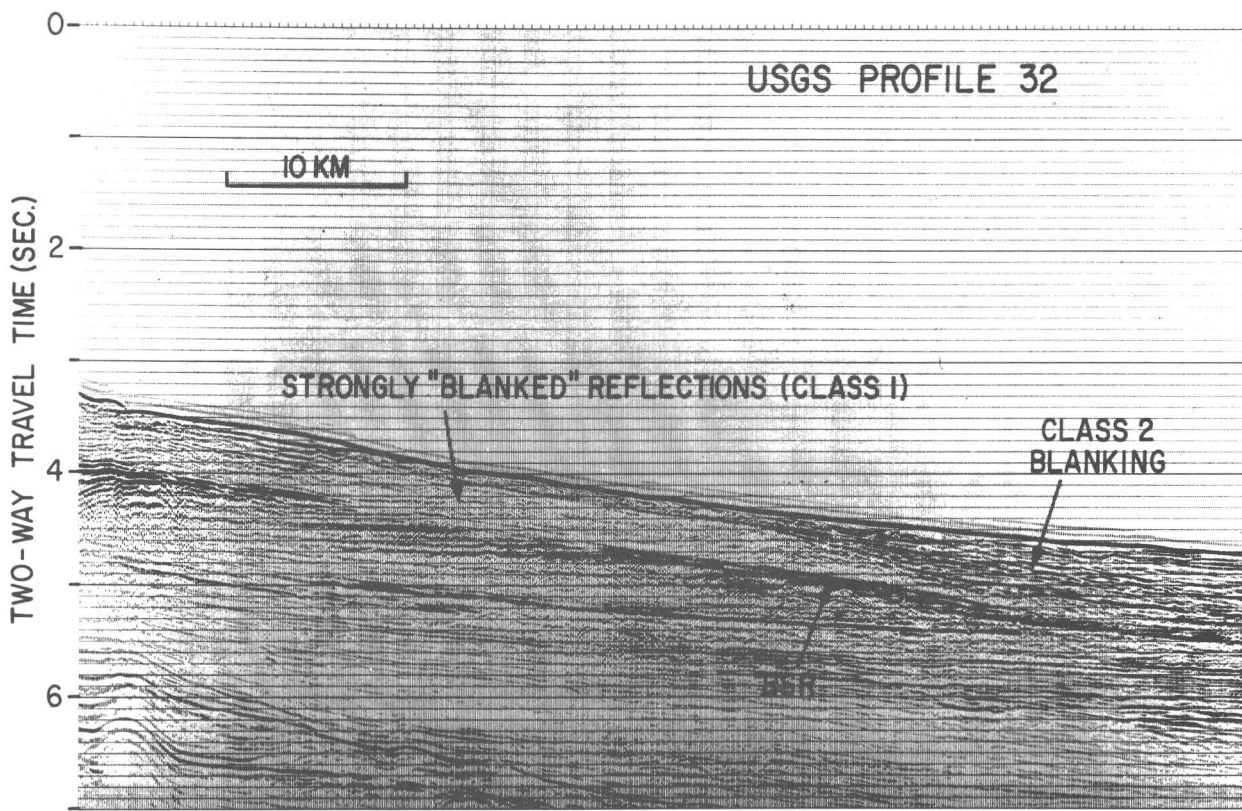


Figure 1 (Dillon and others). Part of seismic reflection profile from the continental rise off North Carolina, showing examples of seismic blanking caused by gas-hydrate cementation and the bottom simulating reflection (BSR) that marks the location of the base of the gas-hydrate stable zone. Location of this profile is shown on inset map of figure 2.

hole will be to obtain core of probable source rocks for the Florence field oil, which will be useful for determining trends of organic richness and thermal maturation. The sedimentary sequence to be recovered from this drill hole, deposited in relatively deep water on the west side of the Western Interior seaway, will include cycles of terrigenous-clastic and pelagic-marine sediments that will contrast with the pelagic carbonate-dominated cycles of Kansas and the clastic-dominated cycles of western Colorado and Utah.

Gas Hydrates in Deep Ocean Sediments Offshore Southeastern United States—A Future Resource?

William P. Dillon, Richard F. Mast,
Kristen Fehlhaber, and Myung W. Lee

Gas hydrates hold immense amounts of methane in deep-sea marine sediments worldwide (they also bind methane in onshore and shallow-water offshore deposits

in Arctic regions; see abstract by T. Collett, this volume). A gas hydrate is a crystalline solid, which is formed of a gas molecule surrounded by a cage of water molecules, stabilized by hydrogen bonding; such material occurs at the temperatures and pressures that exist in oceanic sediments. Although marine gas hydrates have the disadvantage of being located in relatively deep water (several hundred to a few thousand meters depth—approximately 1,000 to 12,000 feet), they occur at very shallow drilling depths and may be located in energy-poor regions and at relatively short distances from significant markets. We are examining a region of the continental rise off North and South Carolina where the existence of gas hydrate has long been known. Our purpose is to identify unusual concentrations of gas hydrate and determine the geologic, physical, and chemical factors that control these accumulations.

We are using their characteristic acoustic signatures in seismic reflection profiles to map concentrations of gas hydrates. Formation of hydrate in the pore space causes significant changes in acoustic characteristics because gas hydrate has a high

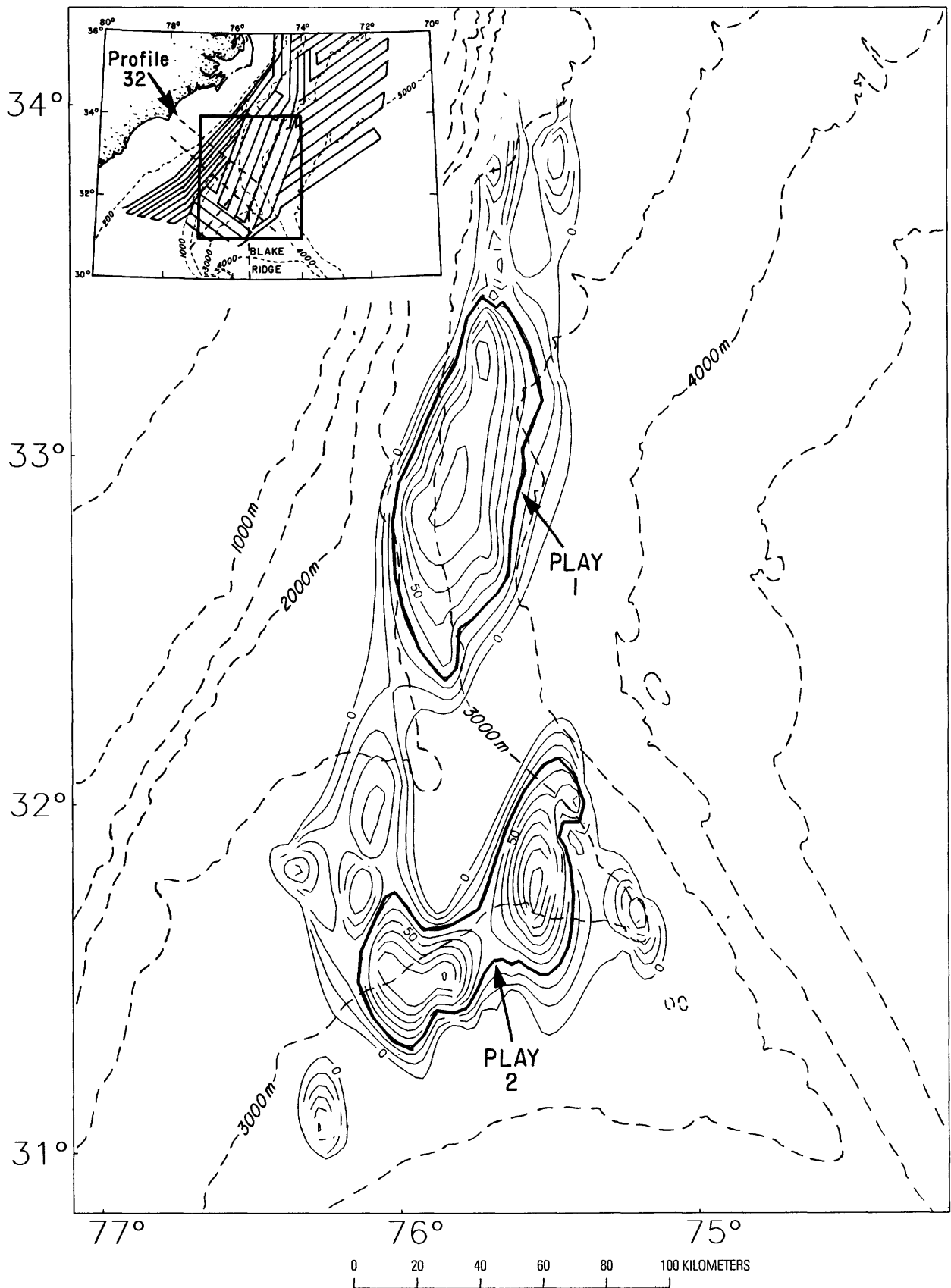


Figure 2 (Dillon and others). Contours of inferred thickness of pure gas hydrate within Class 1 deposits in the study area. The two plays were chosen where the amount of pure gas hydrate in Class 1 deposits exceeded 30 m. Inset map shows location of the larger scale map relative to the coasts of North and South Carolina, as well as track coverage.

compressional wave velocity compared to sediments. Velocity of the sediments is increased, and cementation of sedimentary strata by gas hydrate also has the effect of reducing the amplitude of reflections from stratal boundaries in seismic profiles (known as “blanking” of reflections). We have used seismic modeling to estimate the amount of hydrate that would cause various amounts of blanking, and have chosen three classes of blanking that we believe represent predictable ranges of gas-hydrate admixture into sedimentary pore space (fig. 1). Distribution of these classes has been mapped in the study area and used to estimate volume of hydrate (see abstract by K. Fehlhaber and others, this volume).

The thickness of the layer of hydrate is described by mapping the distance from the sea floor to a reflection horizon that is caused by the change from higher velocity above to lower velocity below. This reflection follows the phase boundary conditions for gas-hydrate stability, that is, hydrate is stable above, and unstable below that boundary because of increasing temperature with depth. Because this reflection approximately parallels the sea floor, it is known as the Bottom Simulating Reflection, or BSR (fig. 1). It had been believed that the zone of hydrate stability (sea floor to BSR) would increase consistently as water deepened, based on the assumptions of steady-state conditions, uniform thermal gradient, and a pressure value dependent only on water depth. Mapping shows that this is not the case, and that great variations occur in thickness of the gas hydrate-stable zone, unrelated to water depth.

Considerable variation also exists in concentration of hydrate within the stable zone, which we have described by mapping calculated thickness of pure hydrate across the study area. The three blanking classes display varying patterns of hydrate distribution. In the class having lowest concentration (Class 3), in which hydrates occupy about 2 percent of the sediment volume, hydrate is distributed nearly uniformly across the study area. Conversely, in the highest-concentration class (Class 1), in which hydrate occupies about 8 percent (to as much as 14 percent) of the sediment volume, the hydrate is strongly concentrated at two locations (fig. 2). These two locations also represent high concentrations of hydrate when the amounts contributed by the three classes are totaled, and they will be treated as plays for this report. The high-concentration areas are defined as the area surrounded by the 30-m contour of Class 1 hydrate (fig. 2).

Play 1.—This area occurs at the head of a very large landslide and near a trend of diapirs that follow the seaward side of the Carolina Trough, one of the four principal continental-margin troughs of the Eastern U.S. continental margin. Possibly the concentration occurs because of increased sources of gas here. The gas might be thermogenic gas that rose from deeper sources along

fractures provided by the diapirism, or it might be biogenic gas that was released when the landslide occurred (probably in Pleistocene time). The landslide would have removed lithified sediment (lithified by hydrate cementation) and therefore would have lowered pressure on underlying hydrate, causing it to break down; the released gas might then have migrated updip within continental rise strata to nourish development of hydrates at shallower water depths.

Play 2.—This area is located on the crest of the Blake Ridge, a sedimentary drift deposit formed by relatively rapid deposition since Oligocene time. Gas hydrate might be concentrated here because the rapid deposition would have caused the sea floor to become shallower, which would be accompanied by upward migration of the sediment isotherms. This would cause breakdown of hydrate at the BSR, releasing free gas that would be available to nourish hydrate formation in the overlying sediments. The ridge shape of the accumulation could have aided this, as the concave-down shape of the BSR would create a trap, with hydrate-cemented sediment acting as a seal to retain the gas within the ridge. Velocity analyses imply that free gas is presently trapped beneath the BSR in the Blake Ridge.

Estimates of gas volumes for the two plays and for the total area were calculated using Monte Carlo simulator. Uncertainties in the volumes of hydrated sediment for each class and the porosity of the hydrated rock were accounted for. The resource estimates were made for only the lower one-half of the hydrated layer, which contains the higher concentration of hydrates. The results of the assessments of estimated gas volume are as follows:

ESTIMATED VOLUMES OF GAS

	Trillions of cubic meters			Trillions of cubic feet		
	F95	Mean	F5	F95	Mean	F5
Play 1	13	20	28	459	706	989
Play 2	12	18	25	424	636	883
Total area	88	117	144	3,108	4,132	5,085

(Note that fractile values (F95, F5) are not additive. F95 represents a 19 in 20 chance and F5 represents a 1 in 20 chance of the occurrence of at least the amount tabulated.)

The estimated mean volume of gas contained in the study area is 117 trillion cubic meters at a temperature of 15 °C and pressure of 1 bar. Estimates range between 88 and 144 trillion cubic meters. The gas is concentrated in the two play areas. Play 1 contains 19.4 percent of the gas in the study area but covers only 11.5 percent of the area; Play 2 contains 17 percent of the gas but covers only 9.4 percent of the area. Class 1-type deposits account for 94.2 percent of the gas in Play 1 and 88.2 percent in Play 2. These plays are in approximately 3,000 m (10,000 ft)

of water, ≈ 240 km (150 mi) from shore. The volume of gas contained in a cubic meter of Class 1 hydrated rock is estimated in this study to be 22.3 m^3 . Gas reservoirs onshore are estimated to hold about 17 m^3 of gas in place per cubic meter of rock.

At present, we know that very large amounts of gas are locked in gas hydrates in deep-sea sediments. Estimates of exactly how much exists at specific locations and analyses of the geological/geochemical controls, as suggested here, are speculative, but ideas are developing. The technology for extracting gas from gas-hydrate deposits surely is undeveloped; however, the amount of energy represented by such deposits is immense, so that continued study is imperative.

Undiscovered Oil and Gas Resources of Federal Lands and Waters

G.L. Dolton, R.F. Mast, and R.A. Crovelli

In 1987, the U.S. Geological Survey (USGS), in conjunction with the Minerals Management Service (MMS), completed an assessment of the undiscovered

conventional resources of crude oil and natural gas of the United States. The USGS was responsible for assessment of the onshore United States and adjoining State waters, and the MMS for the Outer Continental Shelf (OCS). Resources were: (1) those considered recoverable under current technology, and (2) those that could be developed and produced economically, once found, using an extrapolation of costs and prices prevailing at the time of assessment. Resources beneath Federal lands and waters were estimated as part of this assessment.

More than half of the Nation's estimated undiscovered recoverable conventional oil and gas resources are beneath Federal lands and waters. Approximately 87 percent of these estimated Federal recoverable resources are located in the OCS and Alaska, which areas also are estimated to have potential for very large hydrocarbon accumulations as opposed to the smaller estimated accumulation sizes in the onshore lower 48 States. These areas of large potential can have major impact on domestic supply, but they are also areas where long lead-times are required for development and where the economically recoverable portion of resources is significantly lower than the technically recoverable portion due to the high costs associated with operations.

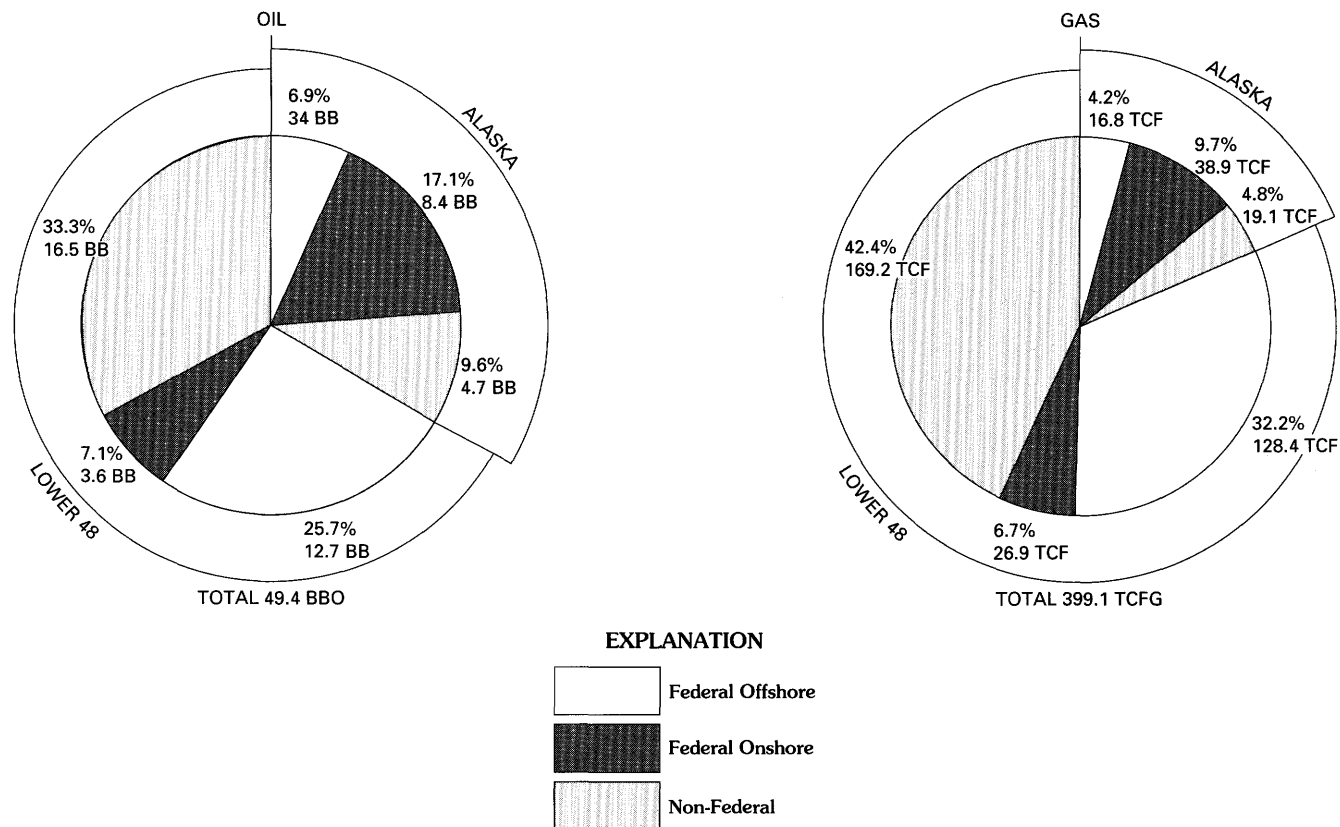


Figure 1 (Dolton and others). Distribution of undiscovered conventionally recoverable crude oil and natural gas resources in Alaska and the lower 48 States.

ESTIMATED UNDISCOVERED RESOURCES

[BBO, billion barrels of oil; TCFG, trillion cubic feet of gas]

	Recoverable			Economically recoverable		
	F95	Mean	F5	F95	Mean	F5
Onshore Federal						
Oil (BBO)	4.0	12.1	26.4	1.8	8.3	21.6
Gas (TCFG)	25.4	65.8	132.6	14.8	26.2	42.0
Offshore Federal						
Oil (BBO)	9.2	16.1	25.6	4.0	8.2	14.3
Gas (TCFG)	97.8	145.1	204.8	44.3	74.0	113.8
Total U.S. Resources						
Oil (BBO)	33.2	49.4	69.9	20.7	34.8	53.8
Gas (TCFG)	306.8	399.1	507.2	208.2	262.7	325.5

The geographic distribution of undiscovered conventionally recoverable crude oil and natural gas resources in Alaska and the lower 48 States is shown in figure 1, and the importance of Federally owned resources is readily apparent.

This assessment addresses only those undiscovered resources in oil and gas reservoirs that are amenable to production by conventional well-bore production techniques in use at the time of the assessment. The estimates of resources *do not* include intractable heavy oil deposits or tar deposits, oil shales, gas from fractured shale reservoirs or low-permeability "tight" gas sandstone reservoirs with in-place reservoir permeabilities to gas less than 0.1 mD (millidarcy), coalbed methane, gas in geopressured shales and brines, or gas hydrates (clathrates). These kinds of occurrences, which are treated as "unconventional" resources, are recognized as potentially important future sources of hydrocarbons, and some oil and gas is currently produced from them.

Two recent publications expand on the derivation of these estimates: a USGS/MMS publication, "Estimates of undiscovered conventional oil and gas resources in the United States—A part of the Nation's energy endowment," by R.F. Mast and others, 1989, and USGS Open-File Report 90-705, "Estimates of undiscovered conventional resources of oil and gas for Federal lands, and for Indian and Native lands of the continental United States," by G.L. Dolton and others, 1990.

Field Growth in the Gulf of Mexico— A Progress Report

Lawrence J. Drew and Gary L. Lore

The idea that oil and gas fields grow in size throughout their productive lives dates from at least the

time of World War II, as reported in a 1960 study by J.R. Arrington. However, field growth is not a concept that has gained universal acceptance as a long-term stable process. Before we can say that we understand the phenomenon of field growth in the United States or elsewhere in the world, certain problems need to be solved, whose solutions require that tedious tasks be completed in data collection and data file construction at the field level. We need to determine the relationships among the mortality of fields, their size, and their economic setting and to resolve several philosophical issues that bear on the assumptions needed to structure a forecast that can predict how fields will grow in the future.

In this study we report progress made in the analysis of the growth of oil and gas fields discovered between 1947 and 1987 on the Federal portion of the Gulf of Mexico Outer Continental Shelf (OCS). The field level data, taken from the Field and Reservoir Reserves Estimates file maintained by the New Orleans office of the U. S. Minerals Management Service (MMS), are available only from 1975 onward: Thus, the growth of all fields across all years cannot be examined. For example, data do not exist to compute a growth rate for 5-year-old fields in 1960 or 1970. Data can only be extracted from the time window 1975-onward to estimate field growth and mortality as a function of field size and type (salt dome versus non-salt dome fields).

In the Gulf of Mexico OCS the annual growth rates for all oil and gas fields range from about 10 percent per year during the first decade of productive life to around 5 percent during the second decade and about 3 percent during the third decade (fig. 1A). The fields that have been producing more than 30 years continued to grow in the fourth decade of their productive life at rates of about 2 percent per year (fig. 1A). The high variability in the growth rate profile covering the 38th through the 41st year of life of the fields in the Gulf of Mexico OCS is caused by individual changes in the estimates of the ultimate productivity in the very few fields that reach this age (1 to 3 fields) (fig. 1A).

The annual growth rate for small fields is typified by the scatterplot shown in figure 1B for fields in the 3.04 to 6.07 million barrels of oil equivalent (BOE) size range. This panel shows that the variability from year to year is high, and no fields of this size have produced for more than 19 years. Either they migrated (grew) into a larger field size class or they were abandoned before the 20th year of their productive life.

The mortality of fields in the Gulf of Mexico OCS is shown in table 1: 69 of the 750 total fields discovered between 1947 and 1987 have been exhausted and the leases returned to the Federal Government. The size of the most frequently abandoned field is in the 3.04 to 6.07 million BOE size class with 15 fields having been abandoned by the end of 1988.

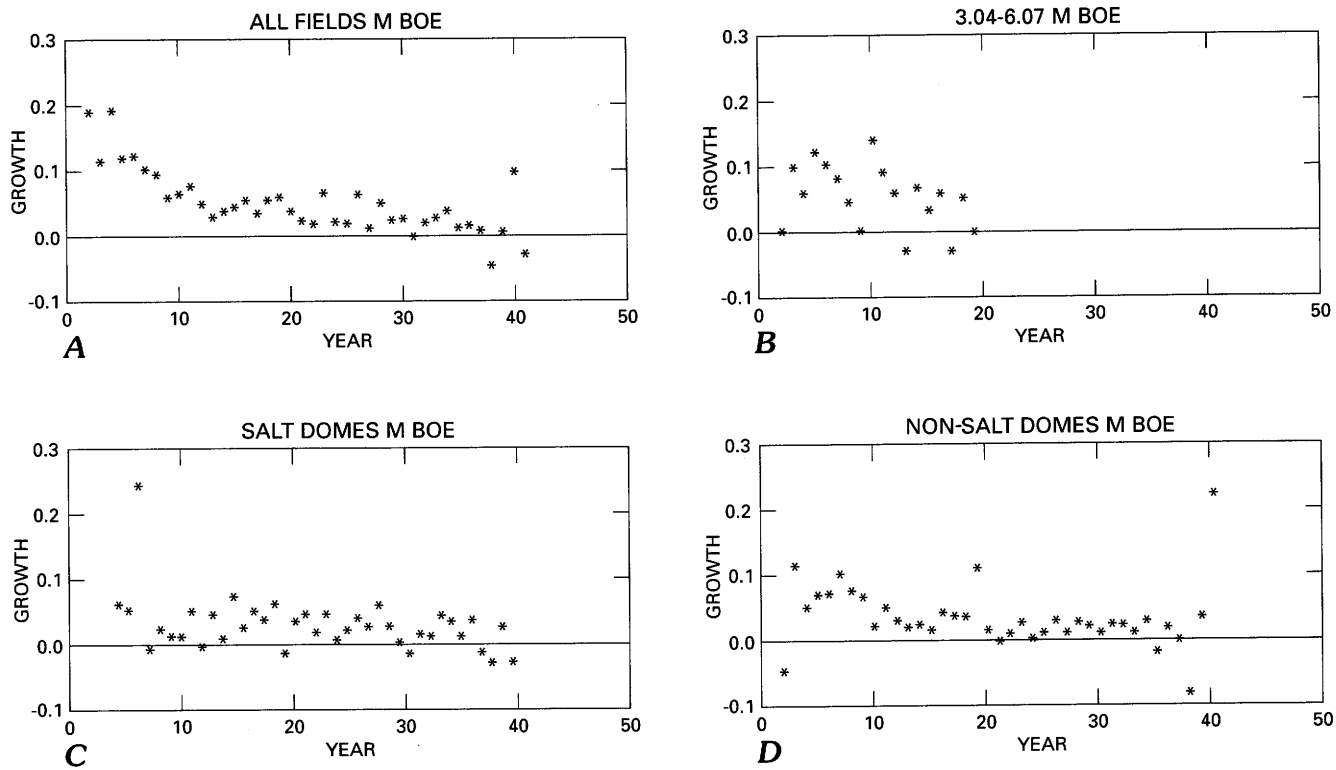


Figure 1 (Drew and Lore). Growth profiles for four classes of oil and gas fields in the Gulf of Mexico OCS. BOE, barrels of oil equivalent. Growth is a proportion; for example, 0.1 equates to 10 percent growth rate per year. *A*, all fields; *B*, small fields; *C*, salt domes; *D*, non-salt domes.

Another aspect of the problem of understanding the dimensions of field growth is determining whether fields with different geologic and engineering characteristics have different rates of growth and mortality. Salt domes with their numerous and disparate reservoirs are widely believed to have higher overall growth rates and longer productive lives (lower mortality). Our total data set of 750 fields was separated into subsets, and the growth rates for salt domes versus non-salt domes were computed. (Compare fig. 1C and 1D.) The rate of growth in the estimated ultimate productivity of the non-salt dome fields is higher during the first 10 years of productive life than for the salt dome fields. Subsequently the salt dome fields have a higher and more variable rate of growth than the non-salt dome fields.

Analyses by a USGS-MMS team are in progress to isolate the structural elements in field growth data, so that a statistical model can be constructed to predict the ultimate productivity within field size classes. These predictions will be used to estimate the volume of crude oil and natural gas forthcoming from the growth of previously discovered fields and to adjust field size data used in discovery process models to forecast future rates of discovery of fields and their associated volumes by size class.

Table 1 (Drew and Lore). Mortality table for oil and gas fields in the Gulf of Mexico OCS

[Leaders (-), not applicable]

Size class	Size range 10^6 BOE	No. fields in range	Avg. life	Min yr	Max yr	Previous class
3	0.01-0.02	1	9	—	9	1-10
4	0.02-0.05	1	3	—	3	1-8
5	0.05-0.10	2	7	3	10	2-10
6	0.10-0.19	1	9	—	9	1-9
7	0.19-0.38	7	8	3	16	1-7; 2-8; 2-9; 1-10; 1-13
8	0.38-0.76	7	9	4	16	2-8; 3-9; 1-10; 1-12
9	0.76-1.52	13	9	5	16	3-9; 3-10; 4-11; 3-12
10	1.52-3.04	12	11	4	16	4-10; 6-11; 2-12
11	3.04-6.07	15	13	7	21	4-11; 8-12; 3-13
12	6.07-12.14	8	14	6	30	6-12; 1-13; 1-14
13	12.14-24.3	0	—	—	—	—
14	24.3-48.6	1	20	—	20	1-14
15	48.6-97.2	1	13	—	13	1-15

Fluvial Architecture and Reservoir Heterogeneity—Triassic and Tertiary Examples from the Colorado Plateau

Russell F. Dubiel, Steven C. Good, and Christopher J. Schenk

Reservoir heterogeneity is an important aspect of petroleum geology because internal permeability barriers at several scales may impede the recovery of hydrocarbons from sandstone reservoirs. Modeling of fluvial sandstone reservoirs can be improved over vertical profile analysis by incorporating data on three-dimensional sandbody architecture and the geometry and extent of bounding surfaces, which are commonly delineated by impermeable facies. Fluvial sandstone reservoirs present acute challenges to reservoir modeling because they are formed by dynamic alluvial systems that produce numerous lateral facies changes and because preservation is determined by a complicated interplay between sediment accumulation rates and the rate of basin subsidence. Fluvial reservoirs are rarely tabular, they have complex internal geometry, and they vary widely in size within individual fluvial systems.

We report preliminary data from outcrop examples of two low- to moderate-sinuosity fluvial sequences on the Colorado Plateau that contain sandbodies with complex three-dimensional internal geometry. Examples are from ribbon and sheet sandbodies of the Upper Triassic Chinle Formation in southeastern Utah and ribbon sandbodies of the lower to middle Eocene Wasatch Formation in western Colorado. In the study of each sequence, photomosaics of the outcrops were constructed in order to map and measure dimensions of individual depositional elements. We emphasized recognition of intermediate-scale third- and fourth-order bounding surfaces because they form the large-scale permeability barriers that significantly affect hydrocarbon migration in fluvial reservoirs. Smaller scale heterogeneities that delineate bedforms and sedimentary structures were not examined in detail, although we recognize that these small-scale features, along with inhomogeneities produced by diagenesis and bioturbation, are crucial for studies of individual fields.

The Chinle Formation along White Canyon in San Juan County, southeastern Utah, contains three units deposited primarily by fluvial processes: the Shinarump, Moss Back, and Petrified Forest Members. The Shinarump and Petrified Forest fluvial systems deposited small ribbon sandbodies (5–15 m thick and 30–100 m wide), whereas the Moss Back fluvial system produced large sheet sandbodies (20–30 m thick, and 300–1,000 m or more wide). Despite these large-scale differences in sandbody dimensions, each of the three fluvial systems is

composed internally of large-scale lateral accretion stratification (LAS) elements produced by migration of point bars in low- to moderate-sinuosity streams. Among the Chinle fluvial systems, the LAS elements vary in thickness and width corresponding to the overall size of the sandbodies. Shinarump and Petrified Forest LAS elements are from 2 to 3 m thick and 5 to 10 m wide, whereas Moss Back LAS elements are from 10 to 20 m thick and about 100 m wide. Within each sandbody, point bar components are complexly stacked to produce a three-dimensional point bar mosaic. In the Shinarump and Petrified Forest Members, sandbodies can be traced as far as 1 km, and in the Moss Back Member, they can be traced as far as 10 km; however, in each sandbody, LAS elements are generally no longer than 2 to 3 times their width.

The Shire Member of the Wasatch Formation in the Piceance basin of western Colorado is well exposed in outcrops north of Interstate 70 from Rifle west to DeBeque. Fluvial systems deposited ribbon sandbodies 5–15 m thick and 30–100 m wide that are encased by floodplain sandstones and mudstones. The Wasatch ribbon sandbodies mainly consist of LAS elements. The LAS elements are 3–5 m thick and 15–30 m wide and, like the Chinle examples, are vertically and laterally amalgamated to form three-dimensional point bar mosaics. Sandbodies can be traced as far as 0.5 km, but LAS elements are no longer than 2 to 3 times their width.

Fluvial sandstones in the Wasatch Formation similar to those studied here produce gas farther north of this study area at White River dome in the Piceance basin, and although the Chinle sandstones described herein are not known to produce hydrocarbons, they provide comparative data and contribute to the evaluation of the variability of sandbody architecture in sinuous fluvial systems dominated by point bar deposition. These examples provide an initial data base on the different scales of point bar deposits, the three-dimensional complexity of point bar sandbodies, and their potential effect on fluvial reservoir heterogeneity.

Origin of the Challenger Knoll Oil, Gulf of Mexico

N. Terence Edgar and Jerry L. Clayton

DSDP Site 2, located in the Sigsbee abyssal plain, central Gulf of Mexico, was drilled into Challenger Knoll, a topographic high (3,572 m water depth) that is underlain by cap rock and a salt diapir (fig. 1). Oil recovered from the cap rock (cores 5 and 6) was described as being a young immature oil of low gravity

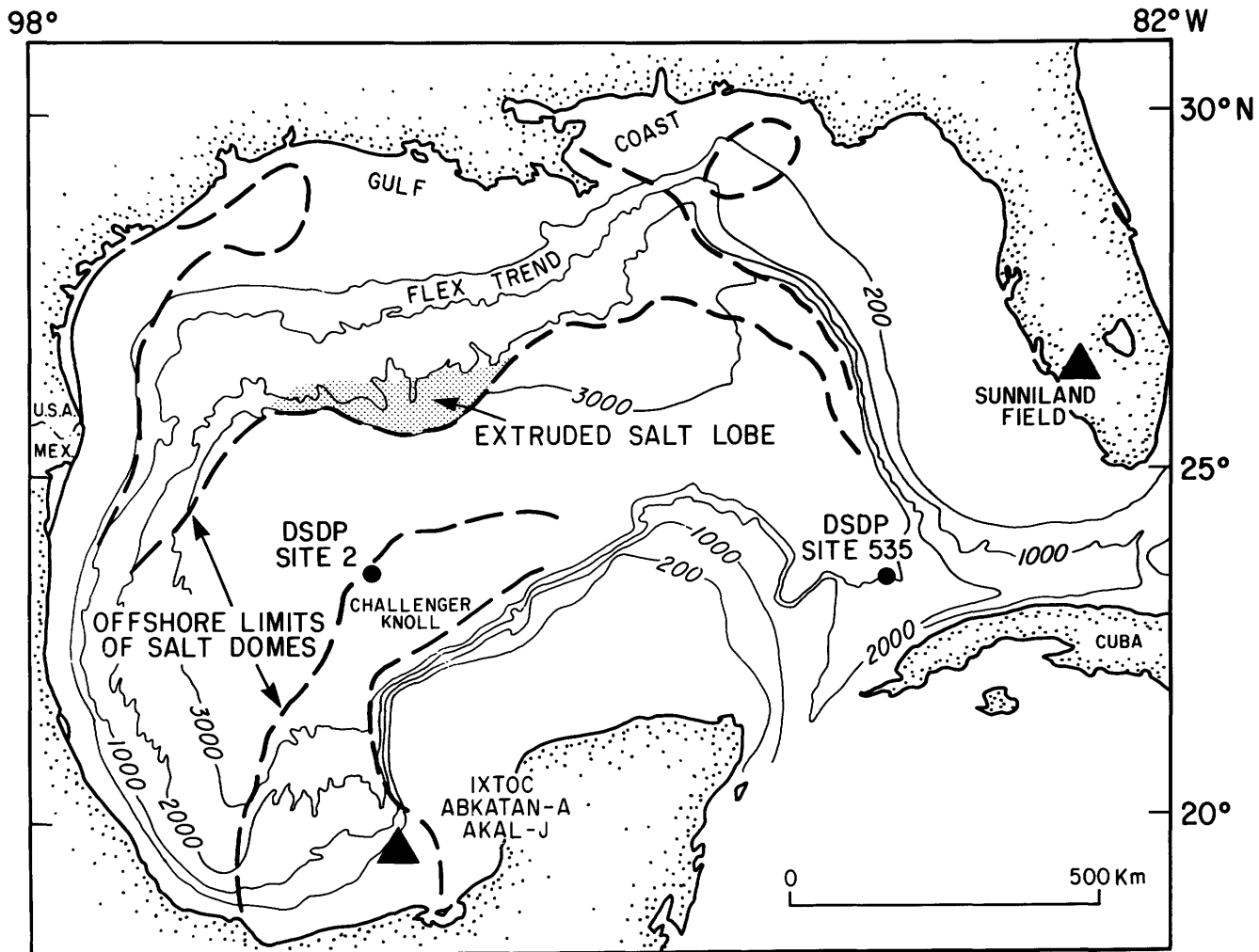


Figure 1 (Edgar and Clayton). Map of the Gulf of Mexico showing the locality of oil samples discussed. Bathymetric contours in meters.

and high sulfur content and (from analysis of it by J.B. Davis and E.E. Bray published in 1969) is similar to Gulf Coast Tertiary oils recovered from cap rock elsewhere. Since these analyses were conducted, analyses of oils from deep-water sites on the continental shelf edge and slope (Flex trend), from the Campeche shelf of Mexico, from DSDP Site 535 in the eastern Gulf of Mexico, and from the Lower Cretaceous Sunniland Limestone of south Florida have become available. In a 1986 study, J.A. Nunn and Roger Sassen suggested the Flex trend oils to be derived from Cretaceous and lower Tertiary sedimentary rocks. In 1990, K.F.M. Thompson and others concluded that deep-water Gulf Coast oils (Thompson's type 1b) are similar enough to Mexico, Challenger Knoll, and DSDP Site 535 oils to represent a single broad superfamily and that no compelling reason exists to reject the hypothesis that all these oils are derived from the same or similar source facies.

To further elucidate the origin of the Challenger Knoll oil, we determined the polycyclic biomarker composition of the Challenger Knoll oil and three oils produced from Mexico (Ixtoc, Abkatun-A, and Akal-J wells; fig. 1) using coupled gas chromatography-mass spectrometry. We determined the sterane (m/z 217) and terpane (m/z 191) distributions on whole-oil samples. We report the following results (bold type), with comments on each:

1. All three Mexico oils are characterized by low pristane:phytane ratios; pr:ph averages 0.75, which compares closely with the value of 0.74 reported in a 1969 study by Bruce Koons and P.H. Monaghan for the Challenger Knoll oil. The pr:ph is a useful oil-oil correlation parameter, and to a lesser degree, an indicator of depositional environment. This ratio differs from those of the Tertiary Gulf Coast oils, which are > 1.0 .

2. Two of the Mexico oils (Abkatun and Akal-J) have a slight predominance of long-chain *n*-alkanes containing even numbers of carbon atoms. Oils from the Gulf Coast Flex trend typically have no predominance or a slight odd-carbon predominance. This subtle but important level of predominance indicates modest to high levels of thermal maturity; even- or odd-carbon predominances diminish irreversibly with increasing thermal maturation but cannot switch from one to the other. Even-carbon preferences are common in oils generated from carbonate and carbonate-evaporite source rocks deposited under strongly reducing conditions. These even-, odd-carbon values suggest that the Mexico and Gulf Coast oils came from different types of source rocks.

3. Oleanane is absent in the Challenger Knoll sample. Oleanane, a pentacyclic compound, is common in Tertiary Gulf Coast oils but not reported in samples older than Late Cretaceous. Its absence does not restrict the source rock to Late Cretaceous or younger age; its presence would have.

4. Terpane distributions in the Challenger Knoll oil are fairly typical of thermally mature oils, but the C₃₅ hopanes are slightly elevated with respect to C₃₄ hopanes. An elevated C₃₅ hopane value is common in oils generated from carbonate-evaporite source rocks, but the differential commonly is more pronounced than in these samples.

5. Sterane distributions (m/z 217) show consistent differences between Challenger Knoll oil and Mexico oils in the relative amounts of 24-ethylcholestanes compared to the other steranes, and in the ratio of 20S:20R diastereomers of 24-ethylcholestane ($\alpha\alpha\alpha$ configuration). The Mexico oils contain more diasteranes. These differences in sterane distributions are unexplained but may be the result of low thermal maturity of the Challenger Knoll oil.

6. Whole-oil stable carbon isotope ratios for the Challenger Knoll and Mexico oils fall within the range of values of Group 1B (Flex trend) oils, but Challenger Knoll oil is slightly heavier than the Mexico oils. The differences between saturates and aromatics (1.12‰ and 0.67‰, respectively) are greatest between the Challenger Knoll and the Mexico oils. The isotopic differences among the Challenger, Mexico, and Group 1B samples are not sufficiently great to discount a common source, because the range of values for oils of common origin in general is greater than observed here.

Individually, these results are not definitive, but combined they lead us to the following conclusions:

1. Our data are consistent with Thompson and others' 1990 hypothesis that the oils from the Flex trend, the Campeche shelf, and west Florida may be derived from the same or similar source facies.

2. The Challenger Knoll oil appears to be derived from a Mesozoic source rock, based on the absence of oleanane, on evidence for a carbonate-evaporite source, and on its high organic sulfur content. High sulfur content indicates a carbonate-evaporite source rock, whereas low sulfur content (generally <0.5 percent but as much as 1.5 percent) is characteristic of Tertiary oils derived from siliciclastic sediments of the northern Gulf Coast. During the Mesozoic, sedimentation in the Gulf of Mexico was primarily carbonates and evaporites, whereas during the Cenozoic, siliciclastic sedimentation prevailed.

3. Although the Challenger Knoll oil is similar to the Mexico oils, certain notable differences, such as the sulfur content, suggest that the source rock of the Challenger Knoll formed in a subbasin characterized by high evaporation and restricted ocean circulation.

4. Properties of oil derived from widely distributed Mesozoic source rocks from Challenger Knoll(?), DSDP Site 535, Mexican wells, and from the Gulf Coast continental slope indicate that an extensive Mesozoic source rock may underlie a large part of the Gulf of Mexico. If this is correct, the amount of undiscovered petroleum resources in the Gulf of Mexico may be considerably underestimated.

Estimation of Gas Hydrate Concentrations Using Seismic Methods

Kristen Fehlhaber, William P. Dillon, and Myung W. Lee

We are applying a new method of evaluating the volume of gas hydrates in sea-floor sediments in the Blake Ridge area (continental slope, U.S. Atlantic margin). We estimate volumes using two-channel seismic data and seismic models that analyze amplitude variations of the seismic profiles to predict the amount of hydrates in the sediments. Initial volume estimates indicate that more than 0.7 trillion cubic meters of gas hydrates are present beneath the 29,000 km² study area.

Gas hydrates exist in the pore space of the upper several hundred meters of ocean-floor sediment. Areas containing gas hydrates are identified by the presence of a BSR (bottom simulating reflection) and by "blanking" of the seismic reflections above the BSR. (See also Dillon and others, this volume.) The BSR parallels the sea-floor topography and represents the pressure/temperature-controlled base of hydrate cementation at the bottom of the gas-hydrate stability zone. The reflection occurs due to the impedance contrast between hydrated and nonhydrated sediments. "Blanking" is the result of the cementing effect of the

hydrate, causing a reduction in the impedance contrast in these upper sediments. We have created seismic models to divide the profiling data into three classes of blanking, each class corresponding to a different level of bulk hydrate in the sediments.

Seismic reflection data were collected specifically to image the shallow subbottom region, where hydrates exist. The seismic source was a single 160 in.³ airgun, and the data were recorded digitally from a two-channel streamer. We used the seismic processing system SIOSEIS to apply a gain function, and to stack, deconvolve, and filter the two-channel data. The processed, true-amplitude profiles were then interpreted for the presence of hydrate, as indicated by the presence of the BSR and (or) blanking. Next, the various blanking classes were marked on the seismic records. The visual interpretation and assignment of the blanking classes were checked using PSEUDO, a subprocess of SIOSEIS, which passes a window along the seismic profile in the depth range of 250–500 milliseconds below the sea floor, and estimates the median reflection amplitude in the window. The median reflection amplitude correlates directly to the three classes of blanking. The interpreted sections were then digitized and fed into a surface-modeling program. The upper and lower surfaces of the hydrate classes were gridded to produce contour maps of total hydrate and to calculate the volume of sediments and hydrate equivalent belonging to each class.

Preliminary results indicate that the 29,000 km² study area contains 7.86×10^{12} m³ of bulk methane hydrate within 1.67×10^{13} m³ of sediment. Because hydrate expands to 160 times its volume when it breaks down to form gas, the hydrate is equivalent to 1.26×10^{14} m³ (4,440 TCF) of methane gas. This represents approximately 0.7 percent of K.A. Kvenvolden's 1988 published estimate of methane hydrates contained in all ocean sediments.

increase in production of less than 20 percent for all U.S. coals. Although this rapid growth has slowed in recent years, continued growth is projected for this region. However, stiff competition from western coal and natural gas and increased environmental constraints on coal utilization necessitate better understanding of the quality of Gulf Coast lignite. Increased knowledge of lignite quality should lead to more efficient and environmentally sound use of Gulf Coast lignite. Despite more than 100 years of lignite mining in the Gulf Coast and the economic impact of the lignite (more than 58,500,000 short tons produced in 1990), relatively little information on lignite quality is publicly available. The U.S. Geological Survey's National Coal Resources Data System contains the largest publicly available coal-quality data base in the U.S. It includes information on the physical and chemical properties of slightly more than 250 Gulf Coast lignite samples in a data base of more than 13,000 entries. Information in the literature on lignite petrography and mineralogy is almost nonexistent.

The Gulf Coast lignite-quality attributes that we expect to attract the most attention during the 1990's are as follows:

Coal Quality Attribute	Significance
Mineralogy	Contributor to corrosion, erosion, and fouling.
Petrography	Indicator of conversion efficiency and spontaneous heating potential.
Sulfur content	Environmental impact, boiler design.
Trace elements	Environmental impact, byproduct recovery.
Ash chemistry	Contributor to fouling and slagging; environmental impact.
Equilibrium moisture	Used for rank determination - impact taxes.

As new technologies, for example, fluidized bed combustors, coal/water fuel mixtures, and briquetting, are implemented, and as new problems appear, other coal-quality attributes will attract attention. The ultimate goal of coal-quality research in the 1990's will be to develop predictive models—models to predict attributes that will affect lignite utilization and quality variation throughout a mine or prospect site.

The Gulf Coast lignite-quality needs of the 90's represent a broad array of problems that impact on virtually every aspect of coal utilization. These needs can best be addressed through joint efforts of industry, State and Federal governments, and academia—perhaps by a jointly funded regional consortium dedicated to solving the Gulf Coast lignite needs of the 90's.

Gulf Coast Lignite Quality— The Needs of the 90's

Robert B. Finkelman, W.R. Kaiser,
Susan J. Tewalt, and James A. Luppens

During the 1980's Gulf Coast lignite production was among the faster growing segments of the United States coal industry; seven surface mines were opened in Texas and Louisiana and a test pit was opened in Arkansas. From 1980 to 1989 production of Gulf Coast lignites increased by almost 80 percent compared to an

Synsedimentary Authigenic Illite and Implications for Geothermometry in Sedimentary Basins

Neil S. Fishman and Christine E. Turner

Authigenic illitic mixed-layer illite/smectite (I/S) occurs in three distinct altered tuff beds in Pleistocene Lake Tecopa, an ancient alkaline, saline lake complex in eastern California. Within each tuff a concentric zonation of diagenetic mineral zones forms a crude bull's-eye

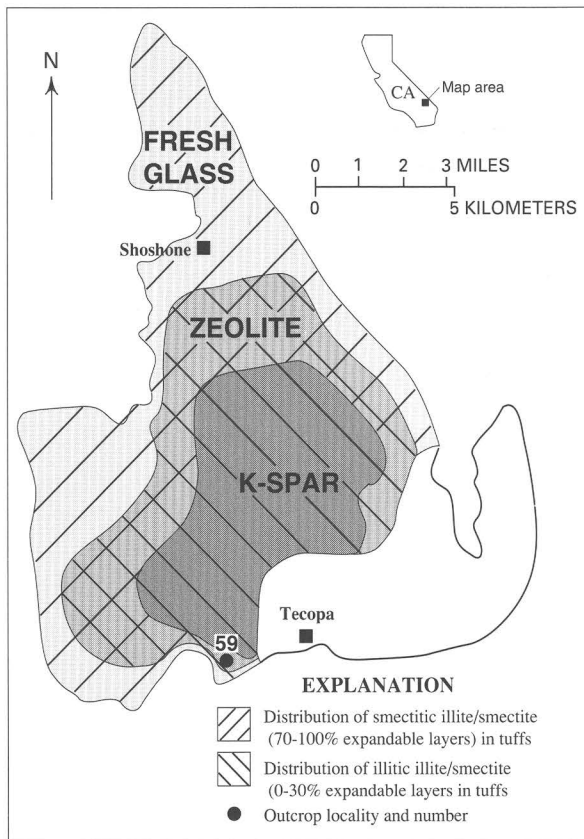


Figure 1 (Fishman and Turner). Generalized map showing diagenetic mineral zones in tuffs of Lake Tecopa (modified from a 1968 study by R.A. Sheppard and A.J. Gude, 3rd) and the crude bull's-eye pattern of zones, from fresh glass along the margins of the lake, to zeolites (chiefly phillipsite and clinoptilolite) farther basinward, to potassium feldspar (\pm searlesite) in the center of the lake (fig. 1). The illitic clays (0–30 percent expandable layers) occur in tuffs in both the potassium feldspar and zeolite zones (fig. 1). Smectitic I/S (70–100 percent expandable layers) occurs in the fresh glass zone, as the only authigenic aluminosilicate present, and also in some zeolitized tuffs (fig. 1); but it is rare in tuffs that contain potassium feldspar. Tuffs containing illitic clays occur in close proximity to those containing smectitic clays (fig. 1).

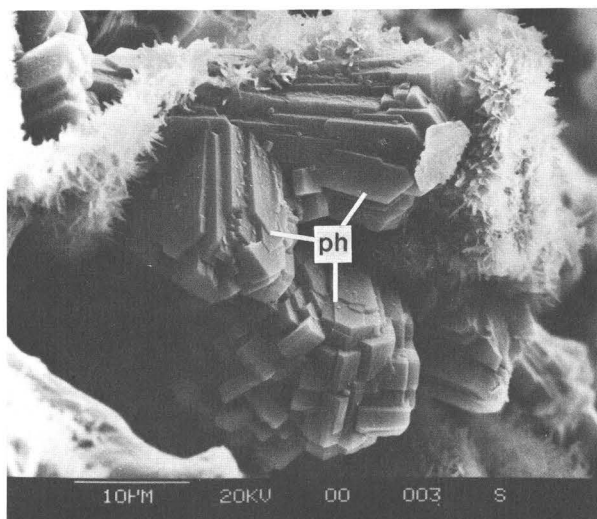


Figure 2 (Fishman and Turner). SEM photograph of illitic clays from a sample from site 59. (See fig. 1 for location.) Illitic clays are fibrous, contain iron, and coat authigenic phillipsite (ph). Bar is 10 μ m in length.

pattern, from fresh glass along the margins of Lake Tecopa, to zeolites (chiefly phillipsite and clinoptilolite) farther basinward, to potassium feldspar (\pm searlesite) in the center of the lake (fig. 1). The illitic clays (0–30 percent expandable layers) occur in tuffs in both the potassium feldspar and zeolite zones (fig. 1). Smectitic I/S (70–100 percent expandable layers) occurs in the fresh glass zone, as the only authigenic aluminosilicate present, and also in some zeolitized tuffs (fig. 1); but it is rare in tuffs that contain potassium feldspar. Tuffs containing illitic clays occur in close proximity to those containing smectitic clays (fig. 1).

SEM observations indicate that the illitic clays are fibrous, postdate the authigenic zeolites (fig. 2), and appear to have precipitated directly from solution. Compositionally, the illitic clays are iron bearing, as indicated by SEM-EDS (scanning electron microscope—energy dispersive spectrometry) analyses, weak 5 \AA peak intensities, and the position of $d(060)$ reflections (1.5090–1.5095 \AA). In contrast, the smectitic mixed-layer clays typically display a honeycomb texture and contain 10–20 percent illite layers, as indicated by the positions of the $d(002)$ and $d(003)$ peaks (8.67 \AA and 5.58 \AA respectively) determined from X-ray diffraction analyses on oriented, glycolated samples. The nonintegral spacing of $00l$ reflections corroborates the mixed-layer nature of these clays. Smectitic clays are likely dioctahedral Al-smectite as indicated by the $d(060)$ reflection at 1.497 \AA .

A similar burial history has been experienced by each of the tuffs throughout the lake basin, and none has

ever been buried to depths in excess of about 50–75 m. The similar burial history experienced by illitic and smectitic tuffs alike, and the close proximity of tuffs containing different clays suggest that elevated temperatures due to burial did not play a role in the formation of illitic clays. Instead, the distribution of the illitic clays in the tuffs and their association with authigenic zeolites and feldspar argue strongly for pore-water chemistry as the main control on illite formation. Because pore waters at near-surface temperatures can control formation of authigenic illite, investigations should be cautious about using illitic phases as a geothermometer when evaluating the thermal history of a sedimentary basin.

High-Resolution Paleoclimate Reconstruction From Alaskan Ice-Core Records

J.J. Fitzpatrick, T.K. Hinkley, G.P. Landis, R.O. Rye, and G. Holdsworth

Deep ice cores from the large continental ice sheets of Greenland and Antarctica provide long-term climate records. From Alaska, however, where the ice contains a record of a climate influenced by Northern Pacific Ocean weather patterns, little information is available.

We selected as our study site the 4,420-m col between Mts. Churchill and Bona in the St. Elias Range of southeastern Alaska. The ice core we plan to recover will contain a high-resolution paleoclimate record dating back to as long as 1,200 years B.P. The site is a broad, relatively flat expanse of snow and ice, about 1.0×1.3 km, sloping gently to the east.

In late spring 1991 we conducted an initial, reconnaissance field season. This emphasized observation, sampling of snow strata from dug pits, and sampling of gases in the snow and firn using shallow and deep probes.

The site is located in the dry facies zone and is part of the ultimate source of the Klutlan Glacier, well above the equilibrium line. No significant melting horizons were observed in snowpits. Net annual accumulation of snow is 1.9–2.0 m per year (approximately 70 cm water equivalent), judging by the minimally compacted most recent year's strata. Snow densities of the topmost year range from a minimum, near the spring surface, of about 0.18 g cm^{-3} to a maximum of about 0.43 g cm^{-3} at a depth of 2 m.

Preliminary analytical results show the following:

The light stable isotopic composition of snow within 1 year's accumulation exhibits a large seasonal range ($\delta D = -157$ to -292), indicating at least two sources of moisture and a correspondingly large range in

temperature. Concentration of biologically produced oceanic methanesulfonic acid (MSA) in snow strata closely parallels the isotopic extremes, with a small time lag. MSA maxima appear with the most negative isotopic values (cold times). This may suggest that different latitudinal sources of moisture exist for different seasons, and that the more arctic regions produce more biogenic sulfur. Alternatively, these variations in stable isotopic composition, and biogenic sulfur, may be related to the tropospheric stratification proposed to dominate in these altitudes and latitudes. (See a 1991 study by Holdsworth and others.)

Gases adsorbed from the atmosphere on accumulating snow crystals are present in different proportions than in the atmosphere. Upon recrystallization of snow grains, with aging and burial of the strata, excess adsorbed gases are released, and residual adsorbed gases approach atmospheric proportions, exchanging in an open system with the atmospheric gases that circulate through the permeable snowpack. At least a decade may be required in this locality for desorption and redistribution of gases from the snow and equilibration of firn gases with the atmosphere. Strata isolated by impermeable layers may retain the fractionated and anomalous proportions of adsorbed atmospheric gases.

We anticipate that concentrations of rock-forming, sea-salt, and volcanic-exhalation metals in seasonal snow strata will give additional information about changing air mass sources.

Tectonic and Climatic Changes Expressed as Sedimentary and Geochemical Cycles in Paleogene Lake Systems, Utah and Colorado—Implications for Petroleum Source and Reservoir Rocks

Thomas D. Fouch and Janet K. Pitman

Paleogene Lake Uinta strata in the Uinta and Piceance basins, Utah and Colorado, record both long- and short-term changes in climate and tectonic regime. Large, tectonically induced reconfigurations of the lake gave rise to relatively thick (several hundred meters), lithologically distinct stratigraphic sequences. Simultaneous changes in climate brought on by variations in solar radiation initiated very rapid rises and falls of the lake, as well as shifts in alkalinity and salinity of the water that resulted in the development of sedimentary and carbonate-geochemical cycles (parasequences) of up to tens of meters thick. Tectonically induced stratigraphic sequences represent environments that lasted several

million years whereas climate-induced parasequences lasted several thousand years: together they brought on rapidly changing conditions. The resulting lake deposits, which reflect both tectonic and climatic cycles, now constitute the principal source and reservoir rocks for petroleum in the Uinta Basin.

Middle Paleocene to late Eocene lake deposits are characterized by halite, sodium bicarbonate salts, and kerogen-rich shales containing organically derived carbonate minerals, indicating a highly organically productive, closed hydrologic system during much of the existence of the lake. Strata are cyclic: some cycles extend over several hundred meters of section, corresponding to a time span of several million years, while other cycles occur within millimeters and probably represent approximately 1 year.

Throughout the lake system, a cyclic depositional sequence in a marginal-lacustrine setting from oldest to youngest consists of: (unit 1) mud-supported, laminated carbonate rock or oil shale with a flooding surface at the base shoaling to an ostracode-, pisolite-, and (or) oolite-grainstone; (unit 2) mudcracked mudstone and (or) stromatolitic carbonate; (unit 3) mudcracked overbank mudstone or sandstone; and (unit 4) coalesced channel sandstone that locally eroded down to the underlying carbonate (unit 1) and aggraded laterally to form a composite sandstone sheet. Each interval within the sequence can vary greatly in thickness and areal extent depending upon its position within the depositional system.

Major open-lacustrine units reflect expansions of the lake such as those associated with the carbonate marker, Flagstaff Member, and Mahogany oil-shale zone of the Green River Formation. They formed in response to episodes of tectonic reactivation of regional faults such as the subsurface Basin Boundary fault along the north flank of the Uinta Basin. Large reconfigurations of the Lake Uinta system are defined by unconformity-bounded sequence boundaries. Strata that bracket these boundaries represent major cycles and consist of thick, lithologically distinct tongues of open-lacustrine, marginal-lacustrine, and alluvial rock that extend over large regions of the depositional system. Flooding surfaces document major episodes of shore transgression and record deposition of open-lacustrine, mud-supported, laminated carbonate rocks that make up the condensed section for each sequence.

Green River Formation strata contain numerous cycles of smaller dimensions than the large regional sequences just discussed. Recurrent and continuing climate change initiated very rapid expansions and contractions (and rises and falls) of the lake as well as shifts in alkalinity and salinity of its water. These changes resulted in small- to large-scale sedimentary and carbonate-geochemical parasequences within the larger

regional sequences. Solar radiation-induced sedimentary and geochemical cycles are similar in style to tectonic cycles, except that they commonly are recorded within a sedimentary thickness of 3–30 m and represent a few thousand to tens of thousands of years. In kerogenous open-lacustrine source rocks, carbon and oxygen isotope profiles for calcite and dolomite show generally synchronous geochemical cycles in which positive and negative excursions correspond to cyclic variations in organic carbon content and to changes in lithology. Small-scale carbon isotope cyclicity in carbonate matter documents salinity-induced changes in primary organic matter productivity and the amount of reduced carbon available for carbonate precipitation via methanogenesis. Large-scale carbon enrichment trends on carbonate curves record the effects of progressive acetate metabolism on the isotopic evolution of the inorganic carbon reservoir in a restricted, extended-residence-time system. Small-scale cyclic variations in oxygen in carbonates are related to climate-induced salinity changes that resulted from alterations in hydrologic balance during the lake's history. Major oxygen trends on the carbonate curves correspond to large-scale variations in lake level and salinity due to large alterations in inflow-evaporation balance coincident with major paleoclimate changes.

The principal reservoirs for oil and gas are found in marginal-lacustrine channel sandstones. Channel sandstones in surface exposures on the basin's south flank can be separated into two types (I and II) with respect to geometry and width/depth (W/D) ratios. The channel sequences (unit 4) occur within the parasequences described. Type I sandstones are characterized by a tabular geometry controlled by a planar lower bounding surface, an average channel depth of 7.6 m, and an average W/D ratio of 8.9. The planar channel bottom results from underlying resistant carbonate-rock units whose early lithification restricted downcutting and caused more extensive lateral aggradation compared to that of streams forming type II bodies. Type II sandstones are characterized by a lenticular geometry, with an average channel depth of 5.7 m, an average W/D ratio of 3.6, and a concave-upward lower bounding surface. The absence of resistant carbonate rocks (because of erosion or nondeposition outside the limits of the lake) underlying streams that deposited type II bodies resulted in stream channels that, although similar in size, did not migrate laterally as much as those of type I. As a result, the size of individual channel sandstone bodies, and therefore reservoir units, is largely dependent upon induration of the substrate across which streams flowed.

Late Cretaceous and Early Tertiary Evolution of the Uinta and Piceance Basins (Northeastern Utah and Northwestern Colorado) and Associated Development of Hydrocarbons

K.J. Franczyk, T.D. Fouch, R.C. Johnson, C.M. Molenaar, and W.A. Cobban

Paleogeographic reconstructions for Late Cretaceous through early Oligocene time in an area that includes the Uinta and Piceance basins and surrounding vicinity illustrate several major geologic events: the incursion of a Cretaceous sea, thin-skinned thrusting in the Sevier orogenic belt, eustasy, the breakup of a Late Cretaceous foreland and withdrawal of the sea, the formation of intermontane basins, and the appearance and disappearance of large lakes. Throughout most of the Late Cretaceous, the area was part of a foreland basin in which depositional patterns were controlled both by thrusting in the Sevier orogenic belt to the west and by eustasy. Organic detritus that accumulated in open-marine waters and in coastal plain swamps and marshes later produced the gas now found in low-permeability reservoirs in the Uinta and Piceance basins. In late Campanian through early Maastrichtian time, the sea withdrew from much of the paleogeographic map area, centers of greatest subsidence shifted, basement-involved uplifts developed, and small intermontane basins began to form in the western part of the map area. These basins formed on top of the thrust allochthon in the west-central and southwest parts of the map area and between the thrust front and the rising San Rafael structure east of the thrust front.

By latest Maastrichtian time, the sea had withdrawn completely. Movement on the Uinta and Sawatch uplifts, in the north-central and southeastern parts of the map area, respectively, had begun; and sediment accumulated in the small intermontane basins in the western part of the map area. The more extensive intermontane basins that characterized much of this area during the Paleogene were developed by the middle Paleocene. Initially, in the last Maastrichtian through middle Paleocene, sediments were deposited primarily in alluvial fans and plains, shallow lakes, and lake-margin wetlands. The lakes expanded in late Paleocene and early Eocene time, and in the early Eocene they occupied large parts of both the Uinta and Piceance basins. Organic sediment was deposited locally in the older, smaller lakes as well as the younger, larger lakes. These deposits became the principal source rocks for the oil in areas of the Uinta Basin where they are thermally mature. Fluctuating lake levels produced interbedded lacustrine and fluvial reservoir rocks and source rocks. In the

middle Eocene, the lakes in the Uinta and Piceance basins expanded further, covering the Douglas Creek arch that had separated the lakes, and joined to form a single major lake, Lake Uinta. The Mahogany oil-shale bed formed during this time of maximum lake development, but it is too thermally immature to generate oil or gas.

During the late middle Eocene, volcaniclastic sediments from the north began to fill the lake in the Piceance basin. From then through the late Eocene, Lake Uinta retreated westward and disappeared from the west end of the Uinta Basin in latest Eocene or earliest Oligocene time. The Uinta Basin was filled with clastics shed during the final tectonic event in the Uinta uplift; concurrently, volcanic material and reworked volcanic detritus accumulated in the western part of the map area.

Bridging the Gap Between Third- and Fifth-Order Cycles in Carbonate Sequences—The Western Margin of the Great Bahama Bank

Robert B. Halley and R. Jude Wilber

Almost 100 km of high-resolution single-channel seismic data (200–300 ms two-way travel time) has been collected in the vicinity of published multichannel seismic records (1.0–1.5 s two-way travel time) from the western margin of the Great Bahama Bank. Comparisons of the overlapping portions of the two data sets, together with an understanding of the modern surface and shallow-subsurface sediments, provide insights into the interpretation of the upper portion of the multichannel lines. Both data sets are characterized by laterally stacked sigmoidal reflectors, attesting to western progradation of the shelf edge. The two uppermost sequence boundaries are clearly recognizable in the lower slope sediment wedge, but tracing these surfaces to their banktop equivalents is uncertain because correlations must pass through a reflection-free area, often interpreted as “reef?”, associated with steep relief at the platform margin.

Reefs do not occur on the platform margin today, yet shallow drilling has revealed reefal sediments beneath the platform edge. Westward flow of bank water, highly variable in salinity and temperature, generally precludes modern reef growth along this margin. Instead of reefs, the modern margin is characterized by sandy deposits in a band up to 4 km wide and a slope break between 55 and 65 m water depth. Below the shelf break, the upper slope is a steep (15°–30°) rocky incline characterized by sediment bypassing. At 140 to 180 m, the rocky slope gives way to a soft-sediment slope of bank-derived

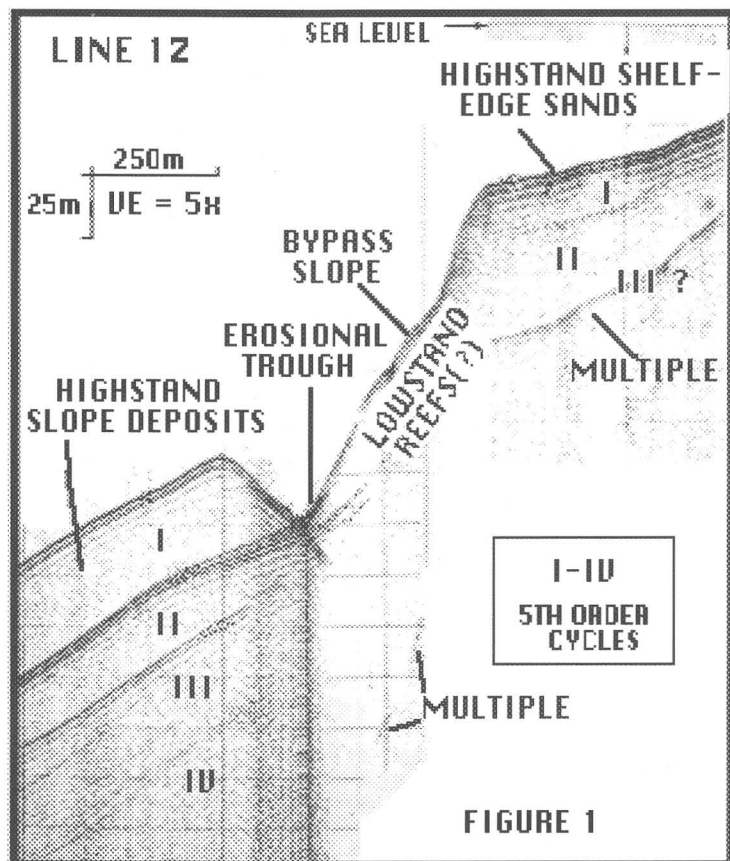


FIGURE 1

Figure 1 (Halley and Wilber). High-resolution seismic profile across the west edge of the Great Bahama Bank.

carbonate mud and sand. This sediment wedge dips away from the base of the rocky slope at increasingly gentle angles into the Straits of Florida.

Strong reflectors in lower slope sediments form the basinward portion of sigmoid oblique sequences. Sediments recovered from the youngest subsurface reflector yielded a ^{14}C age of 10,000 yr. This reflector, when traced bankward, clearly underlies the base of the rocky upper slope before disappearing into the reflection-free area (fig. 1). Underlying reflectors mimic the morphology of the present sediment surface, suggesting that they are relict surfaces formed during hiatuses in sedimentation. Lower slope sediments presently exhibit evidence of rapid sedimentation at the surface and may be seen to onlap the base of the rocky upper slope.

These observations have led to a conceptual model of platform aggradation and progradation during sea-level fluctuations, summarized in two stages: (1) When sea level falls below the general level of the platform, large carbonate-producing areas are subaerially exposed,

resulting in lithification and the development of strong reflectors. Sediment production on the bank is minimal except in the immediate vicinity of the shoreline, which may host fringing reefs. Basinward, the sea floor is sediment starved, allowing the formation of hardgrounds and winnowed coarse sediments that serve as reflectors. Allochthonous debris fields do not appear to be a major contributor to slope sediments in this area. As sea level rises and falls along the margins of the platform, accumulations of reef sediments build and maintain steep profiles on the slope. (2) During highstands, major aggradation and progradation take place when the bank-top carbonate "factory" produces copious amounts of sediment, more than half of which is transported to the outer shelf and slope. On leeward margins, highstands are not characterized by reef development, but rather by shelf-margin carbonate sands and thick (up to 80 m) accumulations of bank-derived slope deposits. Steep portions of the upper slope become sediment-bypass areas subject to marine lithification and eventual development of strong reflecting horizons.

The consequences of these complex sea-level/carbonate-sedimentation relations are that basinal and lower slope reflectors as well as banktop reflectors form when sea level is below the bank margin. At the platform margin, facies changes may be abrupt and the lateral distance between reflectors may be small, inviting correlation of horizons that appear continuous on multichannel seismic sections. Upper slope reflectors may form during highstands or not at all. Sequence boundaries may be inadvertently crossed through the reflection-free zone in areas where reflectors have not developed within the reef facies. Where sedimentation rates are high, fifth-order sequences approach the spatial scale of third-order sequences. Under these circumstances, additional control for making correlations is critical. Careful attention to complementary stratigraphic data is essential for detailed age assignments and interpretations of multichannel lines across leeward carbonate-bank margins.

Hydrocarbon Source-Rock Evaluation of Desmoinesian (Middle Pennsylvanian) Coals from Southeastern Iowa, Missouri, Southeastern Kansas, and Northeastern Oklahoma

Joseph R. Hatch

Coals in the Desmoinesian (Middle Pennsylvanian) Cherokee Group and Marmaton Group in the Western Region of the Interior Coal Province, U.S.A., are potential source-rocks for methane and liquid hydrocarbons. To help evaluate this potential and better understand the organic geochemistry of these coals, 85 samples were collected from core and surface-mines at 21 locations in southeastern Iowa, Missouri, southeastern Kansas, and northeastern Oklahoma. Analyses performed include Rock-Eval pyrolysis, vitrinite reflectance (R_o), CHCl_3 extraction of coals, and gas chromatography to compare saturated hydrocarbon distributions from coals with those from Cherokee Group oils. The analyses are summarized from three geographic areas defined by increasing thermal maturity. Organic matter in coals from area 1 (southeastern Iowa and northern Missouri) is marginally mature with respect to petroleum generation (Rock-Eval $T_{\max} = 430 \pm 4$ °C, $n = 48$; $R_o \leq 0.55\%$, $n = 9$); in area 2 (southwestern Missouri, southeastern Kansas, and northeastern Oklahoma near the outcrop) organic matter is mature ($T_{\max} = 446 \pm 5$ °C, $n = 25$; $0.57 \leq R_o \leq 0.80\%$, $n = 7$); and in area 3 (cores from Osage County, northeastern Oklahoma) organic matter is near peak oil generation ($T_{\max} = 460 \pm 5$ °C, $n = 12$; $0.80\% \leq R_o \leq 1.0\%$, $n = 3$).

For coals from area 1, mean genetic potential (Rock-Eval $S_1 + S_2$ mg HC/g sample) is 126 ± 41 mg/g; from area 2, 139 ± 46 mg/g; and from area 3, 115 ± 35 mg/g, which shows that coals from the three areas all have excellent potential to generate hydrocarbons. For coals from area 1, mean carbon-normalized volatile hydrocarbon content (S_1/TOC , mg HC/g TOC) is 4.4 ± 3.1 mg/g; from area 2, 6.8 ± 4.6 ; and from area 3, 12 ± 5 mg/g, which indicates that some hydrocarbon generation has taken place.

For coals from area 1, mean content of CHCl_3 extractable organic matter is 27 mg/g sample (geometric deviation [GD] = 1.7; $n = 14$); from area 2, 15 mg/g (GD = 1.6; $n = 9$); and from area 3, 9 mg/g (GD = 1.1; $n = 5$). This decrease is thought to be caused by a decrease in micropore interconnections with increased thermal maturity, which results in lower extraction efficiencies. In coal extracts from area 1, saturated hydrocarbon:aromatic hydrocarbon ratios are 0.31 ± 0.12 ; from area 2, 0.33 ± 0.08 ; and from area 3, 0.41 ± 0.22 . For coals from areas 1 and 2, saturated hydrocarbon distributions are dominated by pristane with low relative amounts of $n\text{-C}_{25}$ through $n\text{-C}_{31}$; in area 3, relative amounts of n -alkanes and isoprenoids are similar. In coals from area 1, mean pristane:phytane ratio is 6.5 ± 2.3 ; from area 2, 5.7 ± 1.9 ; and from area 3, 3.7 ± 1.2 . This decrease in pristane:phytane with increased thermal maturity follows trends observed in coals by previous researchers. Extracts from Desmoinesian coals immediately overlain by marine black shales are intermediate in composition between those of the black shales and other coals. This may result from the addition or preservation of bacterial biomass in the upper layers of the peat during early diagenesis or from migration of hydrocarbons from the overlying shale down into the coal.

All coal extract compositions are dissimilar to oils produced from the Cherokee Group in southeastern Kansas and northeastern Oklahoma suggesting minimal generation or migration of liquid hydrocarbons from these coals. However, active exploration for coalbed methane is taking place in southeastern Kansas, and at least 74 gas wells have been completed.

Anadarko Basin Reservoir and Non-Reservoir Sandstones—A Comparison of Porosity Trends

Timothy C. Hester and James W. Schmoker

Sandstone porosity normally decreases during burial and is commonly treated as a function of burial depth. Treating sandstone porosity as a function of vitrinite reflectance (R_o), however, minimizes the effects

on porosity data of regional differences in burial history. Thus, porosity data from areas with regional differences in burial, uplift, and thermal gradient may be combined and (or) compared within a normalized context.

Two porosity- R_o data sets representing sandstones of the Anadarko basin, Oklahoma, have been compiled: (1) non-reservoir sandstones of the central and southern Anadarko basin, and (2) hydrocarbon-reservoir sandstones of the Anadarko basin as a whole. Each of these data sets is compared to a composite set of sandstone porosity- R_o data from numerous basins that represents a preliminary porosity framework of sandstones in general, and the two are also compared to each other (fig. 1).

Porosity data of non-reservoir sandstones in central and southern Anadarko basin consist of two populations; in both, porosity generally declines as a power function of increasing thermal maturity. For $R_o < 1.1$ percent, Anadarko basin non-reservoir sandstone porosity decreases more rapidly than does porosity of sandstones in general. For $R_o > 1.1$ percent, Anadarko basin non-reservoir sandstone porosity decreases less rapidly than does porosity of sandstones in general.

Reservoir sandstones of the Anadarko basin, however, follow a different pattern. Reservoir sandstones lose porosity much more slowly than do non-reservoir sandstones (for $R_o < 1.1$ percent) and sandstones in general (fig. 1). This slower rate of porosity decline with increasing R_o could be due to geologic factors such as overpressuring or the inhibiting effects of early hydrocarbon emplacement on diagenesis, and (or) to economic factors inherent in the selection of hydrocarbon reservoirs.

In any case, as R_o increases from about 0.65 percent to about 1.1 percent, the porosity trends of Anadarko basin reservoir and non-reservoir sandstones rapidly diverge. Above about $R_o = 1.1$ percent, however, the porosity trends of Anadarko basin reservoir and non-reservoir sandstones have similar slopes, suggesting that sandstones of the central and southern Anadarko basin may retain sufficient porosity for economic accumulations of hydrocarbons, even at high thermal maturities.

develop sequence stratigraphic models that relate coal deposition and quality to climate, tectonism, and eustasy. The study interval includes, in ascending order, the Smoky Hollow, John Henry, and Drip Tank Members of the Straight Cliffs Formation. The members are approximately 40, 260, and 60 m thick, respectively, and are late Turonian to early Campanian in age. In 1991, we collected continuous core from two 300-m holes drilled through these strata in the central regions of the plateau. With this core, we hope to test our models and gain additional insight into the controls on coal accumulation by integrating coal petrography, geochemistry, and palynology with sedimentologic and stratigraphic data.

A sequence stratigraphic model published in 1991 by K.W. Shanley and P.J. McCabe divided the Straight Cliffs Formation into several systems tracts based on the recognition of unconformities, variations in stacking patterns, and sandstone geometries. The Calico bed, located in the upper part of the Smoky Hollow Member, and the Drip Tank Member consist of fluvial, valley-fill deposits that are underlain by thick, rooted paleosols. The intervening John Henry Member accumulated as a highstand deposit along the western margin of the Western Interior seaway.

Stratigraphic sections described from the northeast flank of the plateau show that the John Henry Member is dominated by 225 m of thick shoreface parasequences characterized by upward-coarsening units that contain hummocky and swaley cross-stratified sandstone and marine fossils. In exposures 2 km to the southwest, several shoreface parasequences grade laterally into coastal plain strata characterized by rooted mudstone, carbonaceous shale, and coal. Here, the John Henry Member has a total coal accumulation of 9 m, and individual coal beds are as thick as 4 m. Core collected from the John Henry Member, 5 km inland from the stacked shoreface parasequences, is dominated by interbedded tidal and coastal plain strata; only 45 m of swaley bedded sandstone remains. Tidal strata are characterized by trough cross-stratified sandstone, wavy-lenticular bedding, double mud drapes, *Teredolites* burrows, and oyster shell fragments. Here, the total coal accumulation has increased to 20 m, and individual coal beds are as thick as 7 m. Ten kilometers farther inland, a second core indicates that the John Henry Member consists entirely of interbedded coastal plain, tidal, and fluvial rocks; its total coal accumulation is 30 m, and individual coal beds are as thick as 7 m. By contrast, stratigraphic sections described along the south flank of the plateau, 35 km inland from the shoreface strata, show that the John Henry Member consists entirely of stacked alluvial strata containing only rare coal beds less than 2 m thick.

Preliminary interpretations indicate that peat accumulated in a 35-km-wide belt of coastal plain strata that accreted immediately landward of the vertically

Testing New Coal Models—The 1991 Kaiparowits Plateau Drilling Project

R.D. Hettinger and P.J. McCabe

During the past 4 years, the USGS has conducted detailed stratigraphic studies on Upper Cretaceous strata exposed along the flanks of the Kaiparowits Plateau in southern Utah. The purpose of these studies was to

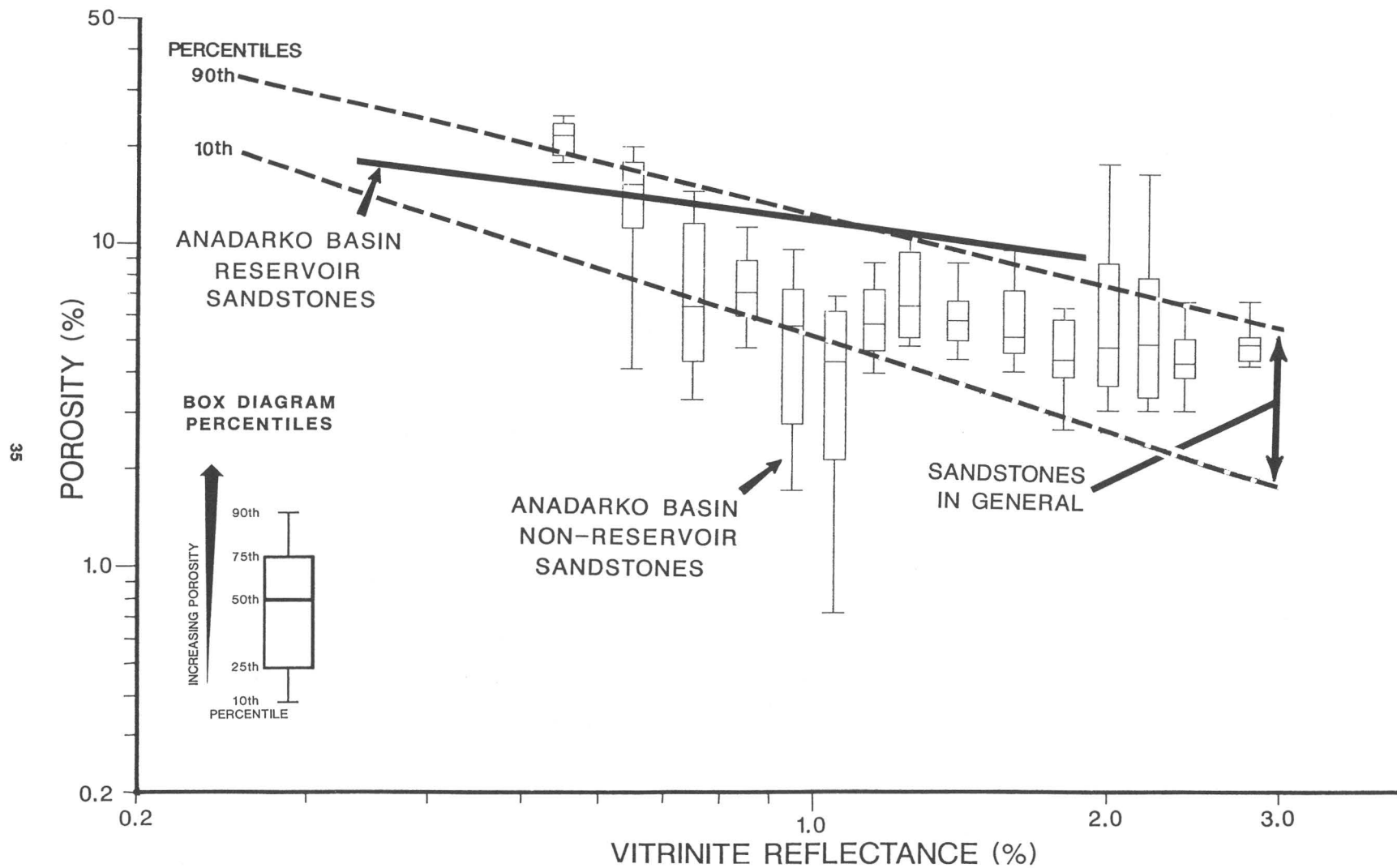


Figure 1 (Hester and Schmoker). Plot of porosity versus vitrinite reflectance for Anadarko basin non-reservoir and reservoir sandstones, and for sandstones in general.

stacked shoreface parasequences. Several distinct deepening events are recognized in the core where thick tidal deposits overlie coal-bearing coastal plain strata. We were able to correlate these deepening events to minor transgressive episodes recognized on outcrop and depicted in our sequence stratigraphic models. Recognition of these transgressive episodes refines our models by allowing for a higher degree of correlation between shoreface, coastal plain, and fluvial strata than was previously possible; and it enhances our interpretations regarding the controls on coal accumulation.

$\delta^{13}\text{C}$ of Terrestrial and Marine Organic Matter in Cretaceous Rocks of the Western Interior of North America

Charles W. Holmes, John M'Gonigle, and Brent Dalrymple

Measurement of $\delta^{13}\text{C}$ composition of upper Phanerozoic coals demonstrates a relative decrease in $\delta^{13}\text{C}$ beginning in the middle Cretaceous. $\delta^{13}\text{C}$ determination in coals from the Upper Cretaceous (Cenomanian to Coniacian) Frontier Formation of western Wyoming suggests that the shift occurred prior to the Cenomanian. Values of $\delta^{13}\text{C}$ of coals within these middle Cretaceous strata range from -25.6 to -26.4 ‰ , averaging -26.0 ‰ . The narrow distribution of $\delta^{13}\text{C}$ values indicates that the composition of the carbon source was nearly constant during this time. The composition is approximately 2 ‰ more negative (lighter) than older Phanerozoic coals and 3 ‰ more positive (heavier) than late Cenozoic coals:

Plants growing in a low-lying environment, such as the Okefenokee swamp, Georgia, obtain carbon from both the atmosphere and the waters flowing through the swamp mire. During the evolution of such an environment, the submerged portion of the mire is infilled, which produces a stratified hydric- to mesic-derived peat deposit. The resulting peat contains varied (4 – 6 ‰) $\delta^{13}\text{C}$ values, heavier because of the hydric-derived peat and lighter because of the mesic-derived peat. In contrast, plants growing in a raised mire, in which the water comes from rain, obtain carbon solely from the atmosphere. Studies by C. Geissler and L. Belau in 1971 and H.M. Chung and W.M. Sackett in 1978 have shown no apparent effect on the $\delta^{13}\text{C}$ of the residual organic matter during coalification, and as the raised-mire plants assimilate their carbon from the atmosphere, the $\delta^{13}\text{C}$ of the resultant coals may serve as a monitor of the atmosphere $\delta^{13}\text{C-CO}_2$ at the time of deposition. Sedimentologic and chemical data on coals from the Frontier Formation in western Wyoming suggest that

these coals formed in raised mires on a fluvial plain near the shoreline; if so, we suggest that the distribution of $\delta^{13}\text{C}$ in the coals contains the middle Cretaceous atmosphere $\delta^{13}\text{C}$ signal, and the data indicate that it was relatively constant during this time.

In contrast, L.M. Pratt and C.M. Threlkeld in a 1984 study noted that the marine $\delta^{13}\text{C}_{\text{org}}$ record for Cenomanian and Turonian rocks from many localities in the interior sea has a 2 – 4 ‰ positive excursion over a background value of $\approx -26\text{ ‰}$ that spans the Cenomanian-Turonian boundary. W.E. Dean and others in 1986 tentatively concluded that this excursion results from increased $p\text{CO}_2$ in the atmosphere. This conclusion contradicts the data from the terrestrial material on the adjacent land mass. An alternative explanation for the positive excursion is that it is due to an increase of productivity in the sea. Unpublished data by Holmes of the distribution of $\delta^{13}\text{C}_{\text{org}}$ in the Mowry Shale shows a positive excursion (2 – 3 ‰) immediately above bentonite beds. As the isotopic excursion lies within the rocks whose time of deposition spans the Cenomanian-Turonian boundary, and as the excursion is associated with numerous bentonite beds, we propose that the volcanic ashes were sources of nutrients that increased productivity. This increased productivity led to the change in marine organic matter $\delta^{13}\text{C}$ but did not affect the terrestrial record perceptually.

Collisional Tectonics and the Global Generation of Oil and Gas

David G. Howell

Models that integrate the principles of plate tectonics with the requirements for hydrocarbon accumulation (source, maturation, expulsion-migration, and entrapment) provide a way to evaluate the worldwide distribution of oil-and-gas resources. If tar sands and heavy oils are included along with the more conventional oil and gas, the principal habitat for the world's petroleum resources is seen to be fold-and-thrust belts and their associated foreland basins.

The distribution of oil and gas in foreland basins is dictated by thermotectonic processes related to the collisional process. To create the petroleum habitat of fold-and-thrust belts and forelands, continental shortening, or A-subduction, is required. Such shortening can be caused by either of two distinct plate-tectonic events: (1) accretion of one or more volcanic arcs to a continental margin, or (2) the collision of two continents. Event 1 has produced such features as the Brooks Range of Alaska and the North American

Cordillera, whereas event 2 has produced such features as the Appalachian-Ouachita-Marathon, Zagros, and Ural orogens.

Regardless of the specific plate-tectonic process that triggers intracontinental shortening, the styles of continental crustal deformation are essentially identical. For these crustal-shortening settings to be petroliferous, however, one additional ingredient is required: an extensive, thermally immature, organic-rich source rock. This preexisting source rock is commonly, but not exclusively, Devonian, Triassic, Jurassic, and (or) Cretaceous black shales. Thus, the superimposition of a tectonic orogen across older, thermally immature source strata is a critical requirement in the generation of nearly all of the world's petroleum.

Tectonic thickening in the orogen imposes a crustal load that creates a crustal sag, which is the foreland basin. The sedimentary fill within this basin depresses the older strata and effects petroleum maturation. In addition, the architecture of the foreland provides pathways toward a lithospheric bulge, above which vast amounts of oil can accumulate. Owing to inefficiencies in the expulsion of oil from source rocks, the extant oil and much of the still-rich source rock are depressed far below the oil-generating window, such that natural gas becomes the primary hydrocarbon generated during the later stages of the orogenic cycle.

In young systems, oil may remain preserved in the fold-and-thrust belt, but in fully developed orogenic areas, multiple deformational events in the fold-and-thrust belt result in the destruction of the early-formed architecture of traps and seals. Thus, the initial oil either remigrates or cracks, owing to increasing temperatures, to gas. In either case, the new structural configurations become gas habitats. The flux of gas continues long after the initial migration of oil. Therefore, in tectonically mature fold-and-thrust belts, we would expect to find primarily oil accumulations in regions distal from the orogen and primarily gas accumulations in regions proximal to the orogen.

Seismic Reflection Studies of Lake Baikal, U.S.S.R.

D.R. Hutchinson, A.J. Golmshtok,
T.C. Moore, M.W. Lee, C.A. Scholz, and
K.D. Klitgord

Approximately 1,500 km of 12-fold multichannel seismic-reflection data was collected in Lake Baikal in 1989 by the U.S.S.R. Academy of Sciences. These data were processed jointly by the U.S. Geological Survey and the U.S.S.R. Academy of Sciences. Shots were fired every

50 m using a 17-liter (1,000 in.³) airgun and recorded through a 1,200-m, 24-channel streamer for a total recording length of 7 s. Velocities are resolved in this configuration to about 2-s subbottom. We assume velocities of 2.5–4 km/s for the deeper sedimentary units. Data were processed 12-fold.

The data show that Lake Baikal contains three rift basins (South, Central and North) that are separated by fault-bounded basement highs, Academician Ridge and the Selenga Delta (fig. 1). The South and Central basins contain the thickest rift deposits (7.0 and 7.5 km respectively). Complex depositional patterns and the presence of boundary faults on both sides of the basins suggest that the style of deformation has varied through time and that these basins have not evolved as simple half-grabens. In contrast, the North basin has a simpler structural style with consistent depositional patterns, more suggestive of a uniform deformational regime; and maximum sediment thickness is much thinner, about 4.5 km. These differences suggest that the South and Central basins are older than and (or) have extended (and subsided) more than the North basin.

The geometry of each of these basins is asymmetric. From south to north, the greatest fault offset occurs on the north, northwest, and west sides of the basins (fig. 1). This overall geometry consists of rift segments that change orientation from east/west in the south to north/south in the north. The intervening basement highs are complex accommodation zones in which fault orientation therefore changes between adjacent rift segments.

The seismic data indicate at least three phases of deposition, separated by significant tectonic movements and faulting. The oldest episode of faulting, which offsets basement blocks and the oldest acoustically opaque sedimentary units, is most prominent in the South and Central basins but may be locally present in the North basin. The second phase of faulting is characterized by steep primary and antithetic faults ($>50^\circ$) that generally die out upward at about 0.5–1.0 s beneath the lake floor. This phase of faulting occurred contemporaneously with a seismic depositional unit which contains clear internal, laminated reflections. The youngest faulting is also very steep, occurs near the edges of all basins, offsets the lake floor, and rejuvenates some of the older faults. Some areas near Academician Ridge show indications of fault dip-reversal and slight compression. The steepness and linearity of the faults, the evidence for dip-reversal, and the progressively rotated orientation of the three basins suggest that oblique-sinistral slip tectonics have played a significant role in the development of the structures and stratigraphy beneath Lake Baikal.

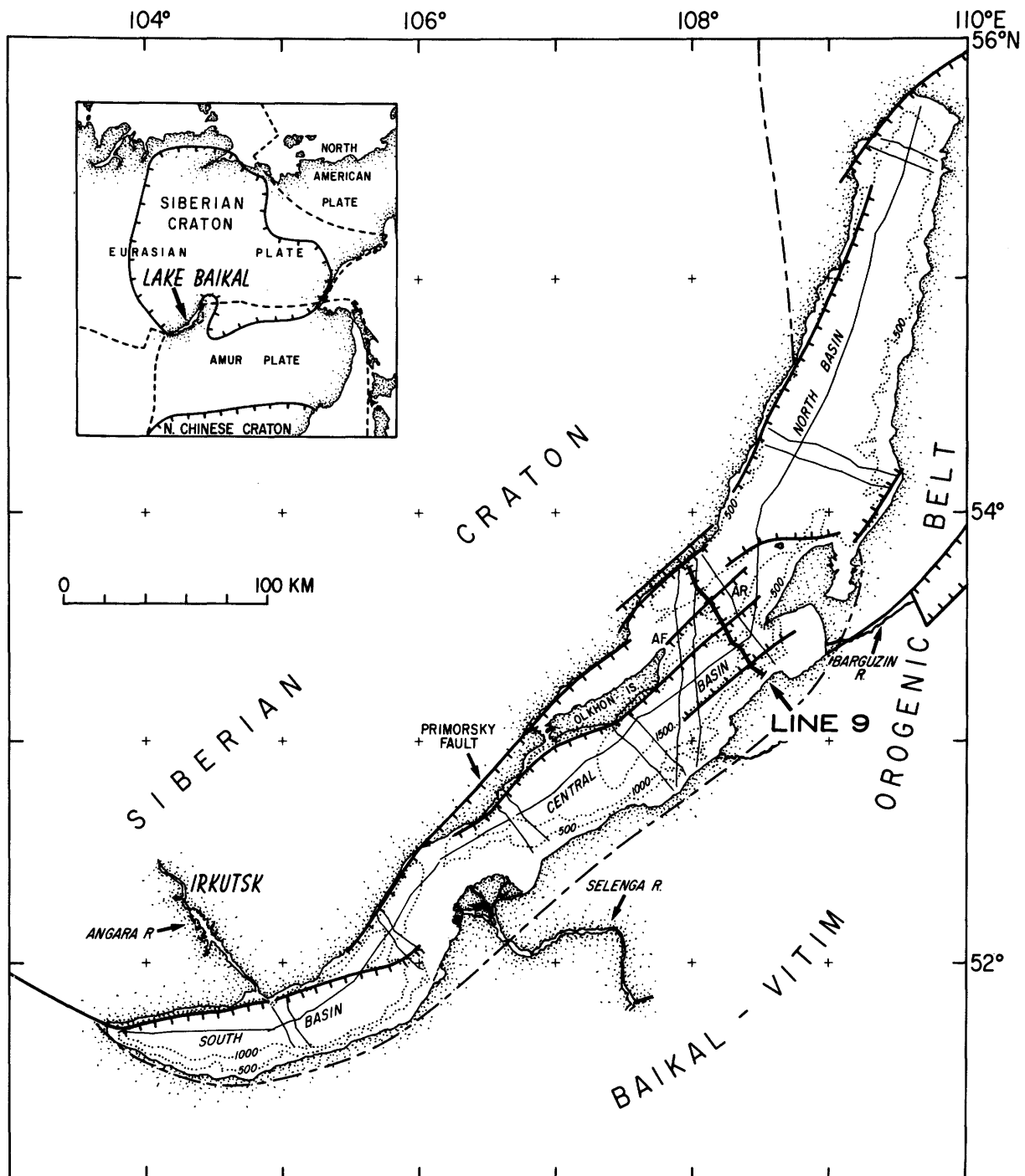


Figure 1 (Hutchinson and others). Total sediment thickness (kilometers) beneath Lake Baikal from multichannel seismic reflection profiles. Dashed line indicates inferred thickness; query, contour position unknown. Dotted line, multichannel track line. Hachured line, fault.

Petroleum Geology Research in the Santa Maria Province, California

Caroline M. Isaacs

The USGS Onshore Oil and Gas Investigations Program has ongoing research focused on the petroleum geology of the Santa Maria province. This research centers on the Miocene Monterey Formation, the principal source and reservoir of petroleum in the onshore and offshore Santa Maria basins, and a major source and reservoir in the Santa Barbara–Ventura basin.

Current stratigraphic research on the Monterey Formation is focused on establishing a firm age and facies framework, with the long-term goal of developing reliable regional correlations and paleogeographic reconstructions. Problems currently being addressed include (1) poor age control in much of the province, especially in the interval 5–10 Ma; (2) high small-scale (< 1 ft) variability, which has made comparison of sequences difficult and determination of regional trends unreliable; and (3) complex and poorly understood expression of lithotypes and lithofacies on well logs. Research has focused on detailed interrelation of the composition, well-log characteristics, age, and paleobathymetry of select subsurface sequences in the Orcutt, Point Arguello, South Elwood, and Hondo oil fields.

Source-rock characteristics, another major topic of research, are being investigated mainly by the USGS-sponsored Cooperative Monterey Organic Geochemistry Study. This international study group involves about 30 organic geochemists and 10 geologists working in collaboration on the deposition, diagenesis, oil generation, and oil-source correlation of the Monterey Formation. The center of the source-rock study is the comprehensive geologic and organic geochemical analysis of 22 rock samples and 11 oils from the Santa Maria and Santa Barbara–Ventura basins. Rock samples include a variety of lithotypes from two stratigraphic sections of differing maturity, and oil samples include a variety of gravities and sulfur contents from eight oil fields. Also part of the source-rock study is selected research on organic geochemical maturity of a deep (> 13,000 ft) offshore well profile. Topics addressed by the source-rock study include the interpretation of provenance and paleoenvironmental indicators in organic matter, compound identification, effect of sulfur on organic maturation, source-rock maturity assessment, early oil generation, application of biological marker compounds, and kinetic modeling. Methodological topics, such as interlaboratory comparisons and evaluation of both source-rock potential and maturity assessment by Rock-Eval pyrolysis, are also being addressed.

Other research in the USGS on the petroleum geology of the Santa Maria province includes (1) silica and clay diagenetic profiles in the Orcutt field and Los Alamos syncline of the onshore Santa Maria basin; (2) thermal and kinetic modeling of organic maturation in the same areas; (3) high-quality thermal surveys and regional heat-flow studies; (4) synthesis of petroleum occurrence in the region; (5) coordinated organic and inorganic geochemical research on outcrop weathering of source rocks; and (6) fractured-reservoir characterization by fractal analysis.

Basin Evolution in the Foreland of Thin- and Thick-Skinned Thrust Terranes—Example from the Sylhet Trough, Bangladesh

Samuel Y. Johnson and A.M.N. Alam

The Sylhet trough is a subbasin of the Bengal Basin in northeastern Bangladesh that contains a thick fill (12–16 km) of upper Mesozoic and Cenozoic strata. The trough is bounded on the west by the Indian Shield platform; on the north by the Shillong Plateau, a basement-cored uplift in the foreland of the Himalayas; and on the east and southeast by the Chittagong-Tripura fold-and-thrust belt of the Indo-Burman ranges. To the south and southwest, the trough opens to the main part of the Bengal Basin. The tectonic evolution of this trough, inferred from outcrop, core, well-log, and seismic data, reflects the complex interactions of its bounding orogenic belts.

The Sylhet trough occupied a slope and basinal? setting on a passive continental margin from late Mesozoic through Eocene time (fig. 1A). Subsidence may have increased slightly in Oligocene time (fig. 1B) when the trough was located in the distal part of a foreland basin paired to the Indo-Burman ranges. Oligocene fluvial-deltaic strata (Barail Formation) were derived from incipient uplifts in the eastern Himalayas. Subsidence increased markedly in the Miocene Epoch (fig. 1C) in response to westward encroachment of the Indo-Burman ranges. Miocene to earliest Pliocene sediments of the Surma Group were deposited in a large, mud-rich delta system that may have drained a significant proportion of the eastern Himalayas.

Subsidence rates in the Sylhet trough increased dramatically (3–8 times) from Miocene to Pliocene-Pleistocene time (fig. 1D) when the fluvial Tipam Sandstone and Dupi Tila Formation were deposited. These two units thin markedly over anticlinal crests, indicating that the frontal zone of Indo-Burman ranges deformation had advanced into the eastern Sylhet trough

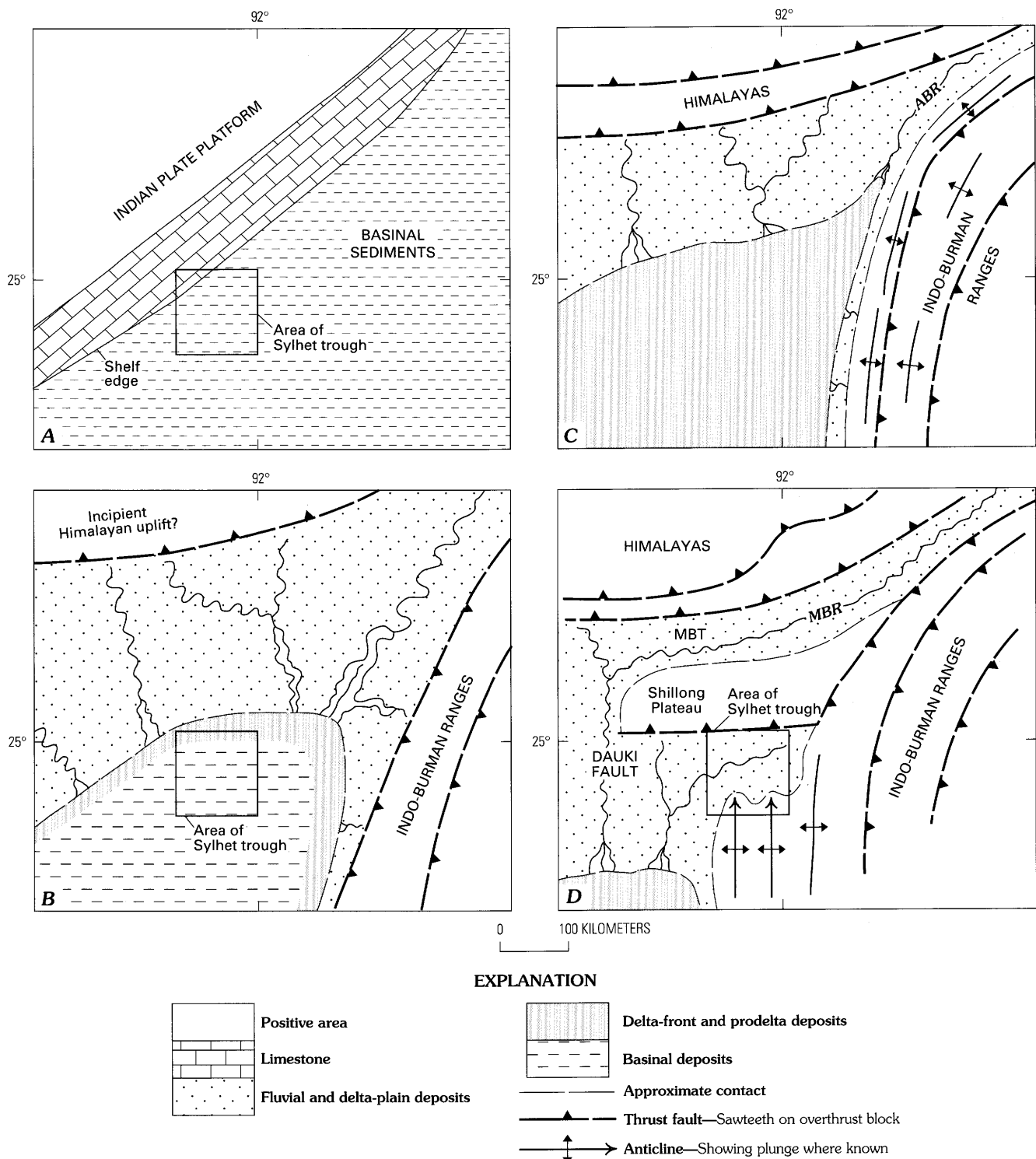


Figure 1 (Johnson and Alam). Schematic paleogeographic reconstructions showing four stages in the Cenozoic evolution of the Sylhet trough: A, middle Eocene; B, Oligocene; C, Miocene; D, Pliocene. Reconstructions A, B, and C restore inferred Shillong Plateau southward displacement. ABR, ancestral Brahmaputra River; MBR, modern Brahmaputra River; MBT, Main Boundary thrust fault. Scale is approximate.

by the early Pliocene. The dramatic increase in subsidence rate is attributed to south-directed overthrusting of the Shillong Plateau on the Dauki fault for the following reasons: (1) Pliocene and Pleistocene strata in the trough thin markedly away from the Shillong Plateau, consistent with a crustal load emplaced on the northern basin margin. (2) The Shillong Plateau is draped by Mesozoic to Miocene rocks, but Pliocene and younger strata are not represented, suggesting that the massif was an uplifted block at this time. (3) South-directed overthrusting of the Shillong Plateau is consistent with gravity data and with recent seismotectonic observations. Sandstone in the Tipam has a marked increase in sedimentary lithic fragments compared to older rocks, reflecting uplift and erosion of the sedimentary cover of the Shillong Plateau.

Southward thick-skinned overthrusting of the Shillong Plateau and westward folding and thin-skinned thrusting in the Indo-Burman ranges have thus occurred in the Sylhet trough area since the early Pliocene. The frontal zone of the Indo-Burman ranges is being depressed by the Shillong Plateau into a foreland basin (fig. 1D). If the Dauki fault has a dip similar to that of other Himalayan overthrusts, then a few tens of kilometers of horizontal tectonic transport are required to carry the Shillong Plateau to its present elevation. Uplift of the Shillong Plateau probably generated a major (about 300 km) westward shift in the course of the Brahmaputra River.

The ARC/INFO Geographic Information System Applied to Geologic Investigations of the Norphlet Formation, Alabama and Mississippi

C. William Keighin and C.J. Schenk

A desirable part of our program to evaluate the natural gas potential of deeply buried reservoirs in the Gulf Coast region was (1) to have a system in which existing map coverage could be integrated with various types of ancillary data, and (2) to display these coordinated data and maps in different combinations at convenient map scales. We found that, although numerous maps of the Gulf Coast area were available, base maps at the desired scale in digital format were not. To provide maximum flexibility in data display in the future, we utilized the GIS (Geographic Information Systems) laboratory of the USGS in Denver. Base maps containing the desired political boundaries and spatial (coordinate) data, obtained as black-line positives, were scanned by Tektronix laser scanning and converted into a data format usable in the ARC/INFO GIS system. Other

information, including location and outline of oil and gas fields, well data, structural data, and location of known salt domes, was added to the GIS system. Using the GIS system, the data could be manipulated to produce different layers of information, and the layers overlaid in different combinations to produce maps.

An initial target for evaluation is the Upper Jurassic Norphlet Formation, because this formation is an important hydrocarbon reservoir in Alabama in Baldwin and Mobile Counties, offshore in Mobile Bay, and it produces condensate from the Flomaton field in Escambia County. Depth to the producing horizon varies, but it reaches approximately 21,000 ft in offshore wells in Mobile Bay. The Norphlet also contributes limited quantities of oil and gas in a few fields in Mississippi. In line with our recognizing the importance of map data integration and the usefulness of the GIS, we wanted to graphically relate distribution, depths, and production levels of Norphlet fields to known geologic features such as faults and salt domes, and to fields producing from other formations. We needed to display these relationships in various combinations and at different scales. Although Norphlet production does not appear directly related to distribution of salt domes in this region, because salt domes are important indicators of Gulf Coast geologic history, we wanted to graphically show their distribution and spatial relationship to other hydrocarbon-producing fields and formations.

The Santa Maria Province Project, California

Margaret A. Keller, Caroline M. Isaacs, and Richard G. Stanley

The Santa Maria Province Project of the U. S. Geological Survey is an undertaking jointly sponsored by the Evolution of Sedimentary Basins and Onshore Oil and Gas Investigations Programs. The project is a 5-year study involving more than 60 researchers from government agencies, academia, the oil industry, and consulting firms. The study area is the onshore region west of the Sur-Nacimiento fault and north of the Santa Barbara Channel together with adjacent offshore areas, a region including the onshore Santa Maria basin proper, the offshore Santa Maria, western Santa Barbara-Ventura, Pismo, and Huasna basins, and several other small basins and basin fragments. Onshore, the Santa Maria province contains the world's largest diatomite deposit as well as major petroleum deposits (>1 billion bbl recoverable). The province includes the most extensive fractured petroleum reservoirs in California and, in the offshore, the largest United States petroleum discoveries since Prudhoe Bay.

The Santa Maria province has a complex tectonic history. Mesozoic and lower Paleogene rocks form a collage of tectonostratigraphic terranes that apparently accreted to the North American continent by late Eocene time. Many questions remain about the sites of origin of the terranes, their travel paths, and the processes and timing of terrane suturing and continental "docking." Overlying the pre-Eocene rocks and fragments of Eocene marine strata is a widespread and thick pile of sedimentary and igneous rocks deposited in numerous basins that began to form along the continental margin during the late Oligocene and early Miocene. The Oligocene to Pleistocene rocks of the province exhibit rapid lateral changes in facies and thickness and include (1) nonmarine alluvial fan, lacustrine, and fluvial deposits; (2) shallow-marine sandstones and conglomerates; (3) bathyal marine mudrocks, including the organic-rich biogenous strata of the Miocene Monterey Formation (source of the diatomite and petroleum deposits); and (4) volcanic rocks ranging in composition from rhyolite to basalt. The origin of the Neogene basins is controversial; wrench tectonism, regional extension, large-scale block rotation, and combinations of these three mechanisms have been proposed. Differences among the mechanisms are great enough that Miocene paleolocations, onshore-offshore orientations, and basin geographies remain uncertain. However, Miocene facies and their subsequent structural, thermal, and compaction history controlled petroleum generation and reservoir formation in this region.

Studies in the Santa Maria Project have focused on the stratigraphic and structural framework, with particular emphasis on detailed mapping in key areas and intensive study of important stratigraphic sections in outcrops and wells. Many good surface exposures occur in the province and extensive subsurface data are available from both onshore and offshore. Major geologic problems addressed by the project are (1) the origin and timing of terrane accretion; (2) the origin and history of the Neogene sedimentary basins; (3) Miocene paleogeography and lateral facies changes; and (4) the thermal and structural history of the province.

Completed or nearly completed projects include (1) geologic mapping in the San Rafael Mountains and Santa Lucia Range; (2) detailed sedimentologic and biostratigraphic study of the Oligocene through Miocene nonmarine and marine sequence; (3) new radiometric dating of Oligocene and Miocene volcanic units; (4) equilibrium temperature surveys in key wells; (5) coordinated study of thermal history utilizing clay diagenesis, silica diagenesis, and biomarker maturation parameters; and (6) analysis of the USGS seismic data collected in 1990 in the offshore Santa Maria and Santa Barbara-Ventura basins. In addition, the following regional summaries are either underway or completed:

(1) major correlation sections based on outcrop, subsurface, and geophysical data; (2) compilations of the geology, gravity, and magnetics; and (3) a synthesis of the province's geologic evolution from Jurassic to Holocene. Completed project publications include a province bibliography, core workshop volume published by the Society for Sedimentary Geologists, numerous USGS Open-File Reports and Maps, numerous abstracts, and journal articles. Publications in progress include USGS Bulletin 1995 (a multiple chaptered series on the province studies), a 1:100,000-scale compiled geologic map of the province, and several more USGS Open-File Reports and Maps.

Fracturing and Reservoir Development in the Katakturuk Dolomite, Arctic National Wildlife Refuge, Alaska

John S. Kelley, Chester T. Wrucke, and Augustus K. Armstrong

The Katakturuk Dolomite of Proterozoic age, a possible petroleum reservoir under the Arctic coastal plain of the Arctic National Wildlife Refuge (ANWR), is about 2,500 m thick in the Sadlerochit and Shublik Mountains. The Katakturuk in this area has a structural setting similar to that north and east of the Sadlerochit Mountains under the coastal plain of ANWR, where pre-Mississippian rocks are involved in Brooks Range thrusting.

Reservoir properties of the Katakturuk Dolomite owing to depositional fabric and diagenesis are poor but likely are enhanced by fracturing. Reservoir properties were examined in thin section and measured from outcrop samples in the Sadlerochit Mountains and core from the Canning River Unit A-1 well west of the Sadlerochit Mountains, but their values are too low to explain the flow rate from a drill-stem test in the Katakturuk. In the Canning River Unit A-1 well, the Katakturuk yielded 134 barrels of fresh water with a calculated flow rate of 4,800 barrels per day (data from the 1987 study of Bird and others). The drill-stem test from which the flow rate was calculated included the interval cored and sampled for porosity and permeability measurements. Enhancement of permeability through fracturing could explain the flow rate. Fractures are pervasive in the Katakturuk in the Sadlerochit Mountains and likely are related to folding and thrust faulting.

Early dolomitization and cementation in the Katakturuk Dolomite largely obliterate porosity and permeability. Dolomite rhombs 2–6 μm across replace framework clasts originally composed of peloids, microbial fragments, microbial-laminated clasts, ooids,

pisolites, oncolites, mud pellets, coated grains, and fragments of microbial mats, early cements, and micrite. Dolomite cement, chalcedony, and spar calcite infill voids consisting of internal molds in oolites and pisolites and fenestral cavities in microbial mats and stromatolites. Much of the formation is massive dolostone composed of xenotropic dolomite rhombs 100–500 μm across. The intercrystal pore space of the massive dolostone is mostly filled with dolospar, calcite, and silica cements.

Forty-three samples of the Katakturuk Dolomite from the Sadlerochit Mountains and 9 samples from core in the Canning River Unit A-1 well have low measured porosity and permeability (according to a 1987 study by K.J. Bird and others). Mean porosity for outcrop samples is 2.3 percent. Although a single outcrop sample had a porosity of 10 percent, all other samples had porosities of 0.8 to 6.2 percent. Measured permeabilities from outcrop samples range from less than 0.1 to 1.6 mD (millidarcies); nearly half the samples have permeabilities less than 0.1 mD. Samples from the Canning River Unit A-1 well have a mean porosity of 0.7 percent and a range from 0.3 to 1.1 percent. Permeabilities for all well samples are 0.1 mD or less.

The Katakturuk Dolomite in the Sadlerochit Mountains crops out in the south limb of an east-trending, doubly plunging regional anticline. The Katakturuk dips 10°–30° more steeply to the south than unconformably overlying Mississippian and younger strata. The steeper dips in the Katakturuk largely result from the angular unconformity beneath Mississippian limestone. The south-dipping Weller thrust at the base of the Katakturuk extends the length of the anticline and emplaces the Katakturuk over steeply dipping strata of Paleocene age in the western Sadlerochit Mountains. Displacement on the thrust diminishes to the east and becomes negligible where the thrust separates the Katakturuk from underlying Precambrian argillite and sandstone in the eastern Sadlerochit Mountains. Two sets of high-angle faults in the Katakturuk subtend the direction of tectonic transport in the Sadlerochit Mountains. One set trends about N. 30° E. and the other set about N. 45° W. The northeast-trending faults have left-lateral separations that typically are greatest near the thrust and diminish upward and away from the thrust. Systematic offset is not recognized in northwest-trending faults. Fracturing in the Sadlerochit Mountains is most intense within the Katakturuk that crops out between the folded angular unconformity at the base of concentrically folded Mississippian strata and the Weller thrust.

The fractures and faults in the Katakturuk Dolomite are thought to have resulted as the dolomite accommodated to concentric folding that developed during Tertiary time in Brooks Range thrusting. As concentric folds became dominant in the Mississippian limestone and younger strata, the angular relation

between the Katakturuk and Mississippian and younger strata severely limited bedding-plane slip as an accommodation to concentric folding within the Katakturuk. Pervasive fracturing and movement by distributed shear within the Katakturuk became the principal mechanism of deformation of the brittle carbonate strata of the Katakturuk as the dolomite became incorporated into the core of the fold during folding and thrusting. The sets of high-angle faults above the Weller thrust and mostly within the Katakturuk are likely conjugate faults that provided a mechanism of mass transport and contributed maximum contraction north-northwest, parallel to the direction of tectonic transport during folding and thrusting.

Major Controls on Accumulation of Upper Cretaceous Coals in North America

M.A. Kirschbaum, L.N.R. Roberts, and P.J. McCabe

Climate, subsidence rates, and eustasy were the primary controls on the accumulation of the extensive Cretaceous coal deposits of North America. To better understand the relative importance of these controls, we constructed a series of paleogeographic and isopach maps for selected biostratigraphically constrained intervals. Our maps suggest that the higher subsidence rates associated with foreland basins were critical in determining the geographic location of thick Cretaceous coal deposits. In these basins, rates of base level change produced by subsidence and eustasy determined the stratigraphic position of the coals within the sedimentary sequence.

Most Cretaceous peat-forming environments developed along broad coastal plains within 60 km of the Western Interior seaway. Restriction of the Cretaceous coals to coastal plain environments suggests that a maritime climate created by the epicontinental seaway was critical in mire development. In the Maastrichtian, for example, extensive non-coal-bearing fluvial strata and variegated paleosols, some containing carbonate nodules, accumulated inland from these coastal plains. Good drainage and lower rates of precipitation in the inland areas precluded the accumulation of peat.

The thickest Cretaceous coals are thought to have accumulated in areas where peat accumulation kept pace with the tectonic subsidence rate. Subsidence rates can be estimated from sediment accumulation rates, which during the Cenomanian were as much as 280 m/m.y. The thickest Cenomanian coals formed in the foreland basin associated with the Sevier orogenic belt where sediment accumulation rates were between 70 and 215 m/m.y. The

east side of the seaway also had suitable peat-forming environments, but because the subsidence rates were lower (sediment accumulation rates < 50 m/m.y.), the coals are thinner and laterally less extensive than those of the foreland basin.

Subsidence rates also affected paleogeographic configurations. For example, high subsidence rates in southern Wyoming and northern Colorado during the Maastrichtian produced a major embayment of the Western Interior seaway covering about 14,000 km². In this area, as much as 2,900 m of Maastrichtian strata was deposited over a period of about 6 m.y., and more than 20 billion metric tons of coal accumulated in the coastal plain environments along this embayment in the Almond, Williams Fork, Laramie, and Lance Formations.

Evolution of the Illinois Basin

Dennis R. Kolata, W. John Nelson,
Janis D. Treworgy, Stephen T. Whitaker,
Michael L. Sargent, Lloyd C. Furer, and
M.C. Noger

The Illinois Basin is one of the major interior cratonic basins of North America, covering an area of approximately 110,000 mi² (285,000 km²) in Illinois, Indiana, and Kentucky. It comprises about 120,000 mi³ (500,000 km³) of Paleozoic rocks containing a wealth of resources, including coal, oil and gas, ground water, and industrial minerals and metals. To the present time, some 4 billion barrels of oil has been produced from depths mainly shallower than 3,000 ft. About 9 billion tons of an estimated 268 billion tons of original in-place bituminous coal resources has been mined in the basin.

Knowledge of the basin's structural and stratigraphic framework and tectonic history has been enhanced by new regional cross sections, subsurface mapping, and geophysical studies.

The origin and evolution of the basin are closely related to the development of the Reelfoot rift and Rough Creek graben, a failed rift situated at the south end of the basin. The rift system formed during breakup of a supercontinent, apparently during late Precambrian to Early Cambrian time. Lithospheric extension within the rift system resulted in tensional block faulting and relatively rapid subsidence and sedimentation. By Late Cambrian the tectonic setting changed from a rift basin to a broad cratonic embayment centered over the rift. During the remainder of the Paleozoic Era, the proto-Illinois basin was a broad trough extending from the continental margin in central Arkansas northward through Illinois, Indiana, and western Kentucky. Sedimentation during the Paleozoic was dominated by

deposition of carbonates and to a lesser extent by sandstone, shale, and siltstone. Basin fill, after Pennsylvanian rocks were deposited, exceeded thicknesses of 20,000 ft (6,000 m) in the Rough Creek graben area of southern Illinois and western Kentucky and probably was even thicker within the Reelfoot rift. Structural deformation in the basin began in Valmeyeran time concurrent with the initial accretion of continents that later formed the Pangea supercontinent. Compressional stresses emanating from the Allegheny and Ouachita orogenies were transmitted to the continental interior, reactivating faults within the Reelfoot rift and Rough Creek graben and causing uplift of basement-block structures throughout the Illinois basin. The compressional phase was followed by a post-Early Permian episode of extension that probably coincided with breakup of Pangea. Tensional stresses reactivated faults within and adjacent to the Reelfoot rift and Rough Creek graben.

Post-Pennsylvanian, pre-Late Cretaceous uplift in the area of the Reelfoot rift structurally closed the south end of the Illinois basin, creating the present basin geometry. By the end of the Mesozoic Era, this uplift had been beveled and overlapped by Upper Cretaceous and lower Tertiary rocks of the Mississippi Embayment. The midcontinent region, including the Illinois Basin, is presently experiencing east-west compressive stress that apparently is reactivating faults within the southern part of the basin, particularly in the Reelfoot rift.

The Illinois Basin Consortium (IBC), consisting of the Illinois, Indiana, and Kentucky Geological Surveys, is presently conducting joint basin-wide studies to gain a better understanding of the basin-forming, -filling, and -modifying processes. One of the primary missions of the IBC is to assess the potential for ground water, coal, oil, natural gas, and industrial-mineral resources. The IBC is conducting basin research in cooperation with geoscientists from universities, the USGS, and other government agencies.

GIS Visualization of Coal Stratigraphic and Geochemical Information

Kathleen K. Krohn, Carol L. Molnia,
Susan J. Tewalt, and William G. Miller

The National Coal Resources Data System (NCRDS) of the USGS is an integrated GIS (Geographic Information System) digital system that accesses a master data base and a suite of 2- and 3-dimensional vector and raster mapping, display, and statistical capabilities for data analysis and visualization.

Currently the system is composed of a network with main nodes in Reston, Va., and Denver, Colo., and

is accessed by scientists and other coal experts within and outside the USGS. Twenty-two State geological agencies have cooperative agreements with NCRDS and either access the system from remote sites via commercial and USGS telecommunications networks or are implementing the public domain software on local workstations. Software modules operate on a range of hardware platforms running Unix and X-windows. Current hardware includes three Sun 4 servers, desktop workstations, microcomputers (IBM-PC compatibles), and mainframes. Enhancement of software and acquisition and integration of hardware are ongoing to provide coal geologists the means to analyze multiple coal data elements and to create a variety of maps with enhanced flexibility and interactivity.

The data-base information includes stratigraphic descriptions and coal-quality data (trace element, Btu, ash, and sulfur analyses) located by latitude and longitude, as well as summary files (coal tonnage and coal-quality information) located by geographical area. The basic geologic data are used primarily to model coal deposits and analyze resource estimates in 2- and 3-dimensional maps and diagrams.

A major concern of NCRDS is to provide cost-effective software solutions. Currently, NCRDS has found it necessary and desirable to use a combination of both in-house developed software and commercial software. A robust suite of raster-based GIS techniques is encompassed in GRASS (Geographic Resources Support System) being developed by the U.S. Army Corps of Engineers. USGS is enhancing GRASS software to meet NCRDS needs as both an analytical tool and a data-base access facility. At present, NCRDS has the following programs available for use for resource assessment and mapping: GRASS, Dynamic Graphic's Interactive Surface Modeling (ISM), a USGS version of semivariogram modeling and Kriging geostatistics, subsets of ARC/INFO, and USGS's GARNET. Image analysis techniques are being investigated for their applicability to coal geology analysis.

Coal resource tonnage analysis provides an example of how multiple digital-mapping software capabilities are used. First, the data specified are gridded and contoured in software of choice. Then the areas of interest are defined by a series of boundaries that include outcrop geology, thickness, sulfur content, structure, overburden, and other variables of interest. Finally, volumes are determined and the tonnage of coal meeting specified criteria is calculated. These techniques have been used successfully in a variety of projects on a local (lease tract, quadrangle-based) and regional (basinal) scale.

Research continues on the integration of object-oriented data-base-management (OODBMS) techniques to provide a link between the GIS data

visualization options and the master data base. Postgres is the extension to Ingres, which is the relational database management system in use by NCRDS. This software is being developed by the University of California at Berkeley. Investigations are underway to determine its suitability as a vehicle to meet the graphical analysis and data-management needs of geologists, for GIS projects of short- and long-range application.

Alteration of Lignin During Biodegradation in Peats and the Early Stages of Coalification

Harry E. Lerch, William H. Orem, and Timothy A. Moore

Lignins are one of the most important groups of biosynthesized, organic macromolecules produced on Earth. They are produced exclusively by vascular plants primarily in wood, and have a cross-linked, methoxy-substituted, polyphenol chemical structure, often bonded to complex carbohydrates in plants via ether linkages (for example, as lignocellulose). The chemical structure of lignins makes this group of compounds resistant to microbial degradation following the death or senescence of plant biomass. Thus, lignins and lignin residues are often abundant in soils, peats, and sediments. In addition, lignin residues are thought to be the major contributors to the aromatic structures of coals.

Details of the changes in the macromolecular structure of lignins that occur during early diagenesis and the early stages of coalification are poorly understood, and our work has focused on the chemical structural changes in lignin biopolymers which occur during these processes. We are using a number of different organic geochemical techniques to elucidate these chemical changes, including solid state ^{13}C nuclear magnetic resonance spectroscopy (NMR), pyrolysis-gas chromatography (PY-GC), and gas chromatography-mass spectroscopic (GC-MS) analysis of cupric oxide lignin oxidation products (LOP). Peat and low-rank coal samples from a number of different locations were studied; however, emphasis was placed on peat and coal samples from Kalimantan (Borneo), Indonesia.

Results of ^{13}C NMR studies of peats have shown that lignin is preserved in some environments and rapidly degraded in others. In all environments studied, carbohydrates are preferentially biodegraded compared to other biomolecules. However, in many extensive acidic peat deposits (such as Indonesian peats and Okefenokee Swamp peats), lignin is also rapidly degraded from the peat. In these low-pH environments, the remaining peat organic matter consists primarily of aliphatic substances

such as cuticular waxes. The biodegradation of lignin produces aromatic-rich organic acids that may contribute to the low pH and dark color of the water in these wetlands. Pyrolysis-GC and GC-MS studies of LOP in these acidic peats have confirmed that lignin degradation is an important process. This process, however, does not involve the preferential biodegradation of individual phenols (such as vanillyl, syringyl, p-hydroxyl and cinnamyl phenols) that constitute the lignin macromolecule. Our LOP studies in a number of wetlands have shown that the relative proportions of the individual phenols in lignin remain about the same during biodegradation. Thus, specific lignin monomers are not selectively degraded.

Our ^{13}C NMR studies of low-rank coals indicated that fragments of the lignin molecule may be present in a relatively unaltered condition in some samples. This was implied by distinct peaks from methoxyl, phenolic, and aromatic carbons in the ^{13}C NMR spectra. However, other samples showed little evidence of preserved lignin in their ^{13}C NMR spectra, although broad peaks in the aromatic region indicated that highly altered lignin was present. Further studies of two of these coal deposits from Indonesia (SS-1 and 1001), conducted using the LOP method and GC-MS, showed the presence of measurable amounts of unaltered lignin in both sets of samples. Thus, relatively unaltered lignin can survive both biodegradation and early stages of coalification and may provide information on the environments of coal deposition. In the case of the two Indonesian coals, the LOP results indicate that the SS-1 samples apparently formed in an angiosperm-dominated swamp and the 1001 samples in a gymnosperm-dominated swamp. We are currently investigating the chemical structures of unknown peaks in the LOP chromatograms of these coals. This may provide information on subtle changes to lignin polymers that occur during the earliest stages of coalification.

Role of Water in Petroleum Formation

Michael D. Lewan

Laboratory experiments show water to be a critical component in natural petroleum generation and expulsion. The significance of water is best demonstrated by an experimental approach referred to as hydrous pyrolysis. Similar to natural maturation in subsiding sedimentary basins, this experimental approach maintains a liquid water phase in contact with a source rock as it is heated. Although these experiments require higher temperatures (250–365 °C) to offset the longer durations at lower temperatures experienced in natural maturation, the products are similar in bulk chemical, molecular, physical, and isotopic character to natural

maturity products. Hydrous pyrolysis experiments conducted on potential source rocks show that petroleum formation involves two overall reactions: (1) partial decomposition of insoluble kerogen to soluble, high-molecular-weight bitumen; and (2) partial decomposition of bitumen to a liquid, expelled oil.

The first overall reaction involves the cleavage of weak noncovalent bonds in the kerogen. Cleavage of these bonds to form the high-molecular-weight bitumen does not appear to be influenced by the presence of water. A volume increase associated with this overall reaction causes the generated bitumen to expand into micropores and along bedding-plane partings. It is crucial to the effectiveness of most source rocks that a continuous bitumen network develop through the rock matrix as a result of this overall reaction. Under hydrous conditions, a significant amount of interstitial water in the rock is dissolved in the bitumen network. This water-saturated bitumen network is maintained in hydrous pyrolysis experiments by the liquid water surrounding the source rock in the reactor, and in nature by the liquid water surrounding the source rock in dissecting fractures or faults and adjacent porous rocks.

Unlike the first overall reaction, the second overall reaction, that of bitumen partially decomposing to oil, involves the cleavage of covalent bonds and is dependent on the presence of water. The role of water in this overall reaction is both chemical and physical. Chemically, the dissolved water in the bitumen network terminates free-radical sites by donating its hydrogen atoms during bitumen decomposition. This process reduces the frequency of β -scission, disproportionation, and cross-linking reactions, thereby enhancing oil generation and inhibiting pyrobitumen generation. Physically, the resulting oil generated by this overall reaction is immiscible in the water-saturated bitumen and forms a separate phase. In addition to the buoyancy force generated by the density difference between the immiscible oil and the water-saturated bitumen, a net volume increase associated with the partial decomposition of bitumen to oil generates an internal force within the confining mineral matrix of a rock. As a result, the immiscible oil is expelled from the rock as it is being generated.

The processes and mechanisms responsible for generation and expulsion of oil in hydrous pyrolysis experiments are considered the same as those in nature. However, the *degree* to which they are operative in nature remains to be determined through additional research. Overburden and confining pressures may have some influence on these processes and mechanisms, but as a first approximation, the higher temperatures used in hydrous pyrolysis are likely to have the greatest influence. The solubility of water in the bitumen network decreases with decreasing temperature. Therefore, a reduction in

the amount of water dissolved in the bitumen under the lower temperatures characteristic of natural maturation may result in a corresponding reduction in immiscible-oil generation. The same processes and mechanisms may thus be operative in hydrous pyrolysis and natural maturation, but the amount of oil generated and expelled by hydrous pyrolysis may to some degree be exaggerated. An implication of this assessment is that thermally immature rocks incapable of generating and expelling oil in hydrous pyrolysis experiments are definitely incapable of becoming effective source rocks in nature.

Thermochronologic Constraints on Relation Between Extensional Geometry of the Northern Grant Range and Oil Occurrences in Railroad Valley, East-Central Nevada

Karen Lund, L. Sue Beard, L.W. Snee, and William J. Perry, Jr.

Geologic mapping in the northern Grant Range, east-central Nevada, has resulted in a new model for Neogene crustal attenuation in the Grant Range and adjacent Railroad Valley and for petroleum generation in Railroad Valley. During attenuation, source rocks in the upper plate may have undergone maturation and release of hydrocarbons due to juxtaposition of hotter mid-crustal lower plate rocks against the cooler upper plate rocks. Thermochronology, which shows the timing of heating and subsequent cooling of metamorphosed mid-crustal rocks, enables us to test whether generation of petroleum by heating of upper-plate source rocks coincided with cooling of the lower plate after Neogene tectonic thinning.

In the northern Grant Range, a stacked set of curviplanar low-angle attenuation faults formed as the range arched about a north-northwest axis and as a structural basin formed in Railroad Valley to the west. The style and amount of attenuation were controlled by lithologic character and structural depth of rock units and, locally, by the geometry of the arch. On the steeper west side of the Grant Range arch, the curviplanar low-angle attenuation faults converge into a single west-dipping low-angle fault zone. Along this zone, unmetamorphosed Mississippian units are juxtaposed over low- to medium-grade metamorphosed Middle Cambrian units and Late Cretaceous granite (fig. 1), creating the greatest amount of attenuation in the range. The distinct geometry of the arched curviplanar low-angle fault array is seen in windows into the structure low on the west side of the range.

Seismic and drill-hole data suggest that the low-angle attenuation faults in the range extend into Railroad

Valley and control the structure buried in the valley. Both petroleum source and reservoir rocks in Railroad Valley oil fields are located in extensively fractured rocks in the upper plate of the major low-angle attenuation fault system. In the valley, as in the range, relatively cold upper plate rocks, immature with respect to hydrocarbon generation, were brought into contact with hotter lower plate rocks by extensional processes. Evidence for Neogene heat in metamorphic lower plate rocks is indicated by static mineral growth that overprints earlier dynamothermal metamorphic fabric. In addition, preliminary $^{40}\text{Ar}/^{39}\text{Ar}$ thermochronologic results show that the dynamothermal metamorphism occurred in Late Cretaceous, but the thermal pulse associated with the secondary static mineral growth began in Oligocene. Protracted cooling of the hot lower plate and transfer of heat to the upper plate allowed maturation of upper plate source rocks.

Oil and Gas—Where in the World and Why

C.D. Masters

From the inception of the World Energy Resources Program of the USGS, one of our most important objectives has been to identify new areas that might make a difference in available supplies of world oil and gas and to determine possible supply quantities that might derive from specific areas. Overall, our studies suggest that the occurrence of ultimate world oil resources (including Cumulative Production, Identified Reserves, and Undiscovered Resources) will be about 2,100 billion barrels (BB) and for gas, about 10,000 trillion cubic feet (TCF). From a Btu perspective (6,000 ft³/barrel of oil), these resource numbers show more oil than gas. This is a surprising outcome in that, worldwide, we can expect to recover about 80 percent from a gas reservoir, whereas 33 percent is an approximate average recovery for oil reservoirs; further, conventional wisdom suggests that more geologic opportunities exist for gas source rock than for oil. An explanation of these seeming contradictions may be in the enormous gas deposits found under unconventional circumstances as well as in the recognition that gas requires better sealing properties to hold it in place. The fact that the gas resource is less well developed than is the oil (80 percent of the ultimate oil resource has been discovered compared to only 60 percent of the gas) offers room for continued adjustment of the ultimate resource proportions, but we judge that the two resources will ultimately be found to occur in approximately equal quantities.

This amount of oil and gas is enormous relative to annual use: Identified Reserve to Production ratios

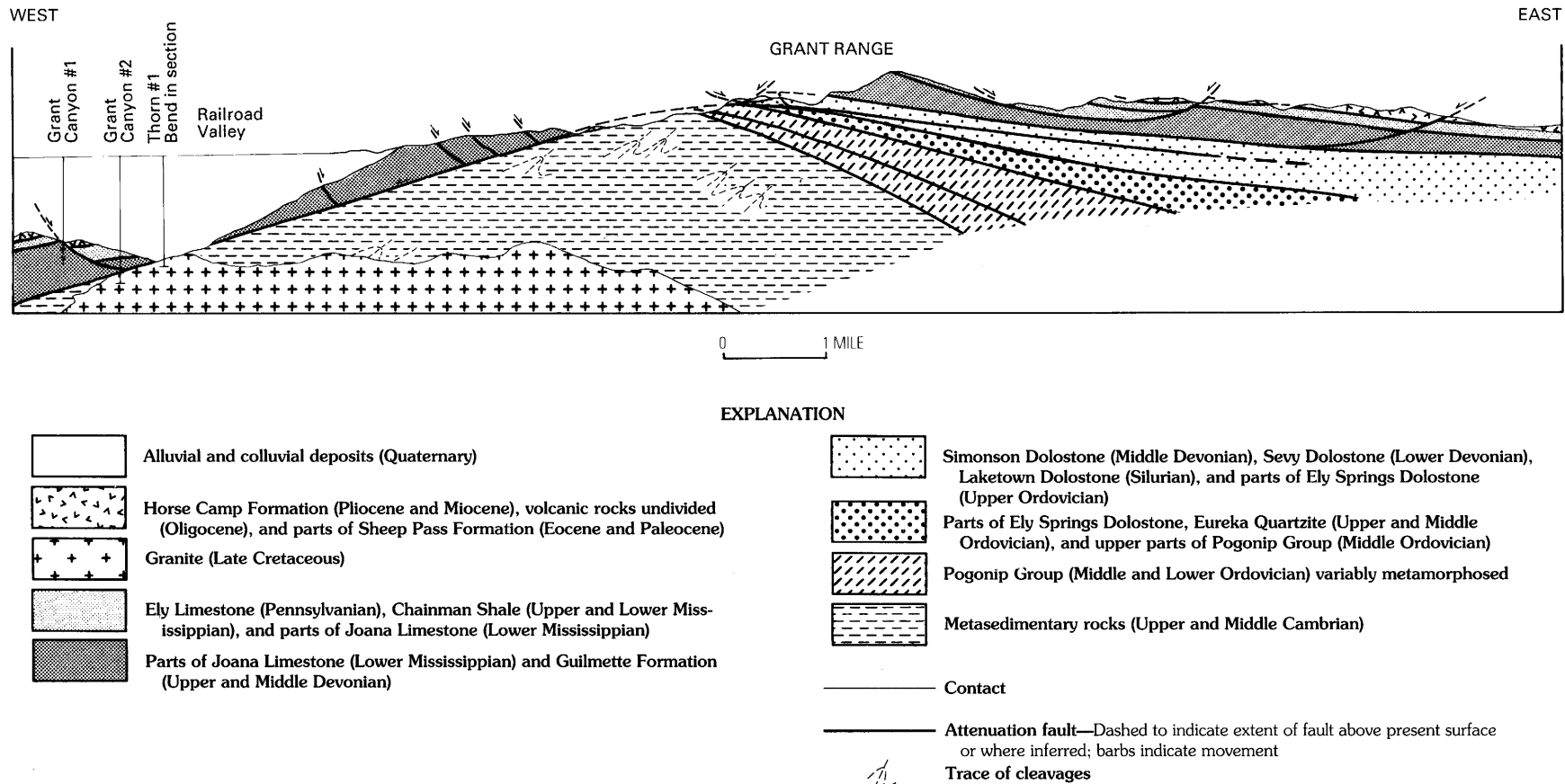


Figure 1 (Lund and others). Cross section showing tectonic relations in the northern Grant Range, east-central Nevada. No vertical exaggeration. Subsurface information generalized from drill-hole data, 1988 study of Veal and others.

EXPLANATION

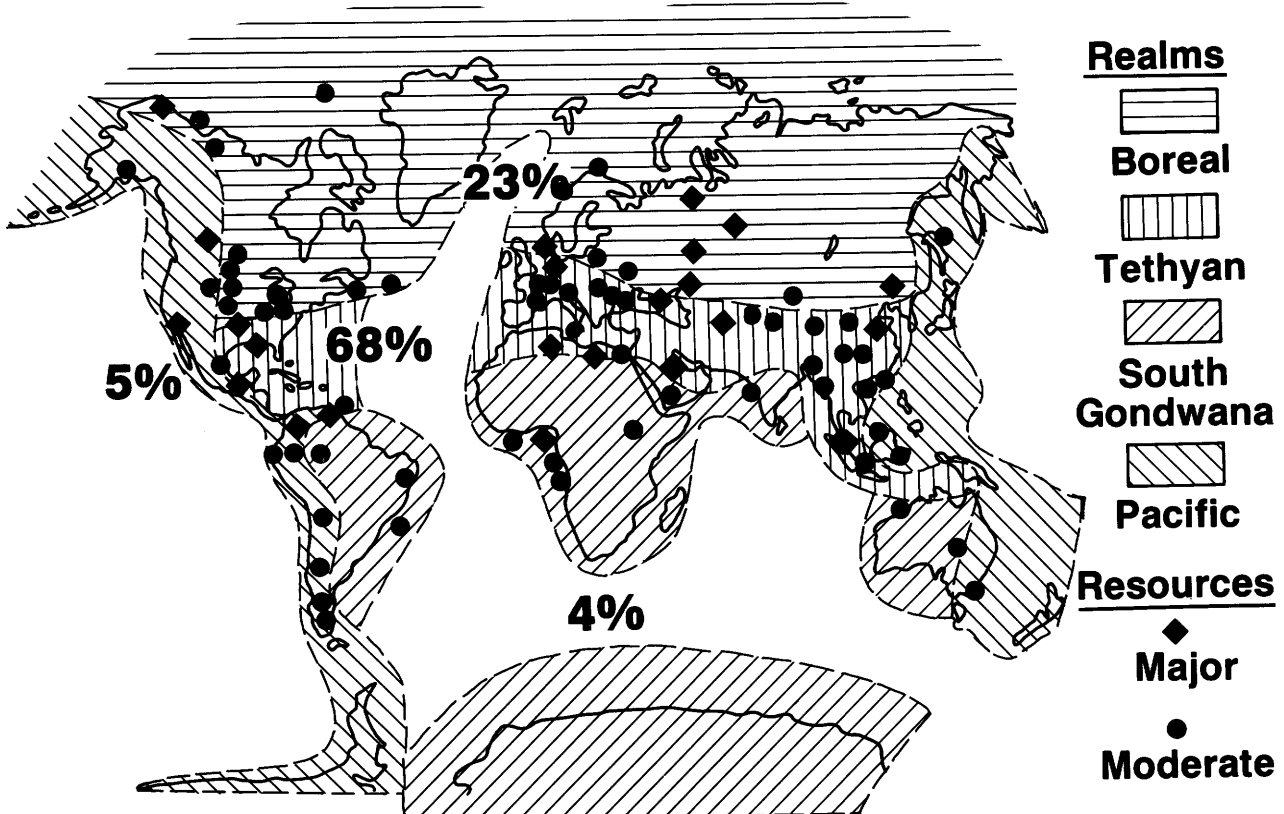


Figure 1 (Masters). Geographic distribution of the four petroleum realms of the world showing the percent amount of discovered oil and gas in each realm. Also shown are the locations of the major and moderate occurrences of world petroleum.

exceed 50:1 for oil and 60:1 for gas. Quantity, however, is not so much an issue as is the distribution of the resources relative to market. Seventy-five percent of the world's ultimate recoverable oil and gas is concentrated in the Middle East, the U.S.S.R., and North America. From an historical perspective, North America clearly is rich, but the data also show that we have been far and away the heaviest users of oil and gas and are, in turn, the most mature in its development and extraction. We have now reached a stage wherein our demand for oil far exceeds our capability to produce, and for best market terms we should prefer a wide spread of foreign suppliers. According to our resource analyses, such a broad supply base at present exists in oil and, given judicious changes to more broadly based gas resources, we can expect to benefit from a diversity of supply sources, but only for a couple of decades. Then, world supply will become increasingly, and more narrowly, the purview of the Middle East.

This scenario assumes that the distribution of world oil and gas has been established. We believe that to

be true, for both statistical and geological reasons. For oil and gas to occur at all, five commonly independent variables, including source rock, reservoir rock, trap, seal, and timing, all must be positive; and for oil and gas to occur in large quantities, one or more of those variables must be unusually favorable. Given these requirements, we expect oil and gas to be distributed sparingly and only rarely present in large quantities. In the 12 years of our program geological studies, we have found confirmation of this statistical probability and we do not expect the discovery of any large new basins that would significantly alter the distribution of world oil.

To explain the distribution of petroleum as we interpret it, two members of our World Energy Resources Program, Gregory Ulmishek and Doug Klemme, propose as a working hypothesis that paleoclimate and tectonics play such a predictable role in the generation and entrapment of oil that we can define four realms of petroleum occurrence (fig. 1): the Tethyan Realm, the Boreal Realm, the South Gondwana Realm, and the Pacific Realm. Three of the necessary

independent variables to the occurrence of petroleum are climate controlled. (1) Source-rock-producing organisms occur in relatively greater quantities in equatorial waters between the 30° paleolatitudes, north and south; also, in low latitudes, the absence of lake turnover precludes an otherwise annual oxidizing event, thereby contributing to source rock development. (2) Carbonate reservoirs, which compose 50 percent of petroleum reservoirs, develop in significant quantities only in low latitudes. (3) Salt, the best of all sealing materials, forms mainly between the 30° latitudes, north and south. The identified Tethyan Realm enjoyed this geographic position throughout geologic history and is responsible for 68 percent of the world's discovered oil and gas. The geographic elements of the Boreal Realm passed Paleozoic time in the low latitudes before migrating into the temperate region. Except for the Upper Jurassic source rocks, which were deposited during an abnormally warm time, dominant source rocks in the Mesozoic and Cenozoic are gas prone; the Boreal Realm is responsible for 23 percent of the world's discovered oil and gas. The continental fragments of South Gondwana did not experience a move into equatorial waters until the Early Cretaceous, and most of its oil and gas, constituting 4 percent of the world's discovered total, is associated with Mesozoic and Cenozoic sedimentary rocks of passive continental margins.

The Pacific Realm, through tectonic action, destroyed most of the sedimentary column below the Miocene and enriched the younger reservoir rocks with volcanic clasts and matrix. Windows of favorable rock, however, survived locally, and the Pacific Realm accounts for 5 percent of discovered oil and gas.

Estimates of Undiscovered Resources suggest that the proportional distribution of the oil and gas assigned to the four different realms is similar to that calculated for discovered sources.

Sequence Stratigraphy in the Search for Hydrocarbons in Nonmarine Strata

Peter J. McCabe

Depositional sequences are produced by the interplay of the basic controls of climate, eustasy, and tectonism. Close to a shoreline, changes in relative sea level, produced by the interplay of eustasy and subsidence, are critical in determining the packaging of strata. For at least tens of kilometers inland from a shoreline, valley incision and rates of change in accommodation space are primarily controlled by fluctuations in relative sea level. Farther inland, changes in stratigraphic base level and rates of sediment flux

increasingly become a function of tectonism in the source area and of climatic change. Some terrestrial strata, such as those deposited in intermontane basins, clearly are not directly influenced by changes in relative sea level; but they contain unconformities of regional extent and can, therefore, be subdivided into sequences. However, climate, eustasy, and tectonism are not independent variables. Eustasy, for example, is controlled in part by global climate, but regional variations in land/sea geometries, controlled by eustasy, influence local climatic regimes. At least in theory, therefore, it may be possible to correlate eustatically driven sequences with climatically driven sequences.

Climate is a critical factor in determining the type and style of terrestrial sedimentation whereas rates of base-level change determine the thickness and stacking patterns of these facies. A clear link should therefore exist between the geometry of stratigraphic sequences and the lateral and vertical variations in facies within them. Recent work at the USGS has related the style and geometry of fluvial sediments and coal deposits to regional sequence stratigraphic interpretations in Cretaceous strata of the Western United States. These studies suggest that laterally amalgamated fluvial channel-sandstones and thin coals form at times of slow rates of base-level rise and are coeval with marked forward- or backward-stepping shoreface parasequence geometries. More isolated channel-sandstones and thick coal deposits form at times of faster rates of base-level rise and are coeval with vertically stacked shoreface deposits. Our studies also suggest that the local climate became more seasonal during lowstands in sea level: as a result, some facies, such as coal, are better developed at highstands, whereas other facies, such as braided river sediments, are better developed at lowstands.

The development of models that relate sequence stratigraphy to depositional facies will allow better correlation of nonmarine strata than is otherwise possible. Such models could be used to predict the size of fluvial and eolian reservoirs and the location of economic facies, such as coal and lacustrine source rocks, or the presence of reservoir seals, such as mudstones. These models will have profound impact in the search for hydrocarbons in nonmarine strata.

Redefining Hutton's Unconformity—Geology in a Digital World

William G. Miller

The USGS (U.S. Geological Survey) is producing many data products and publishing them in machine

readable form. The CD-ROM has become the method of choice for digital publication. Different skills are required to use the digital products than were required of the observational geologists of Hutton's day, and the markedly different approaches of observational versus analytical geoscience have in some instances created a culture clash. The differences inherent in such a clash are often as striking as the geological differences observable in, for example, the sandstone beds of the Yorkshire coast.

Recent releases of digital publications on CD-ROM vary from basic cartography in the form of digital line graphs (1:2,000,000 DLG) to marine sonar studies (West Coast GLORIA) and images from the USGS core library. As of this writing, two disks have been released from the NERSL (National Energy Seismic Library). All these disks are very different from each other: data range from simple lines and polygons (1:2,000,000 DLG) to complete images (West Coast GLORIA) derived from remote sensing data collection. The scientific community requires specific computer skills to use the new digital products; management requires specific computer skills as well, to judge the quality of the USGS products and assess their utility in generating derivative products.

Understanding the spatial resolution of the digital data and its intended use is important in assessing the data set's utility. For example, data points plotted on a map produced from the 1:2,000,000 DLG data may not plot in the State or county expected when displayed at a scale of 1:24,000. This mismatch of the data with its anticipated use will lead some to conclude that digital mapping is not worth the effort. Digital map production will be readily accepted by those who take this kind of information into account.

Equipment must be matched with the intended use of the products. As examples of insufficient equipment, (1) a 9-pin dot matrix printer of the type commonly attached to personal computers will not produce a product of publication quality. (2) A 24-bit true color image cannot be usefully displayed on a 4-bit EGA adapter of a personal computer. (3) The 30-megabyte disk is insufficient to meet the 20,000 megabyte storage requirement for the TIGER data from the U.S. Bureau of the Census (digital cartographic data from the 1990 census). Many USGS digital products are indeed usable on a personal computer; but most, to be used to full advantage, require more advanced hardware and software than generally available on personal computers.

Budgets need to be adjusted to absorb the costs of the new information-producing technologies. For example, a common necessary decision is whether to gather more observations in the field or provide a larger disk for a computer. A balance to strive for allows the gradual evolution of the installed computer hardware base without sacrifice of other aspects of a project: at

some phases of project completion, a technician is more useful than is a scientist. The skill level required to operate many computer systems may require months of training and practice to master, and scientists as such are often unable to invest the time required to master complex computer tools and produce complex products.

Recognizing the virtues and limitations of digital techniques and their products will help establish realistic expectations for their use. Appropriately selected digital products can lead to enhanced productivity by increasing the quality of data produced by a given amount of effort. Digital techniques can also make it possible for a single individual to build upon the skills of others to perform tasks such as cartographic drafting that may be out of that individual's normal experience. Digital products are especially useful in situations where projects must be periodically repeated or the results must be passed on for further examination by others.

Development of the Ellesmerian Continental Margin and the Brookian Orogeny, Alaska—A DNAG Perspective

Thomas E. Moore, Wesley K. Wallace,
Kenneth J. Bird, Susan M. Karl, and C. Gil Mull

A synthesis of the geologic history of northern Alaska developed for the Decade of North American Geology (DNAG) project divides the stratigraphy of the region into the continental Arctic Alaska terrane and oceanic Angayucham terrane. The Arctic Alaska terrane, one of the largest terranes in Alaska, underlies the North Slope and most of the Brooks Range. Rocks of the Arctic Alaska terrane are divided, from bottom to top, into (1) structurally and stratigraphically complex Proterozoic to Middle Devonian rocks of diverse affinity; (2) a laterally extensive succession of uppermost Devonian and Lower Mississippian to Lower Cretaceous nonmarine to marine passive continental margin deposits (equivalent to the Ellesmerian sequence); and (3) upper Mesozoic and Cenozoic siliciclastic foredeep deposits (Brookian sequence). The pre-uppermost Devonian rocks apparently record early to middle Paleozoic convergent deformation and plutonism along the edge of North America, which was followed by rifting in Devonian time. The Devonian rifting event culminated in formation of an ocean basin and paleogeographically complex south-facing Ellesmerian passive margin by Late Devonian time. Subsidence along the passive margin resulted in (1) progressive northward onlap of nonmarine and carbonate platform deposits in Late Devonian and Mississippian time and (2) deposition of neritic to bathyal sediments in Mississippian to earliest Cretaceous

time. The neritic to bathyal deposits are characterized by a southward increase in abundance of condensed basinal deposits. A second rifting event culminated in opening of the Canada basin in Early Cretaceous time and produced the Barrow arch and the modern northern continental margin of Alaska.

The Angayucham terrane, exposed in isolated klippen in the Brooks Range and beneath Jurassic to Lower Cretaceous volcanic-arc rocks of the Koyukuk basin to the south, structurally overlies the Arctic Alaska terrane. The Angayucham terrane consists of two subparallel, allochthonous lithotectonic assemblages, both of oceanic affinity. The structurally lower assemblage consists of imbricated Devonian to Jurassic ocean-island basalts and pelagic sedimentary rocks, whereas the structurally higher assemblage consists of ultramafic and gabbroic rocks of a Middle Jurassic ophiolite. Rocks of the lower unit were metamorphosed to amphibolite facies along the base of the ophiolitic assemblage in Middle Jurassic time. The Angayucham terrane is interpreted to represent an accreted subduction complex and overlying ophiolite that formed the forearc region of a Middle Jurassic volcanic arc in the ocean basin adjacent to the Ellesmerian continental margin.

The Brookian orogeny began in the Middle and Late Jurassic with southward subduction and closure of the part of the Angayucham ocean basin that lay outboard of the south-facing passive margin of the Arctic Alaska terrane (fig. 1A). Fragments of the upper Paleozoic and lower Mesozoic oceanic upper crustal rocks were underplated by subduction beneath an intraoceanic arc and ophiolite and locally metamorphosed amphibolite, thus forming the Angayucham terrane and overlying Koyukuk arc terrane (fig. 1B). In Late Jurassic and Early Cretaceous time, the outer (distal) south-facing passive continental margin succession of the Arctic Alaska terrane was partially subducted and underplated beneath the Angayucham terrane (fig. 1C). Northward thrust imbrication sequentially placed more distal parts of the continental margin over its more proximal parts (fig. 1D). The axis of associated Brookian foredeep sedimentation migrated northward with the thrust front such that older foredeep deposits were involved in later thrusting. The continental substructure of the continental margin of the Arctic Alaska terrane was subducted to deeper levels, resulting in tectonic thickening (fig. 1E) and high-pressure-low-temperature metamorphism (blueschist-facies metamorphic rocks). By Albian time, the rate of underthrusting diminished, and the orogenic belt was rapidly uplifted and unroofed, resulting in setting of isotopic cooling ages and deposition of huge volumes of Brookian clastic detritus southward into the hinterland (Koyukuk basin) and northward into the foredeep (Colville basin) (fig. 1F). Latest Early Cretaceous down-to-the-south, low-angle normal faulting in the southern

Brooks Range contributed significantly to this unroofing and uplift and overlapped in time with the formation of the extensional northern Alaska continental margin. Subsequent Late Cretaceous and early Tertiary Brookian orogenesis resulted in deformation of the southern Colville basin. Deformation has continued to the present in the eastern Brooks Range, where thrusting and foredeep deposition have migrated northward into the offshore region.

Turbidity-Current Processes and Turbidite Elements—What You Get Is Not What You See

William R. Normark

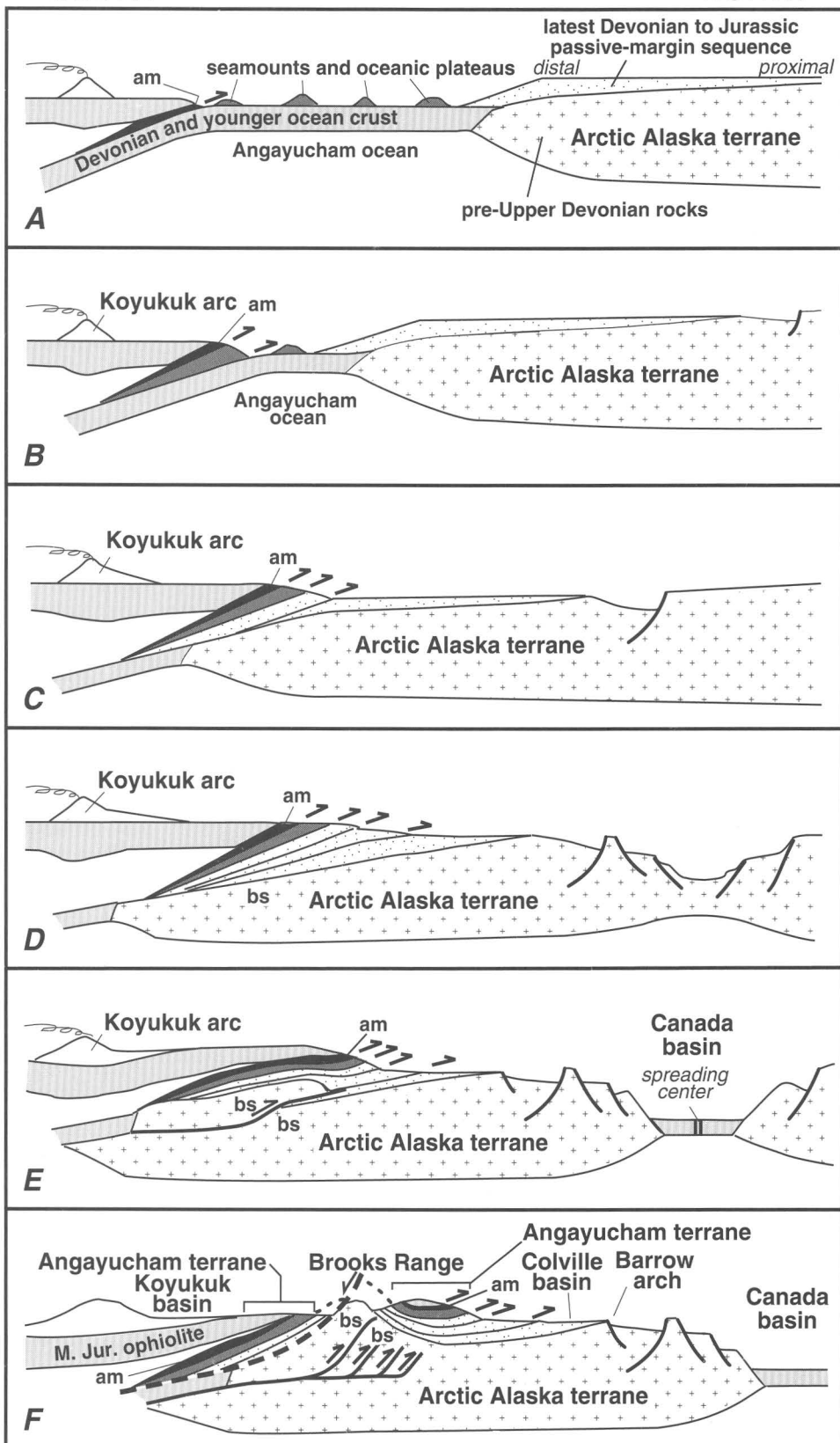
Turbidity-current processes generally are deduced from the physical properties of their conduits and their deposits, from laboratory experiments, or from observations of shallow-water flows in deltaic environments, because direct observation of turbidity currents in a deep-water marine environment has eluded even the most clever and optimistic would-be discoverer. The available data are thus generally restricted to a limited scale range (outcrops and laboratory flumes, shallow-water deltas), or lack resolution of both morphometric characters and bedding features (deep-water marine basins). As a result, existing models tend to underestimate the range in flow properties of turbidity currents in the deep sea. Analogies with subaerial flow processes may provide an intuitive understanding of turbidity currents but can also reinforce the conservative view of what they can do. For example, bankfull flow for rivers indicates near-maximum flow thickness, but in turbidity currents, flow thickness apparently can greatly exceed channel depth based on observations of sediment distribution and key bedform indicators. Average-size turbidity currents overflow and build levee relief; larger flows can erode overbank areas. Flow thickness alone cannot be used to predict depositional conditions; sandy turbidity currents are in general thinner and faster, and muddy flows thicker and slower; thus, the sandier flows remain channelized.

The effect of basin morphology differs between turbidite systems formed on oceanic crust and those in

Figure 1 (Moore and others) (facing page). Development of the Brookian orogeny; am, amphibolite; bs, blueschist-facies metamorphic rocks. Heavy line, fault; dashed where inferred; barb shows direction of relative movement. A, Middle Jurassic; B, Late Jurassic; C, early Early Cretaceous (Berriasian); D, middle Early Cretaceous (Hauterivian); E, late Early Cretaceous (Aptian); F, latest Early Cretaceous (Albian).

SOUTH

NORTH



continental-margin slope basins. In the deep ocean, turbidity currents can rapidly bury extensive areas of low-relief abyssal hills. In general, coarse sediment is deposited close to the termination of a channel as the rapidly spreading and thinning currents lose competency upon leaving the confines of the channel. Deep-water turbidite systems are therefore fan shaped, and the size and position of channel and lobe elements evolve through autocyclic controls. That is, depositional relief from previous turbidity currents greatly influences the fan growth pattern. Within narrow and elongate continental-slope basins, the larger turbidity currents spread laterally until they reach the basin walls, which confine the flow and maintain flow thickness and competence. In such an environment, much coarse sediment can be carried far into the basin, well beyond the end of channel features, and form classic tabular-bedded lobe deposits.

The effects of (1) turbidity-current size and (2) grain-size distribution of suspended sediment in the flow, coupled with (3) effects of both basin and local (turbidite-formed) morphologic relief on the evolution of the flow produce a tremendous range in flow properties. If models of flow do not reflect this heterogeneity, they can lead to incorrect interpretation of the depositional environment (position within the basin and relation to source area). To improve models of turbidity-current flow that rely on observations of their deposits, we must focus on specific mappable features, that is, turbidite elements. Channel-fill, overbank, and lobe deposits are elements produced by deposition and (or) erosion from many events over periods of 10^4 years or longer. Large-scale scours and megabeds are elements produced by single events. These five features are examples of the more common turbidite elements. Similar elements from different sequences can be compared to derive common flow properties, if the effect of scale differences among the examples is considered. An improved understanding of depositional environments of turbidite facies and basin analysis requires improved models of turbidity current initiation and flow evolution.

Controls on Gas Generation and Production, Tight Sandstone Reservoirs, Uinta Basin, Utah

Vito F. Nuccio, James W. Schmoker, and Thomas D. Fouch

Uinta Basin rocks include a thick sequence of low-permeability (tight) sandstones that contain a large volume of gas. Most known gas accumulations occur in the eastern part of the basin in the Upper Cretaceous Mesaverde Group, uppermost Cretaceous to lower

Eocene North Horn Formation, and the Paleocene and Eocene Wasatch, Colton, and Green River Formations. Although the majority of tight-gas completions are in Tertiary strata, rocks in the underlying, sparsely drilled Mesaverde Group in the north-central part of the basin are potential targets as well. To characterize the gas-bearing sandstones, we constructed a series of interrelated maps and cross sections showing vitrinite reflectance (thermal maturity), porosity, lithofacies, and fluid pressure relations for the Uinta Basin.

Vitrinite reflectance (R_m) for each of these low-permeability sequences increases to the north. Levels of thermal maturation for the Mesaverde Group are sufficient for gas generation over large areas of the basin. Values for R_m at the base of the Mesaverde (fig. 1) increase from 0.65 percent at shallow depths along the south edge of the basin to 1.5 percent in the central basin at depths of about 11,000 ft (3,350 m). At the top of the Mesaverde (fig. 2), R_m values increase from 0.50 percent at outcrops along the south edge of the basin to 2.2 percent near the town of Altamont, at depths of approximately 18,000 ft (5,500 m).

Porosity-versus- R_m plots allow prediction of porosity for Mesaverde sandstones in unexplored areas of the basin. Porosity values of nonmarine Mesaverde sandstones with thermal maturity less than about 0.70 percent R_m or greater than roughly 2.0 percent R_m decrease as thermal maturity increases, and follow "normal" sandstone trends. However, between 0.70 percent R_m and 2.0 percent R_m , in the window of hydrocarbon generation, porosities do not decrease as thermal maturity increases (fig. 3). Overpressured, gas-saturated Mesaverde sandstones are likely to have porosities in the 5–9 percent range.

Lithofacies is directly related to reservoir quality in the tight gas sequences of Uinta Basin. In Tertiary and Cretaceous formations, by far the best reservoir rock quality is found in diagenetically altered (both early and late diagenesis) fluvial sandstones (figs. 4, 5). Other good-quality and economically important reservoir rocks are Tertiary open-lacustrine sandstones and Cretaceous lenticular fluvial and blanketlike marine sandstones.

Projecting fluid-pressure and thermal maturity data from drilled areas of the basin into undrilled areas reveals the possibility of a regional, organic-rich, overpressured, basin-centered gas accumulation, where gas generation is probably occurring at present. Published estimates of amounts of erosion in the region vary widely, ranging from 1,000 ft (300 m) to almost 11,000 ft (3,350 m). Our interpretation favors the lesser erosional estimates, because significant cooling of strata due to uplift and erosion would have slowed or stopped the generation of hydrocarbons. Wells drilled in the Mesaverde and lower part of the Tertiary, in the areas where R_m at the base of the Mesaverde is greater than 1.1

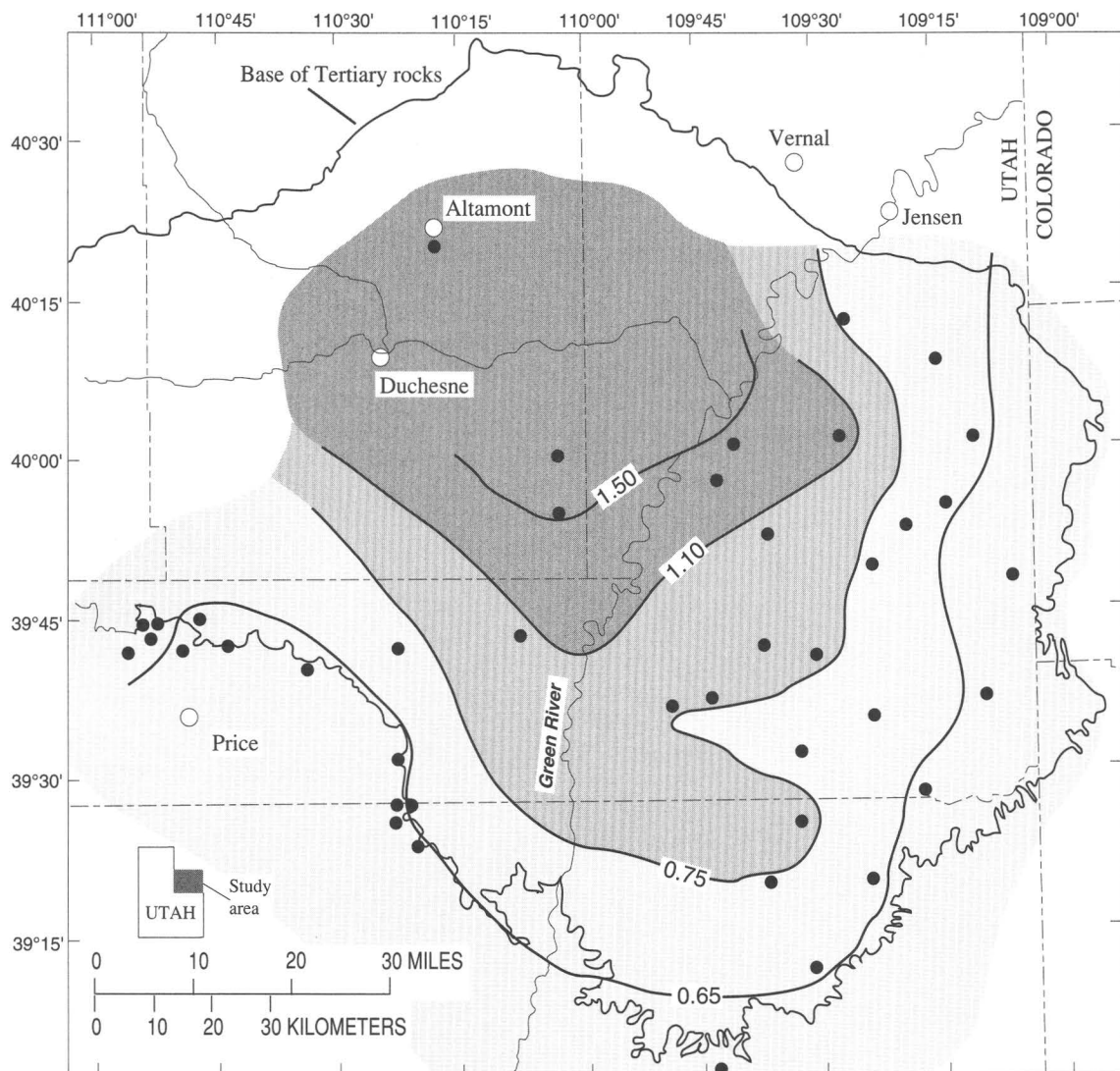


Figure 1 (Nuccio and others). Vitrinite reflectance (R_m) map showing thermal maturity of the base of the Mesaverde Group, Uinta Basin, Utah. Light pattern, area of no gas generation; 0.75 percent R_m isoreflectance line and medium pattern, onset of significant gas generation; 1.10 percent R_m isoreflectance line and darkest pattern, maximum gas generation and expulsion. Dot, location of well and well samples or outcrop samples.

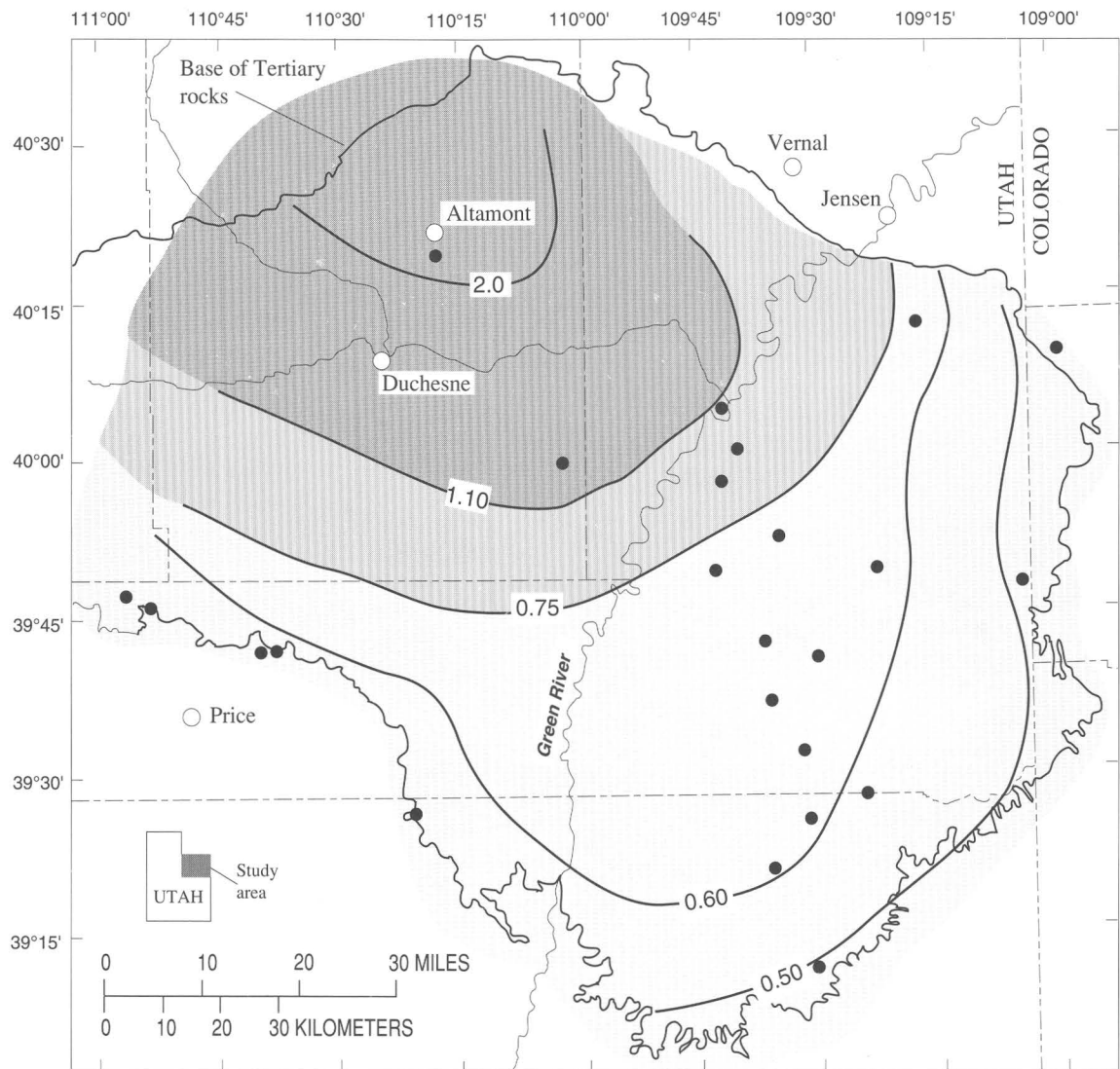


Figure 2 (Nuccio and others). Vitrinite reflectance (R_m) map showing thermal maturity of the top of the Mesaverde Group, Uinta Basin, Utah. Light pattern, area of no gas generation; 0.75 percent R_m isoreflectance line and medium pattern, onset of significant gas generation; 1.10 percent R_m isoreflectance line and darkest pattern, maximum gas generation and expulsion. Dot, location of well and well samples or outcrop samples.

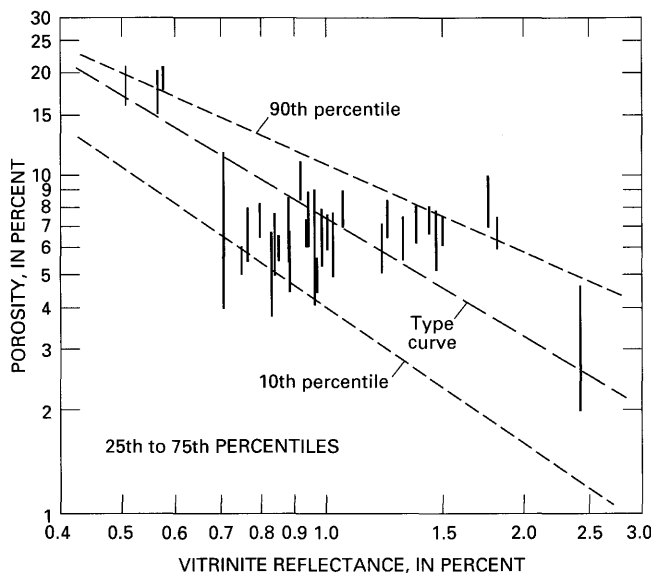


Figure 3 (Nuccio and others). Porosity versus vitrinite reflectance for middle range of core-plug porosity values, nonmarine sandstone intervals of Mesaverde Group, Uinta and Piceance Creek basins. Vertical lines connect 25th and 75th porosity percentiles. Type curve and 10th and 90th porosity-percentile trend lines provide a reference framework that represents sandstones in general.

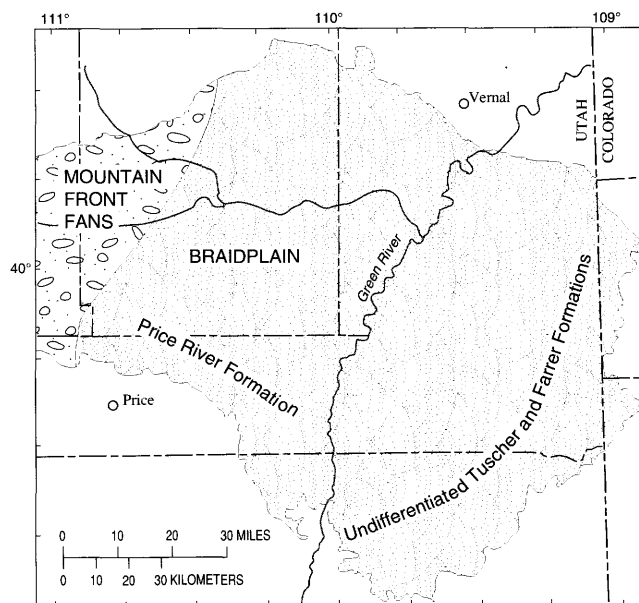


Figure 5 (Nuccio and others). Restored paleogeographic map of Mesaverde Group rocks during the latter part of the Campanian. Gas-bearing rocks of this zone have been identified east of the Green River and are believed to underlie much of the north-central part of the basin.

percent, should have the best potential for gas production. Overpressured gas reservoirs ($Rm > 1.1$ percent) are likely to have no free water and to be surrounded by successive zones of mixed water and gas (Rm 1.1–0.75 percent), and of water only ($Rm < 0.75$ percent).

The Desktop Core Library, A CD-ROM Approach

Michael P. Pantea, Frances E. Gay, and Russell A. Ambroziak

The U.S. Geological Survey, through the Core Research Center in Denver, Colo., maintains a rock core repository containing rock core, thin sections, and core information. Most of the collection comes from oil and gas provinces in the central region of the United States. Other geologic localities in the United States and some international material are also represented. In order to catalog, archive, and distribute core information, we are creating a digital library of the rock core and core information housed at the Core Research Center. Publicly available information will be distributed on Compact Disk—Read Only Memory (CD-ROM) through government distribution centers.

A CD-ROM sampler, prepared in association with the Core Research Center, was designed to help

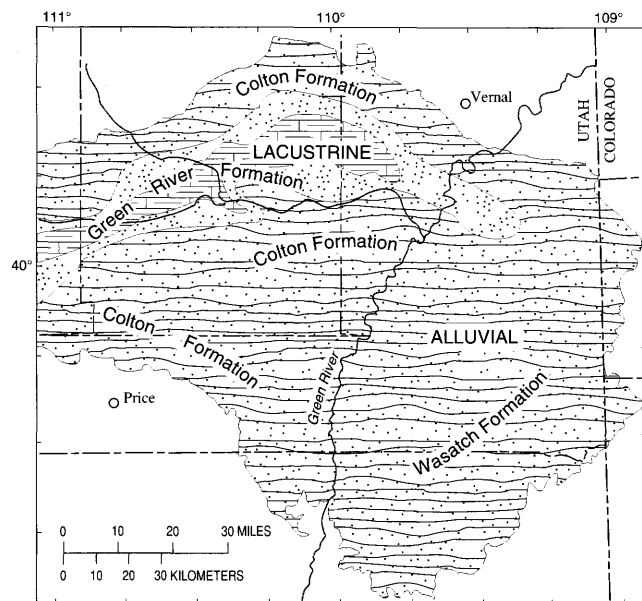


Figure 4 (Nuccio and others). Paleogeographic map of rocks near the boundary between the Paleocene and Eocene in the Uinta Basin. Oil and gas are produced from marginal-lacustrine rocks in this zone in the north-central part of the map area; gas is recovered from Wasatch Formation alluvial units in the east-central part of the basin.

geologists, researchers, and students become familiar with the U.S. Geological Survey's Core Research Center. It presents a way to distribute pictures of rock core and thin section, and core information to a larger audience. This sampler contains rock-core, thin-section, and well-log pictures, as well as index and surface-geology maps, and text information about the wells and core. Text information is the header file for a well and often includes Township, Range, and Section, total depth, and formation picks. All data are displayed using software provided on the CD-ROM. Due to the volume of data being provided, the minimum computer configuration we recommend is an IBM or compatible 80386 PC with 640KB RAM, MS or PC-DOS 3.3 or later, a VGA graphics system capable of displaying 640×480 pixels × 256 colors, and a CD-ROM reader and software capable of reading ISO 9660 standards.

Program features are accessed using a series of menus. An index map can be displayed showing either surface geology or icons marking well locations. Menu choices for use with the map allow display of:

- Latitude and longitude for any spot on the index map
- Primary and secondary roads, streams, lakes, and railroads
- County boundaries
- A zoom feature for detailed viewing of a portion of the index map

Once a well location is chosen from the index map, additional information about that well is available and includes:

- Well header information
- Photo images of rock core
- Photo images of thin sections
- A zoom feature to allow detailed viewing of the rock core and thin-section photo images

Description of data types.—Twenty-one cores from Colorado were selected for this demonstration CD-ROM. These cores come from the Denver basin, the Las Animas arch, the Paradox basin, the Piceance Creek basin, the Axial Basin uplift, and the Sand Wash basin. The rocks range from Cretaceous through Cambrian ages, as identified from well records (current terminology shown in brackets), and include:

- Cambrian carbonate rocks from the Arbuckle Formation [Arbuckle Group]
- Devonian sandstones from the Elbert and McCracken Formations [McCracken Sandstone Member of the Elbert Formation]
- Devonian limestone rocks from the Ouray Formation [Ouray Limestone]
- Mississippian dolomite from the Leadville Formation [Leadville Dolostone]
- Pennsylvanian carbonate rocks from the Lansing, Marmaton, Morrow, and Virgil Formations, and from the Desert Creek Member of the Paradox

Formation [Lansing and Marmaton Groups, Morrowan and Virgilian rocks, and the Desert Creek zone of the Paradox Formation]

- Permian mudstones from the Phosphoria Formation
- Cretaceous Dakota Sandstone siltstones from the Lewis Formation [Lewis Shale]

Future plans.—This CD-ROM sampler attempts to distribute rock core information to the public. It is the authors' intent that this product evolve and be of use in education and research, so comments and recommendations are encouraged. Other plans include migrating this product to the Macintosh platform, and creating CD-ROMs of the frequently viewed core and requested information at the Core Research Center.

Comments and recommendations are welcome and can be addressed to the authors at:

U.S. Department of the Interior
U.S. Geological Survey
Re: Open-File Report 91-355
Mail Stop 975
Box 25046, Denver Federal Center
Denver, CO 80225-0046

Copies of the CD-ROM sampler OF 91-355 can be obtained from the same address or:

Books and Open-File Reports
U.S. Department of the Interior
U.S. Geological Survey
Box 25425, Denver Federal Center
Denver, CO 80225-0046

Petrography and Rock-Eval Studies of Organic Matter in Precambrian Rocks, U.S.A. and U.S.S.R.

Mark Pawlewicz and James G. Palacas

Vitrinite-like particles were isolated from three widely scattered Precambrian terrains: the Late Proterozoic Chuar Group, Grand Canyon, Arizona, and the Middle Proterozoic Keweenawan Group (Nonesuch Shale equivalent), Midcontinent Rift System (MRS), western Iowa, and from the Vendian-Riphean rocks in the Lena-Tunguska Province, eastern Siberia, U.S.S.R. The samples were extracted with chloroform to remove soluble solid bitumen or exogenous hydrocarbons. Some of the remaining material, examined in reflected light, is indistinguishable from post-Silurian vitrinite-group macerals. The particles of organic matter are angular pieces, with a slight expression of internal cellular structure. In addition, in whole-rock samples the distribution of the organic matter was as isolated particles, disassociated

from any bedding feature or mineral fabric, suggesting a nonbitumen macromolecular entity.

With few exceptions, reflectance (R_m) values of the vitrinite-like particles agree with Rock-Eval pyrolysis T_{max} values, providing a measure of validity to the reflectance measurements. Maturity values ranged from immature or marginally mature with respect to liquid hydrocarbon generation for some of the eastern Siberian samples (average 0.42 percent R_m , $T_{max} = 432^\circ\text{C}$), to mature for the Chuar Group (Kwagunt Formation) (average 0.73 percent R_m , $T_{max} \approx 437^\circ\text{C}$), to overmature for the MRS (Keweenawan) rocks (average 2.2 percent R_m , $T_{max} = 503^\circ\text{C}$).

The above factors taken together demonstrate that the reflectance technique can be extended to Precambrian rocks for determination of thermal maturation levels.

Architectural Analysis of Eolian Sandstones—The Lower Jurassic Nugget Sandstone of Northeastern Utah

Fred Peterson and C.J. Schenk

The Lower Jurassic Nugget Sandstone is a heterogeneous eolian reservoir rock that produces oil and gas in the southern part of the Overthrust Belt of southwestern Wyoming and adjacent Utah. The purpose of this study is to examine the three-dimensional sedimentologic heterogeneity of the Nugget in excellent exposures near Vernal, Utah. The chief architectural elements in the formation are cross-stratified eolian dune sandstone and wavy to irregularly stratified sabkha sandstone. Corrugated surfaces, formed by differential erosion of crossbedded sandstone, are fairly common marker horizons in parts of the formation. The Nugget Sandstone is about 277 m (910 ft) thick in the study area and is divided into two informal members.

The lower member is 42 m (137 ft) thick and consists of about equal amounts of sabkha sandstone and small-scale crossbedded eolian dune sandstone. Poor permeability of the sabkha sandstone indicates that these beds are effective barriers to fluid flow and make the lower member a poor reservoir rock.

The upper member, about 236 m (775 ft) thick, is an important reservoir rock in the Overthrust Belt, although the distribution of architectural elements results in significant reservoir heterogeneity. The lower 76 m (250 ft) of the upper member has large trough-shaped sets of cross-strata more than 24 m (80 ft) thick and about 305 m (1,000 ft) wide perpendicular to paleo-wind direction. Poor to moderate permeability of dune apron deposits (composed largely of eolian ripple strata)

at the base of the large troughs laterally and vertically compartmentalizes the permeable eolian dune cross-strata. The overlying 46 m (150 ft) of the upper member consists of tabular-planar sets that are generally less than 6 m (20 ft) thick. Apron deposits composed of eolian ripple strata form the main impediment to fluid flow in this zone. The upper 114 m (375 ft) of the Nugget is the most complex in terms of eolian architecture. This part of the formation consists of cross-stratified sandstone divided vertically into tabular-planar units by thin sabkha beds, generally less than about 1 m (3 ft) thick, or by corrugated surfaces, which are the lateral continuation of the sabkha beds in many cases. The bedding within the tabular units may consist of a single tabular-planar set or it may consist of a complex coset of troughs and tabular-planar sets. The apron deposits tend to impede fluid flow whereas the sabkha beds are effective barriers to fluid flow. The result is a reservoir that is vertically compartmentalized by the sabkha beds and is further complicated, both laterally and vertically, by the apron deposits in the tabular sandstone units that consist of complex cosets.

Relation of Natural Fractures to Composition and Cyclicity in Chalk of the Niobrara Formation, Berthoud Field, Colorado

Richard M. Pollastro

Basic bulk composition was determined from acid-insoluble residue and acid-soluble carbonate contents of 148 samples from core representing the entire section of the Upper Cretaceous Niobrara Formation in the Coquina Oil Corp., Berthoud State No. 3 well, Berthoud field, Larimer County, Colorado. The Smoky Hill Chalk Member comprises mostly impure chalks that contain, on average, about 30 wt. percent insoluble residue; the basal Smoky Hill, however, contains purer chalk beds. The underlying Fort Hays Limestone Member contains the purest chalk beds, some containing as little as 5 wt. percent insoluble residue. In the Berthoud State No. 3 well, fracturing may be related to basic bulk composition; contrast in bed composition and thickness of interbedded chalk and shale beds may be important in understanding fracturing within the Niobrara Formation.

Acid-insoluble residue and carbonate contents of the Niobrara Formation in the Berthoud State No. 3 well represent cyclic variations that correspond to large- and small-scale alternations of chalk and shale. Large-scale cyclicity that produced the major chalk and shale zones in the Niobrara Formation is related to second-order eustatic changes within an overall major transgressive

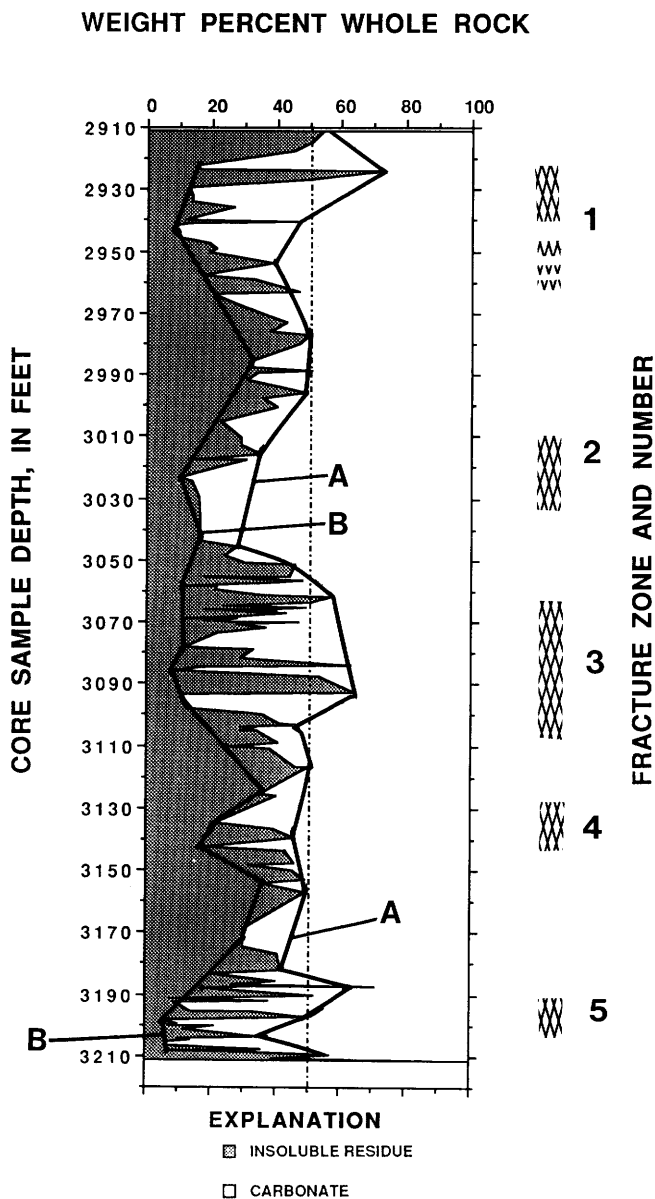


Figure 1 (Pollastro). Insoluble residue and carbonate contents of the Niobrara Formation and numbered fracture zones in the Coquina Oil Corporation, Berthoud State No. 3 well. Bold line A connects insoluble residue maxima, and bold line B connects carbonate content maxima. Note large- and small-scale cyclicity of insoluble- and carbonate-rich zones and the correlation between intervals of fractures and intervals of maximum difference in insoluble residue and carbonate contents (greatest separation of lines). Well depths in feet. Dashed line indicates 50 wt. percent insoluble residue and 50 wt. percent carbonate.

event. Similar large-scale cyclicity of organic matter content in the nearby Coquina Oil, Berthoud State No. 4 well generally correlates with insoluble-residue content. Smaller third-order cyclicity of beds, superimposed on the large-scale cycles, is related to climatic changes due

to Milankovich-type variations in the Earth's orbital patterns.

Five fracture zones, four relatively minor in intensity (that is, size and space), are identified in core of the Berthoud State No. 3 well (fig. 1). Each of the fracture zones occurs in the upper half of a thick chalk unit that is immediately overlain by a thick shale. These thick chalk and shale units correspond to second-order eustatic changes that define the main lithologic units of the Niobrara Formation. Vertical fractures terminate within the overlying shale sequences.

The major and most intense zone of fracturing occurs in the lower midportion of the formation. This zone shows evidence for extensive solution of carbonate, fluid movement, displacement, and related structural deformation. This 35–40 ft interval, informally referred to here as fracture zone 3, contains several beds of chalk with relatively low (< 20 wt. percent) acid-insoluble content that are interbedded with shale having high (> 50 wt. percent) acid-insoluble content (fig. 1). The second-order cycle curve for the Niobrara, as defined by the data, is shortened (thinner units) within this interval. This interval of major fracturing is also characterized by high electrical resistivity. Fracture zone 3 is bounded by two large spikes on the gamma-ray log at about 3,060 ft and 3,140 ft. Fracture zone 3, however, corresponds to a cyclic low in the organic-matter profile for the nearby Berthoud State No. 4 well.

Fractures in Niobrara strata of the Berthoud State No. 3 well appear to be related to composition, as defined by acid-insoluble residue and carbonate contents, and correspond to intervals where strata have insoluble-residue content in excess of 50 wt. percent, and where composition differences among the alternating strata over the interval approach 50 wt. percent (fig. 1). These differences or contrasts in bulk composition, as defined by insoluble residue and carbonate contents, probably produce differences in thermal and mechanical behavior of interbedded units that result in fractures during stress. These tensile fractures that are formed in extremely tight, deeply buried, organic-rich chalks create porosity and permeability required for enhanced recovery of oil for economic production.

The Regional Context of Railroad Valley Oil-fields—An Integrated Geological and Geophysical Transect, East-Central Nevada

Christopher J. Potter, John A. Grow,
Karen Lund, and William J. Perry, Jr.

The Basin and Range province of the Western United States presents an unusual set of exploration

challenges, primarily because of the complex tectonic and thermal history of the region. The province is cut by myriad basin-range extensional faults that are superimposed on Mesozoic contractional structures, middle to late Paleozoic structures related to terrane accretion, and a Proterozoic to early Paleozoic passive margin. Railroad Valley and Pine Valley, the two oil-producing valleys in Nevada, are in zones of complex Cenozoic extensional deformation, and moreover are in close proximity to poorly understood regions of Mesozoic shortening. Detailed understanding of all these structures and their regional significance is essential for the construction of models that guide hydrocarbon exploration in the eastern Great Basin. We are conducting an interdisciplinary investigation in east-central Nevada along a 120-km-long, east-west transect at lat 38°30' N. (fig. 1), which includes the Railroad Valley oil fields and extends from the Pancake Range in the west to Lake Valley in the east. Our approach involves integration of 90 km of regional seismic reflection data (ECN-1 and ECN-2, fig. 1), new geologic mapping, well data, thermal maturation studies, and new gravity and magnetic data.

Contractional structures (including overturned folds, thrust faults that impose older strata on younger strata, and others) have been reported in the ranges that flank Railroad Valley. Geologic mapping by Lund, Perry, and others suggests that these structures fall into three categories: (1) those that formed during regional latest Paleozoic(?)–Mesozoic east-west shortening, (2) those that may record local contraction within a Cenozoic extensional fault system (see Lund and others, this volume), and (3) Cenozoic extension faults that produce fortuitous stratigraphic juxtapositions, mismapped as thrust faults. It appears unlikely that a major continuous Mesozoic thrust belt is a fundamental aspect of the geology of Railroad Valley oil fields.

The magnitude and style of Cenozoic extension vary across the transect. Railroad Valley and the Grant Range (fig. 1) compose a zone of nonuniform east-west extension ranging from 50 percent to 150 percent; a low-angle fault system accomplishes much of this extension. Immediately to the east, the southern White River Valley, southern Egan Range, Cave Valley, southern Schell Creek Range, Muleshoe Valley, and Grassy Mountain make up a block that has undergone 20–30 percent east-west extension along moderately to steeply dipping faults. Major Cenozoic faults that strike obliquely across the southern Egan and Schell Creek Ranges may record significant extension that has no expression on the seismic data, as only one of these faults crosses the seismic line.

In the seismic data across the Grant Canyon oil field of Railroad Valley (fig. 2), a gently west dipping normal fault appears to have controlled the development

of the asymmetric, east-tilted Neogene basin. The fault is clearly defined by fault-plane reflections and by terminations of east-dipping reflections from Tertiary and Paleozoic strata; this fault projects into a low-angle extensional fault system mapped in the Grant Range to the east. Complex reflection patterns in other parts of the hanging-wall probably correspond to chaotically faulted Paleozoic through Paleogene rocks similar to those exposed nearby in the Grant Range. Well-log data suggest that a steep gravity gradient along the east side of the valley is produced in part by steep lateral density gradients within the Neogene basin fill. In the absence of these logs, the gravity gradient and a coincident line of springs could have been interpreted as signatures of listric normal faults that cut Paleozoic rocks and merged into the low-angle fault at depth. Between the Grant Canyon oil field and the front of the Grant Range, a local steepening of the low-angle fault is apparent on seismic data and may indicate modification of the fault system by steeply dipping faults. Alternatively, the steep segment is a minor ramp on the fault system along the western front of the Grant Range. Other workers have interpreted a number of steep faults associated with Railroad Valley oil fields.

East of the Grant Range, extensional structures appear to be simpler. White River Valley (figs. 1, 2) contains several east-dipping subbasins, bounded by moderately to steeply dipping faults. A steep gravity gradient occurs along the eastern margin of the easternmost and largest of these subbasins. This gravity gradient could conventionally be interpreted as the signature of a steep normal fault bounding a thick section of basin-fill; alternatively, varying physical properties within the basin-fill may be a significant contributor to the gravity signature, as in Railroad Valley. The seismic line passes through a homoclinal east-dipping Paleozoic section in the Egan Range that bounds White River Valley to the east. Low-angle normal faults occur in this range north of the seismic line, and a Late Cretaceous to Paleogene extensional(?) basin is exposed in the Egan Range and is encountered in wells in nearby valleys. Related structures have no obvious expression on the seismic data. Pennsylvanian strata exposed in the Egan Range can be traced, as part of a simple homoclinal panel, beneath Cave Valley to the east (fig. 2). Cave Valley contains about 1.1 km of flat-lying Cenozoic strata above a 0.5-km-thick, synextensional, east-dipping sequence, suggesting that most of the basin-fill accumulated after a rapid(?) early extensional phase that was controlled by a west-dipping fault. Muleshoe Valley is a narrow sag basin that has no well-defined bounding faults and records little extension (fig. 2).

All the oil fields in Nevada are intimately associated with Cenozoic extensional structures and basins. Our regional synthesis provides an opportunity to

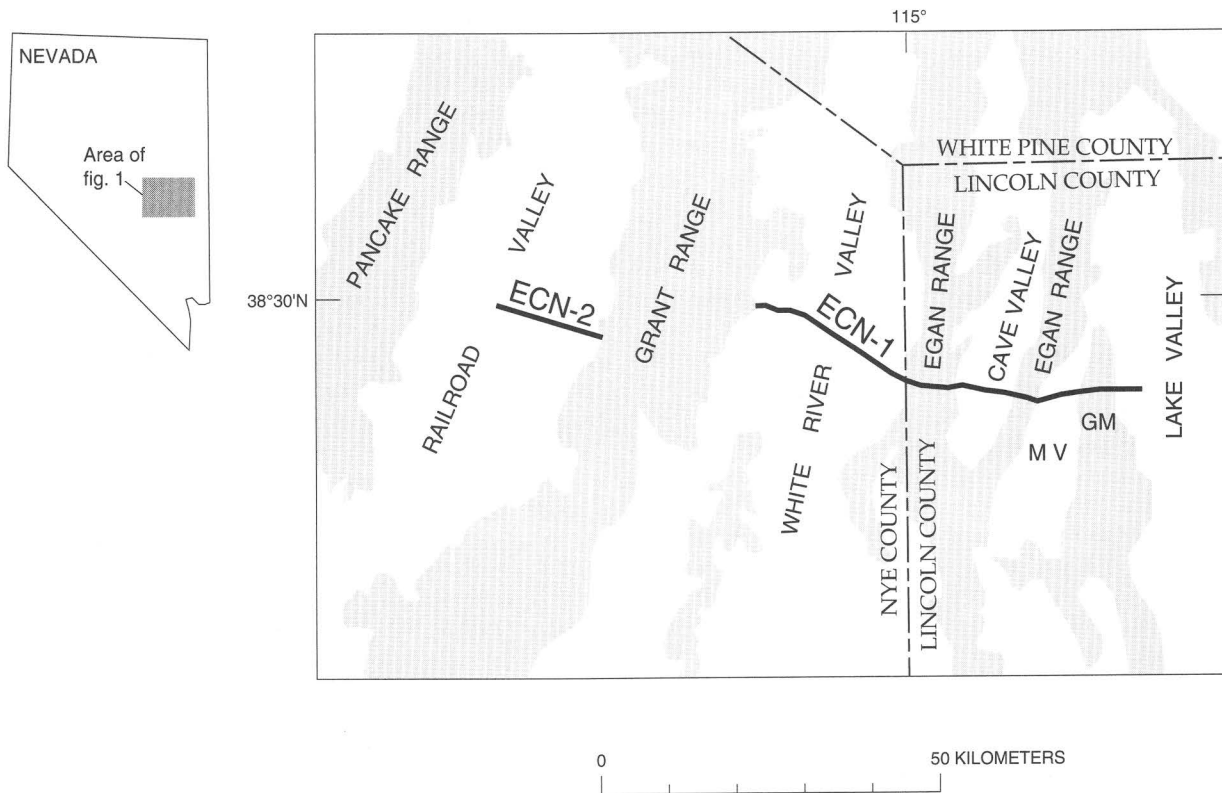


Figure 1 (Potter and others). Location of the geologic and geophysical transect, and ranges and valleys in the study area. ECN-1, ECN-2, seismic lines discussed in text; GM, Grassy Mountain; MV, Muleshoe Valley.

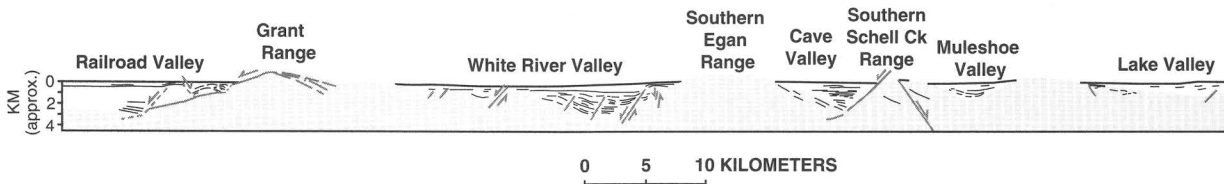


Figure 2 (Potter and others). Cross section illustrating generalized patterns of seismic reflection data and Cenozoic basin-range structure. White areas, Oligocene to recent sedimentary and volcanic strata; patterned area, Paleozoic, Cretaceous, and lower Paleogene rocks that predated basin-range extension. Black line, position of major reflection on the seismic data; stippled line, Cenozoic fault. Bars indicate relative movement.

evaluate the importance of a variety of potentially relevant geologic parameters (fault geometry, basin geometry, basin depth, uplift and sedimentation rates, style of brittle upper-plate deformation, involvement of critical source and reservoir rocks, physical properties of

basin-fill) in combination with thermal-maturation studies. This work will serve as a basis for comparison with other well-studied parts of the Basin and Range province, and will lead to a more useful conceptual framework for exploration in the province.

Huge Indigenous Oil in Mature Source Rocks—Beyond Elephants?

Leigh Price

Numerous Rock-Eval analyses of organic-rich source rocks in different basins show large decreases in hydrogen indices (HI) without concurrent increases in either the Rock-Eval S₁ pyrolysis peak or Soxhlet-extractable hydrocarbons (HC). Thus, many of us geochemists previously concluded that primary petroleum migration from such rocks was very efficient, as almost all the generated HC's appeared to have left the source rocks. However, new research and considerations suggest an alternate possible interpretation. Dramatic increases in electrical resistivity logging values in mature organic-rich source rocks demonstrate large increases in indigenous HC concentrations with increasing maturity in these rocks. Further, historic drilling observations document a large loss of generated HC's from mature source rocks to drilling mud from the large pressure decreases during the rock trip uphole. These pressure decreases cause such large volume expansions of HC gases coexisting with generated oil in fractures in source rocks that the oil is literally blown into drilling muds. If source rocks are both unfaulted and not bounded by hydraulically transmissive rocks, then most generated HC's should remain in mature rocks, even to high maturation ranks. This logic carries the implication of huge in-place oil-resource bases in mature, fractured, organic-rich, self-sourced shales.

The upper and lower shale members of the Lower Mississippian and Upper Devonian Bakken Formation, which are separated by the middle siltstone member, in the Williston basin, Montana and North Dakota, serve as a "type" example. New organic-geochemical studies show that bitumen extracted from the Bakken shales does not correlate to Mississippian mid-Madison Group oils, and that the Bakken shales have contributed only a minor percentage of the oil produced to date in the Williston basin. Also, few pathways exist for vertical migration of Bakken-generated oil to shallower mid-Madison reservoirs. Instead, organic-rich Madison Group marls may be an adequate source for the mid-Madison oils. Published calculations suggest that the Bakken shales have generated 100–150 billion barrels of oil. If the conventional reservoirs were not charged by Bakken-generated oil, this oil would not have leaked from the basin. Thus, an in-place resource base of 100–150 billion barrels of Bakken-generated oil may still exist in fractures in the Bakken "source system," that is, within: (1) all three members of the Bakken, (2) the overlying lowermost Lower Mississippian Lodgepole

Limestone, and (3) the underlying uppermost Upper Devonian Three Forks Shale. Vertical wells in older "Bakken" oil pools (Antelope, Elkhorn Ranch, for example) are perforated in one or all of the three units (Three Forks, Lodgepole, and the middle siltstone member of the Bakken) adjacent to the two Bakken shales, but are not necessarily perforated in the Bakken shales. Rock-Eval analyses of 6–12-inch-spaced core samples taken through all Bakken source system units show that where Bakken shales are thermally mature, the three adjacent organic-poor units contain 10–20 times the HC's they could have generated. Thus, Bakken-generated HC's clearly appear to have moved into the three adjacent units, probably via fractures created by volume expansion of organic matter during HC generation in the Bakken shales.

The mixed results of horizontal Bakken drilling thus far have been attributed to a lack of fractures. However, mature Bakken shales are oil-wet systems with no water in them, and any water introduced into these shales during drilling, completion, or workover operations will decrease or ruin the shales' oil-productive capabilities, due to the principles of two-phase fluid flow and the Jamin effect. Review of vertical and horizontal Bakken well histories reveals that lack of success in some Bakken wells appears due to operational techniques inappropriate to the nonclassical characteristics of the Bakken source system, and not to a lack of fractures. Two other detriments to Bakken productivity also appear probable. First, significant physical damage may be inflicted on the plastic Bakken shales in the beginning and middle portions of Bakken horizontal wells, from the long times the drill bit and string spend there. Second, the overpressured and incompetent nature of the Bakken shales necessitates drilling with overbalanced mud to prevent either blowout or hole collapse, which results in the mud's intrusion into and caking on Bakken fracture walls. Horizontal drilling in the competent units adjacent to the two shale members of the Bakken would avoid both these problems.

The Bakken source system is not unique, as examples exist of other fractured, self-sourced shales that are both currently and historically as productive as or more productive than the Bakken shales. If the Bakken shales have generated and contain 100–150 billion barrels of oil, then given the volume of mature source rocks in other United States basins, it is not difficult to arrive at an in-place oil-resource base estimate in the range of tens to hundreds of trillions of barrels for the lower 48 States. However, if such a large in-place oil-resource base does exist in these mature source rocks, its commercial recovery clearly will depend on development of new exploration, drilling, completion, and production technologies appropriate to the nonclassical characteristics of this resource base.

Some Geologic Controls of Coalbed Gas Generation, Accumulation, and Production, Western United States

Dudley D. Rice, Jerry L. Clayton,
Romeo M. Flores, Ben E. Law, and
Ronald W. Stanton

The presence of gas in coal beds has long been recognized because of explosions which have occurred during underground mining. Coal has been considered as a source of mainly nonassociated gas which has been expelled from and accumulated in adjacent reservoirs in many basins. Recently, coalbed gas has been recognized as a large, relatively untapped energy resource with the coal beds serving as both the source and reservoir rock. In-place estimates of coalbed gas in the United States are as much as 800 TCF; a 1991 assessment by the Potential Gas Committee of the recoverable resource is as much as 145 TCF.

Upper Cretaceous and Tertiary coal beds in Western U.S. basins such as the Piceance, Powder River, and San Juan are estimated to contain large resources of gas. Major efforts have been made to produce this gas, especially in the San Juan Basin where a major regional pipeline system is in place. Several factors, such as coal rank, gas content, pressure, moisture content, and permeability (cleats), have previously been identified as being important in controlling the generation, accumulation, and production of coalbed gas from these western coal beds; two other factors that we have recognized as important are coalbed heterogeneity and composition.

Coal beds are distinguished by heterogeneity, especially lateral variability, which is a most elusive characteristic to determine. This extreme heterogeneity is apparent when closely spaced control points are studied. Closely spaced control points (<0.5 mi) are generally only available from outcrop studies and not from subsurface data sets. In general, coal beds deposited in fluvial and deltaic environments are more laterally discontinuous than coal beds deposited in back-barrier settings. The discontinuity resulting from splitting and pinching out of the coal beds and changes in coal quality is attributed to channel and crevasse-splay deposits. This extreme variability strongly affects the continuity and quality of the coal beds that are both hydrocarbon reservoir rocks and aquifers.

Most Western U.S. coals are composed dominantly of the vitrinite maceral and are classified as humic (type III) kerogen. Such coals are generally considered to be gas prone. However, the examination of macerals in etched polished surfaces under both blue-light fluorescence and white light allows for the identification

of two main genetic types of vitrinite—structured humic material and matrix gels. These two types have different source- and reservoir-rock characteristics.

Both types yield methane-rich bacterial gas in coal beds of low rank (R_m values <0.6 percent), as illustrated by desorbed and produced gas in the Powder River basin. However, at R_m values of 0.6 percent and greater, thermogenic hydrocarbons are generated that vary in composition depending on the genetic type. Structured humic material is more oxygen rich and produces a methane-rich gas (C_1/C_{1-5} values >0.98). Rates of gas and water production are relatively high from coal beds dominated by this facies, indicating higher permeability.

In contrast, matrix gels are more hydrogen rich and produce both liquids and wet gas (C_1/C_{1-5} values \approx 0.90). Liquid hydrocarbons have been produced during early stages of production in the San Juan and Piceance basins in coals characterized by significant amounts of matrix gels of relatively low rank (R_m values of 0.7–0.8 percent). These liquids contain high pristane:phytane ratios, a feature that is typical for coal-derived oils, and a slight predominance of odd-carbon numbered *n*-alkanes in the C_{25+} fraction. However, the saturated fraction consists predominantly of low-molecular-weight components (C_4-C_{10}), which results in the liquids having high API gravities (\approx 50°). In addition, the coal-derived liquids are commonly characterized by high pour points because they contain abundant long-chain *n*-alkanes derived from terrestrial plant waxes. The high pour points of the liquids commonly result in problems by plugging production equipment. The vitrinite-rich coals with abundant matrix gels probably have lower permeability than those with structured humic material, and their gas-production rates are generally lower. However, the negative effect of lower gas production rates is offset by lower rates of water production and higher gas Btu values in the vitrinite-rich coals.

USGS Core Research Center— A Million Feet of Geologic History

Diana L. Richards and Thomas C. Michalski

The Core Research Center (CRC) of the USGS, situated in Denver, Colo., currently houses in excess of 1,000,000 (1 million) feet of core from 25 States, the majority of which are from the Rocky Mountain and Great Plains regions; cores from Wyoming, Montana, Colorado, North Dakota, Utah, New Mexico, and Kansas constitute 95 percent of the collection. Increasing geologic and geographic diversity of samples at the CRC has resulted in its becoming one of the largest, best organized, and most heavily utilized public core repositories in the United States.

Preservation of valuable core material for use by government, industry, and academia has been a concern of the USGS for many years, which resulted in the establishing of a permanent core storage and research facility in 1974. The goals of the repository are to gather cores from a wide variety of sources, process and store them efficiently, and make them available on a daily basis for examination and sampling by all interested scientists. Although gathered from a variety of sources, most cores in the collection were generated as a result of oil and gas exploration and have been donated by a large number of companies in the petroleum industry. A majority of the cores have been slabbed and photographed, and all are available for immediate viewing. In excess of 15,000 thin sections and a large number of analyses made from core in the CRC collection are available to users. The CRC also houses a unique collection of 240,000 feet of oil-shale core.

The recently renovated facility offers a pleasant environment for core examination and sampling: a large, well-lit, climate-controlled examination room provides an ideal setting where 1,500 feet of slabbed core can be examined at one time; a conference room and a small reference library are also available. To facilitate the extensive daily use of the collection, the CRC has established a core information database and provides custom computer searches of its holdings by operator, location, formation, or geologic age. A series of State core catalogs are available for purchase. The CRC encourages use of its facility by all interested geologists and welcomes inquiries about the collection, donation of core samples, computer printouts, and the location of other public repositories. More information can be obtained by contacting the CRC at:

U.S. Geological Survey
Core Research Center
Box 25046, Denver Federal Center
Mail Stop 975
Denver, CO 80225;
telephone (303) 236-1930.

Research Thrusts of the Current Five-Year USGS Evolution of Sedimentary Basins Program—Illinois, Paradox, Eastern Great, and SWANO Basins

J.L. Ridgley, A.C. Huffman, Jr., H.E. Cook, C.J. Potter, S.Y. Johnson, and W.E. Dean

The U.S. Geological Survey has new, five-year, basin-analysis projects underway in the Illinois, Paradox, Eastern Great, and Tertiary southwest Washington and northwest Oregon (SWANO) basin provinces. The

research focus differs for each basin and is coordinated with ongoing research activities of other USGS programs, State geological surveys, academia, and industry.

USGS studies of selected Paleozoic carbonate and clastic rocks in the Illinois Basin will focus on basinwide geochemical, diagenetic, and thermal maturation problems as they relate to movement of fluids in the basin. These studies will use local and regional structure to constrain theoretical fluid flow models and should provide additional insight and constraints on factors influencing hydrocarbon and mineral accumulations.

Paradox Basin studies will concentrate on late Paleozoic development and infilling of the basin and on factors affecting hydrocarbon and mineral resource generation and accumulation. Sedimentologic, stratigraphic, structural, geochemical, thermal maturation, and paleontologic studies of upper Paleozoic carbonate and clastic rocks will provide insights on the structural history, sources and distributions of organic matter and hydrocarbon accumulations, and basin fluid movement. Geophysical studies will examine problems related to the structural evolution of the basin, including the role of salt tectonics and basement faults on basin development and depositional systems.

Research in the Eastern Great Basin (eastern Nevada and western Utah) will focus on the geologic evolution of the region, as defined by a Paleozoic passive margin, an accretionary Paleozoic and Mesozoic foreland basin, and a Mesozoic compressional and Cenozoic extensional tectonic setting. Integrated geologic, geochemical, and geophysical studies from single sites and from defined north-south and east-west transects will evaluate multiple structural events, basin infilling processes, and depositional systems, and the relation of each of these to mineral and hydrocarbon accumulations.

The SWANO basin, a frontier energy province, occupies a fore-arc tectonic setting with a complex Cenozoic history of deformation and subsidence driven by oblique convergence, accretion, and strike-slip faulting. Comprehensive basin reconstructions are being generated from integrated structural, geophysical, stratigraphic, sedimentologic, and geochemical data to provide the framework for regional energy-resource evaluation, and for developing models and principles for analysis of other complex, convergent margins.

Isostatic Residual Gravity Mapping of Wyoming

S.L. Robbins and J.A. Grow

Most complete Bouguer anomaly (CBA) gravity maps show systematic negative values in mountainous

regions that are the effects of crustal thickness variations produced by isostatic adjustments. Isostatic residual anomaly (IRA) gravity maps are created from CBA maps when isostatic corrections are made using an Airy-Heiskanen model, and these are then subtracted from the CBA. The resultant IRA maps usually represent density variations in the upper crust more closely than do CBA maps.

In Wyoming, CBA values range from -80 mGal over the mountains to -288 mGal over the basins. A significant part of this range reflects a regional topographic gradient from 1,200 m above sea level in northeastern Wyoming to 2,500 m in southwestern Wyoming. However, the values associated with the Laramide mountain uplifts are positive relative to those of the basins, and when IRA values are computed using local Airy isostatic assumptions, the positive anomalies become larger. The IRA map values range from -77 mGal in the basins to +75 mGal in the Bighorn Mountains; the average value is, however, near zero. Seismic reflection and two-dimensional gravity models indicate that Laramide mountain ranges are underlain by low-angle thrust faults that flatten within the lower crust. Therefore, the large positive CBA gravity values over the mountains, which are made even larger by assuming local roots beneath these mountains, are in actuality probably due to rootless mountains. In most continental tectonic regions where local mountain roots exist, local algorithms are the optimum choice for isostatic compensation. In Wyoming, however, the use of regional algorithms that average topography over wavelengths of more than 100 km will be required because of the rootless mountains.

IRA maps are significant improvements over CBA maps in that regional effects are removed, and in their effectiveness for interpreting upper crustal anomalies. However, some tectonic regimes require more care in creating IRA maps because local isostatic algorithms may be based on incorrect assumptions. In these instances, regional (as opposed to local) algorithms may be useful in minimizing the relief in the IRA maps and still enhance shorter wavelength gravity anomalies in the upper crust that are caused by structures of economic interest.

Paleocene Paleogeography, Tectonics, and Coal Distribution in the Rocky Mountain Region—An Overview

**S.B. Roberts, M.S. Ellis, R.M. Flores,
D.J. Nichols, W.J. Perry, Jr., and G.D. Stricker**

A study of sedimentologic, tectonic, palynologic, and coal data from Paleocene basins of the north-central

Rocky Mountain region was undertaken in order to understand the relationship of Laramide tectonism to distribution and quality of Paleocene coals. Our study is based primarily on published and unpublished data pertaining to (1) depositional environments and paleocurrent trends in Paleocene fluvial/lacustrine sequences, (2) timing of uplifts, based on fission-track analysis and (or) development of synorogenic deposits, (3) palynomorph biozonation, and (4) coal distribution and apparent rank. Synthesis of the data has led to a current, "working hypothesis" relating Paleocene tectonism to coal-basin paleogeography and coal development

The pattern and timing of Laramide uplifts in the north-central Rocky Mountain region indicate that a Laramide deformational front (LDF) advanced to the northeast from early to late Paleocene. Major coal depocenters in the region recorded a corresponding northeastward shift, suggesting that regional tectonism influenced coal development. The variance in apparent coal rank can also be attributed, at least in part, to regional tectonics, as those coals which formed in depocenters proximal to the LDF tend to have higher apparent ranks.

In early Paleocene time (palynomorph zones P1 and P2), the LDF extended from the Madison Range in southwestern Montana, through the Wind River and Granite Mountains of central Wyoming, to the southern Front Range in Colorado. A network of trunk-tributary fluvial systems flowing east and northeast drained the region. Numerous, areally extensive coal depocenters developed in advance of the LDF (for example, Raton, Denver, and Wind River basins), while fewer coal depocenters developed behind the LDF (for example, Sand Wash/Washakie basin).

During the middle Paleocene (palynomorph zones P3 and P4), the LDF advanced northeastward in Wyoming, as evidenced by uplift in the Washakie and Owl Creek Mountains. Progressive partitioning of the Rocky Mountain foreland at this time is demonstrated by the development of the intermontane Wind River, Bighorn, and Bull Mountain basins. The pattern of trunk-tributary fluvial systems was similar to that of the early Paleocene. However, lacustrine systems, forming in response to rapid subsidence along basin-margin thrust faults, were more widespread than in early Paleocene. Coal depocenters, which developed both ahead (Bighorn, Powder River, and Bull Mountain basins) and behind (Washakie, North Park, and Hoback basins) the LDF, were generally not as numerous or extensive as in the early Paleocene.

In the late Paleocene (palynomorph zones P5 and P6), the LDF in Wyoming shifted farther to the northeast, resulting in thrust-uplift of the Beartooth Mountains, and increased uplift in the Bighorn

Mountains. By this time, the Rocky Mountain foreland had been partitioned into a well-defined network of intermontane basins drained by east- to northeast-flowing, trunk-tributary fluvial systems, and associated lacustrine environments. Numerous, extensive coal depocenters formed ahead of the LDF (Powder River and Williston basins), while fewer coal depocenters developed behind the LDF (Hanna basin).

The apparent rank of 1,482 Paleocene coal samples was determined by calculating Btu/lb values (moist, mineral-matter-free basis) using the Parr formula. Evaluation of these data suggests that apparent rank trends are primarily related to the basinal tectonic history. In general, coal basins can be described as "active" or "passive," with respect to the level of tectonic activity and proximity to the LDF. Active basins (Bighorn, North Park, Hanna, and Raton basins) are proximal to or within areas of deformation associated with the advancing LDF, and are characterized by coal deposits with relatively high apparent ranks (Subbituminous B-High Volatile A Bituminous; mean Btu/lb range = 10,890–14,950). Passive basins (Powder River, Bull Mountain, and Williston basins) developed away from active deformation associated with the LDF, and are characterized by relatively low apparent ranks (Lignite A-Subbituminous B; mean Btu/lb range = 6,980–10,240). Within active basins, the apparent increase in rank is attributed to (1) increased depth of burial (subsidence) and elevated geothermal gradients induced by active tectonism associated with the LDF and (or) (2) subsequent igneous intrusive activity.

Although tectonism seems to have played a significant role in Tertiary coal development, climatic effects were undoubtedly important contributing factors. Continued studies of Paleocene tectonics and coal will necessarily incorporate aspects of paleoclimatology in order to develop a more complete understanding of early Tertiary coal basin evolution.

Reservoir Heterogeneities in the Morrison Formation in Southern Utah—A Prudhoe Bay Analog

John W. Robinson and Peter J. McCabe

Examination of the Salt Wash Member of the Morrison Formation (Jurassic) in the southern Henry Mountains region of southern Utah allows a better understanding of heterogeneities in fluvial reservoirs with high net-to-gross sandstone ratios. The Salt Wash Member is interpreted as the deposits of braided rivers that flowed towards the northeast into a playa lake in central Utah from a source area in north-central

Arizona. Cliffs and canyons provide exceptional exposures that allow a three-dimensional study of vertical and lateral facies relationships of the member over an area of 1,000 km². Interpretation of photomosaic panoramas of cliffs up to 350 m high and 3.2 km long allows for description of the facies architecture and measurement of potential large-scale reservoir heterogeneities. More detailed photomosaics of smaller areas allow an assessment of smaller scale heterogeneities. This work is being supplemented by measurement of detailed stratigraphic sections, minipermeameter analysis of outcrops and freshly cut cores, correlation of subsurface well logs, and petrographic studies.

The Salt Wash Member is 150 m thick, and is composed predominantly of sandstones with <10 percent interbedded siltstones and mudstones. These sandstones have an overall coarsening-upward trend through the unit, with very fine grained quartz-rich beds at the base and chert granule and pebble conglomeratic sandstones toward the top. The sandstones form fining-upward units, from 1 to 5 m thick, that are dominated by trough cross-stratification; the size of individual cross-beds increases higher in the section. The section also contains a few horizontal and ripple-laminated beds. Individual fining-upward units are laterally extensive over tens of meters and are separated by discontinuous, 0.01- to 1-m-thick mudstone drapes and (or) mudstone intraclast pebble lags. Fining-upward units amalgamate to form sandstone sheets that are up to 20 m thick and laterally extensive for 100 m to more than 2 km. These sandstone sheets have flat bases and tops and are separated by rooted and burrowed, red and green mudrock units generally less than 3 m thick. Minipermeameter data from outcrop and core average 600 mD in trough-crossbedded and massive sandstones, 200 mD in horizontal laminated sandstones, and <50 mD in fine-grained deposits.

We believe that conclusions from our study could be used to better model flow unit continuity in large fluvial reservoirs to aid in better reservoir development. Mudrock beds and intraclast conglomerates of varying thickness and continuity would divide a reservoir into flow unit compartments on various scales, influencing fluid migration and drainage. Data from these outcrops provide a guideline to predict the scale of reservoir heterogeneities from field-spaced core and log data. In particular, the Salt Wash Member appears similar to the Ivishak Formation of the Sadlerochit Group (Permian and Triassic) of the Prudhoe Bay field, Alaska. Similarities include (1) an overall coarsening-upward character to the strata; (2) presence of amalgamated sandstone sheets, deposited by braided fluvial streams, separated by discontinuous floodplain mudstones; (3) a vertical evolution of cross-stratification types; and (4) a

high net sandstone composition dominated by a lithic chert component. The scale of our study (1,000 km² area \times 150 m thickness) allows a realistic three-dimensional comparison with a major reservoir such as the Ivishak (770 km² area \times 130 m thickness).

Oil Field Growth in the United States— How Much is Left in the Barrel?

D.H. Root and E.D. Attanasi

Since 1966, the estimated sizes of U.S. oil fields have generally been revised upward every year, as documented first by the American Petroleum Institute in 1966–1979 and then by the Energy Information Administration in 1977–1989. A barrel of production results in less than a barrel reduction in reserves. Indeed, the estimated ultimate recovery from fields discovered in the lower 48 States before 1967 was estimated at year-end 1966 to be 111 BB (billion barrels). As of year-end 1989, the estimated ultimate recovery from these fields was 154 BB. These fields had reserves in 1966 of 31.1 BB; they produced 57.7 BB from 1966 through 1989 and their reserves declined to 16.4 BB. Even fields discovered before 1900 are still growing.

The Energy Information Administration has recently developed a new series of estimates of ultimate crude-oil recovery by year of discovery. We report on research in progress on the application of various methods of analysis to this new series to estimate the expected future growth of crude-oil recovery from known fields in the lower 48 States. Standard methods of field growth analysis as presented in studies by J.R. Arrington in 1960, R.G. Marsh in 1971, and D.H. Root in 1981 require the analyst to make arbitrary choices concerning the level of aggregation between large and small fields, the number of successive years of data used in the analysis, and the cutoff age beyond which fields are assumed no longer to grow.

Projections of future field growth estimated by applying the standard method to this new data series were found to be quite sensitive to these choices. These projections for the lower 48 had a range from 10 to 80 BB of oil. For instance, the future growth calculated when small and large fields are analyzed separately is one-third greater than when all fields are pooled and growth is projected for the aggregate amount of oil. In certain instances when the field growth cutoff age is reduced from 80 to 65 years, projected field growth declines by more than half the original amount. Projected future growth estimates are also sensitive to industry conditions that prevailed during the time period when the historical estimates of ultimate field sizes are made. The projected

future field growth was highest when the historical estimates were made during periods of rising oil prices and increasing development drilling.

Biases in the standard projections of field growth result from the violation of the assumptions that field growth is proportional to ultimate size and fields of the same age are equally developed. It seems more realistic to assume that at any point in time, the annual field growth is proportional to remaining reserves, rather than to ultimate recovery. The uniformity hypothesis assumes that a field discovered in 1957 whose size was estimated in 1987 has the same relative amount of remaining growth as a field discovered in 1947 whose size was estimated in 1977. However, the 1957 field by 1987 had probably experienced more intense development than the 1947 field had by 1977 because of a higher price during its operating period and fewer years under prorationing. So, even at age 30 one would expect to find more growth left in the 1947 field than in the 1957 field.

Alternatives to the standard procedure are presented that are designed to correct for deviations from the uniformity assumptions.

Geochemistry and Origin of Oil in Cambrian and Ordovician Reservoirs, Ohio

Robert T. Ryder, Robert C. Burruss, and
Joseph R. Hatch

Oils from stratigraphic traps along the Middle Ordovician Knox unconformity in Ohio were analyzed to determine their geochemical characteristics and source rocks. Seven samples were collected from the Upper Cambrian(?) Rose Run Sandstone; six samples were collected from the Upper Cambrian part of the Knox Dolomite; one sample was collected from the Upper Cambrian Krysik sandstone of informal usage; and one sample was collected from the Middle Ordovician Black River Limestone. Gas chromatograms of saturated hydrocarbon fractions from these oils show similar geochemical characteristics including (1) full profile of *n*-alkanes from *nC*₅ to *nC*₃₃, (2) slight odd predominance of *n*-alkanes in the *nC*₁₃ to *nC*₁₉ range (carbon preference indices from 1.1 to 1.2), and (3) pristane/*nC*₁₇ and phytane/*nC*₁₈ between 0.28 and 0.45. These similarities suggest that the oils were generated from the same source rocks. Slight differences in the character of the oil are attributed to postemplacement maturation. An Ordovician source is inferred for the 15 oils studied here because they are geochemically similar to oil in the northern Illinois basin and adjoining areas that have been derived from Ordovician source beds. However,

Gloeocapsamorpha prisca, blue-green algae whose distinct gas chromatographic signature is common in Ordovician oils, is not largely recognized in the Ohio oils.

Ninety-two rock samples, predominantly from core, in Ohio, Tennessee, and West Virginia, were analyzed for their TOC (total organic content) and pyrolysis products to evaluate the source of the Ohio oils. Three possible source-bed intervals were tested: (1) Middle and Upper Cambrian strata in the Rome trough, (2) the Middle Ordovician Wells Creek Formation and the equivalent part of the Lower and Middle Ordovician Beekmantown Group, and (3) the Middle and Upper Ordovician Antes Shale and the equivalent Utica Shale. The Antes and Utica Shales have moderate TOC values ($\bar{x} = 1.6$, $n = 32$; 20 values from other published sources) that identify them as potentially good petroleum source beds. The Wells Creek Formation and the upper part of the Beekmantown Group ($\bar{x} = 0.3$, $n = 40$) and the Middle and Upper Cambrian strata in the Rome trough ($\bar{x} = 0.3$, $n = 22$) have several samples whose TOC values fall in the 0.5–1.5 percent range, but most of them are too low in organic carbon to be considered source beds. A plot of the hydrogen index (HI) of these 92 rock samples against oxygen index (OI) of the samples shows low HI values (< 200 mgHC/gC) and a wide range of OI values (50–650 mgCO₂/gC). The low HI values are attributed to the low organic content of most of the samples and to the high thermal maturity of the few samples that have a greater-than-average organic content. The high OI values probably represent the CO₂ generated from partial thermal decomposition of the carbonate minerals in the samples during pyrolysis rather than CO₂ generated from the kerogen. When HI and OI values of the Antes Shale from this study are combined with previously published values from the thermally immature to marginally mature Utica Shale in eastern and central Ohio, they indicate that the compositions of kerogens from the Antes-Utica sequence plot between organic matter Types II and III and, thus, are oil and gas prone. Based on these combined values, we conclude that the black shales of the Antes and Utica Shales are the most probable source of the Ohio oils. Locally, strata in the Wells Creek Formation, the upper part of the Beekmantown Group, and the Middle and Upper Cambrian strata in the Rome trough may also have been a source for some oil and gas.

The required downward expulsion of oil through 1,000 ft of the Middle Ordovician carbonates to reach the Knox unconformity probably was accomplished by high fluid pressure in the Antes-Utica interval. Once oil reached the porous beds accompanying the Knox unconformity, it easily migrated up the eastward-dipping slope of the foreland into Ohio. The superior sealing capacity of the overlying Upper Ordovician Reedsdale Shale and Juniata Formation, compared to the underlying Middle

Ordovician Black River and Trenton Limestones, may also have facilitated the preferred down-section migration of oil derived from the Antes and Utica Shales.

Algodones Depositional System—Modern Analog for the Upper Jurassic Norphlet Formation, Mississippi and Alabama

C.J. Schenk

The Upper Jurassic Norphlet Formation is a prolific gas reservoir in several offshore Alabama fields, and produces minor amounts of oil from several onshore fields. The Norphlet Formation was deposited along the southern margin of North America following rifting of North America and Africa-South America. The Appalachian Mountains formed the northeastern margin of the rift zone, and clastics of the Norphlet Formation were shed southwestward from the highlands, accumulating in alluvial fan, braidplain, sand sheet, interdune, playa, and eolian dune environments. Most of the gas in offshore fields is trapped in eolian dune sandstones, and most cores from the offshore are dominated by thick sequences of eolian stratification. However, the proximal facies of the Norphlet Formation are a complex intercalation of alluvial and eolian sandstones. These facies are well represented in cores from Escambia County, Alabama.

The Algodones eolian dunes and related environments in the Salton trough, southeastern California, are an excellent analog for the intercalation of fluvial and eolian facies of the Norphlet Formation. The Salton trough is a complex extensional basin related to the rifting event that formed the Gulf of California. The Cargo Muchacho and Chocolate Mountains form highlands along the eastern boundary of the Salton trough, similar to the geography that existed along the Jurassic basin margin during Norphlet deposition. Clastics shed westward from the mountains adjacent to the Algodones form alluvial fan, braidplain, and sand sheet deposits. Small alluvial fans adjacent to the mountains grade to extensive braidplains characterized by ephemeral channels that are wide and shallow. Processes on the braidplains are dominated by flash-flood discharge through numerous shallow channels in proximal areas, and by sheetflooding on distal braidplains. Distal braidplain deposits commonly exhibit an intercalation of fine to medium sand with thin layers of pebbles and cobbles. This facies is common in the Norphlet Formation along the basin margins, where it is called the wadi facies. The Algodones braidplains grade to partially vegetated eolian sand sheets, on which sediment transport by wind dominates surficial

processes. Alluvial sheetflood processes resulting from storms can inundate the eolian sand sheets, leaving thin layers of pebbles and cobbles and mud layers in otherwise laminated eolian sand.

Basinward from the braidplains and sand sheets are the eolian dune sands of the Algodones. Overall, the Algodones dune field is about 70 km long and as much as 10 km wide, and the dune sand is as much as 100 m thick. The dunes are large, complex transverse and barchanoid forms that are covered with small superimposed dunes. The dunes are generally migrating to the south and east, over the braidplain and sand sheet sands. Migration of these complex dunes would produce a thick sandbody composed of a complex assemblage of eolian dune deposits, with rare interdune deposits, similar to the eolian sandstones of the Norphlet Formation.

Reservoirs and Source Rocks of the Upper Jurassic Norphlet Formation, Mississippi and Alabama

C.J. Schenk and J.W. Schmoker

The Upper Jurassic Norphlet Formation in the offshore region of Alabama contains gas resources estimated to be in the range of several trillion cubic feet. The remarkable reservoir properties of the productive eolian sandstones of the Norphlet Formation, particularly porosity values as high as 15 percent at depths on the order of 20,000 ft, have been the subject of several studies. Our purpose in this study is to determine why the reservoir properties of the Norphlet are what

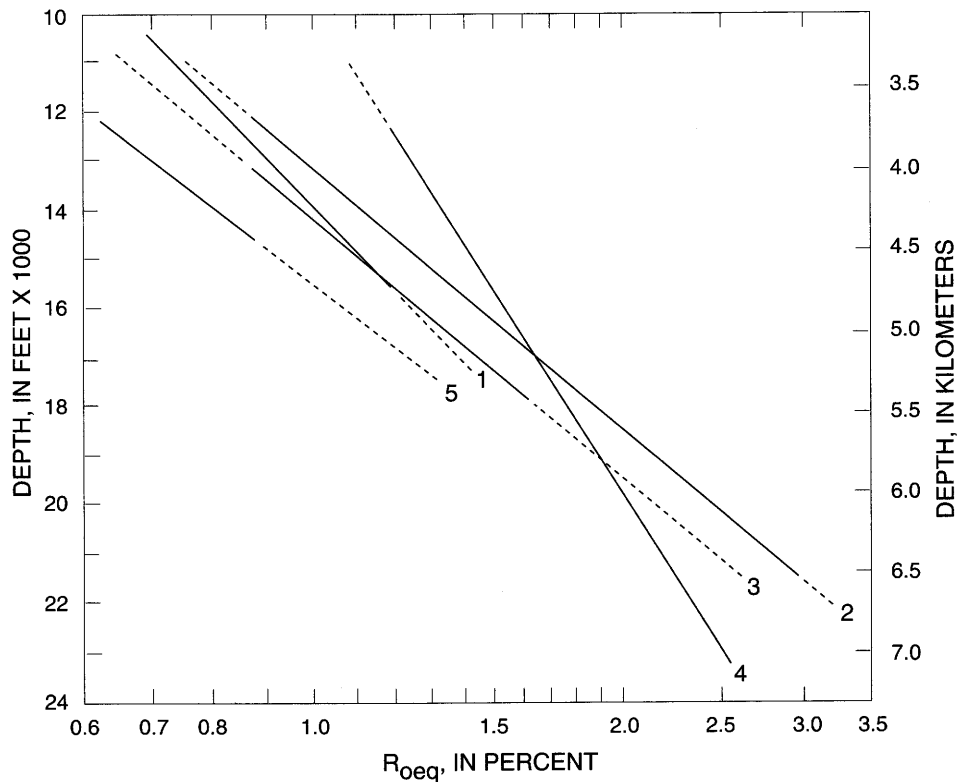


Figure 1 (Schenk and Schmoker). Preliminary working trends of equivalent vitrinite reflectance (Ro_{eq}) versus present depth for five areas in southern Mississippi, southwestern Alabama, and the western Florida panhandle. Trends are derived from published and unpublished data that include vitrinite reflectance, bitumen reflectance, T_{max} (Rock-Eval pyrolysis), and modeling based on time-temperature history. These Ro_{eq} -depth relations are subject to modification as additional data become available. Trend labeled (1) is from vicinity of Escambia County, Alabama, and Escambia County, Florida; (2) represents area of Mississippi and Alabama south of Wiggins arch; (3) represents Mississippi Interior Salt basin; (4) represents area centered on Rankin County, Mississippi, influenced by the thermal effects of the Late Cretaceous Jackson Dome; (5) represents northern peripheral fault zone of Mississippi Interior Salt basin near the Mississippi-Alabama border. Dashes represent extrapolations of data sets.

they are. Figure 1 represents a preliminary attempt at relating thermal exposure to depth for several regions in the Mississippi Interior Salt basin and southwestern Alabama, including offshore; regional thermal exposure has been shown to correlate with average porosity. The curves indicate that thermal maturity increases with increasing depth. Maturation values of about 1.5 to 3.0 percent Ro characterize sandstones of the Norphlet Formation at depths ranging from about 15,000 to 22,000 ft. Given these general trends of thermal maturation, average sandstone porosities of the Norphlet Formation from the Mississippi Interior Salt basin and offshore Alabama are much higher than average porosities of sandstones from numerous hydrocarbon-bearing sandstones worldwide. The reasons for this are not obvious, particularly because sandstones of the Norphlet Formation are not strikingly different petrographically from other productive eolian sandstones outside the Gulf Coast. The anomalously high porosities may be related to (1) the role of early cements such as halite, anhydrite, and carbonate in preserving intergranular space during burial, (2) the role of clay minerals, particularly chlorite, in preserving some porosity during burial, (3) the timing of diagenetic events such as clay growth and cement and framework-grain dissolution relative to gas emplacement, and (4) the role of hydrocarbons in inhibiting porosity-degrading diagenesis.

Source rocks for Norphlet Formation hydrocarbons are generally considered to be the overlying organic-bearing algal carbonates of the Smackover Formation, but source rocks may also include a marine facies of the Norphlet shown by the Alabama Geological Survey to exist down depositional dip from the Norphlet Formation eolian sandstones.

Geologically Oriented Overview of Horizontal Drilling in the United States

James W. Schmoker

A patent application for equipment designed to drill horizontal wellbores was filed in 1919. In 1929, horizontal laterals were successfully drilled from a vertical oil well. By 1954, drilling of horizontal drain holes was sufficiently common to warrant a review article on the subject by John Eastman. Despite these early beginnings, however, the pace of horizontal drilling remained relatively stagnant through the 1970's.

The present cycle of horizontal-drilling activity stems from developments in the early to mid 1980's. Since 1985, the annual number of wells drilled with

horizontal segments longer than 1,000 ft (300 m) has been increasing worldwide at an exponential rate. Although such logarithmic growth cannot be sustained, most observers predict that significant numbers of horizontal wells will continue to be drilled. In the United States, horizontal wells have been tried in a majority of producing basins, but large numbers of individual formations and plays remain to be tested.

The positive atmosphere associated with the oil-price boom of the early 1980's probably helped set the present horizontal-drilling cycle into motion. In the United States, where few horizontal wells have been drilled for exploration, a shifting emphasis from petroleum exploration to the exploitation of known hydrocarbon accumulations has driven horizontal drilling.

In heterogeneous formations where pay zones are difficult to efficiently contact with wellbores, horizontal holes offer an alternative to the drilling and stimulation of vertical wells. In the United States, large volumes of movable oil are known to be present in heterogeneous formations. If the bulk of these known accumulations could be economically recovered through systematic horizontal drilling, the long-range energy outlook for the United States would be dramatically improved.

Results of horizontal drilling to 1991, however, do not support such optimism. Drilling results argue instead for the localization of favorable production characteristics (sweet spots) within the regions encompassed by large oil accumulations. Successful horizontal wells in both the Austin Chalk and Bakken Formation plays, for example, are limited to comparatively small areas of the potential producing trends.

The need to better comprehend the nature of sweet spots within regional trends offers opportunity for geologists. Improved understanding of sweet spots equates to improved understanding of the heterogeneity of sedimentary rocks in the subsurface. Fracture systems are only one aspect of the problem: depositional and diagenetic heterogeneities, on scales ranging from millimeters to kilometers, also significantly affect reservoir behavior.

Relatively little is known about the distributions and characteristic dimensions of depositional and diagenetic heterogeneities. Field mapping, core examination, and thin-section studies, for example, are commonly used to investigate geologic processes but usually not the three-dimensional geometries resulting from such processes. Better understanding of depositional, diagenetic, and fracture geometries is needed for improved reservoir modeling and the reduction of horizontal-drilling risk.

Tectonic and Climatic Controls on the Sedimentary Record of the Early Mesozoic Newark Supergroup Rift Basins, Eastern North America

Joseph P. Smoot

The Newark Supergroup consists of continental sedimentary and igneous rocks of Late Triassic to Early Jurassic age that fill a series of exposed half-graben basins along the eastern coast of North America. The rift basins formed along reactivated Paleozoic faults during extension that later led to the opening of the Atlantic Ocean. The basins had internal drainage systems, with local base level controlled by lake levels. Although the ages of the deposits differ in some basins, each basin exhibits a similar vertical succession of depositional facies from bottom to top: (1) Thin (<200 m), discontinuous immature fluvial conglomerates unconformably overlie Paleozoic or Precambrian rocks; these deposits reflect local provenance and small drainages. (2) Moderately thick (500–1,000 m) conglomerates, cross-bedded sandstones, and siltstones, deposited by braided rivers or low-sinuosity anastomosed streams, exhibit greater maturity than the basal conglomerates that they overlie, possibly unconformably. (3) Thick (500–2,000 m) crossbedded to ripple crosslaminated, medium- to fine-grained sandstones and siltstones were deposited by high suspended-load meandering streams and on vegetated muddy plains. The fluvial deposits typically become finer grained and exhibit greater sinuosity upward in the section. (4) Very thick (1,000–6,000 m) lacustrine mudstones and siltstones, in most basins forming 2- to 10-m-thick cycles of deep-water to sub-aerial deposits, encompass deep and shallow perennial lakes, ephemeral lakes, dry-playa mudflats, saline mudflats, and vegetated mudflats. Dry-playa mudflat and saline mudflat deposits are absent in the southernmost basins and are restricted to discrete stratigraphic intervals in the northernmost basins. Fluvial conglomerates and sandstones and deltaic sandstones and siltstones commonly intertongue with the lacustrine deposits near the axial margins. Alluvial fan deposits, dominated by shallow-stream and debris-flow fabrics, are restricted to the faulted margin of the half-grabens where they intertongue with lacustrine and fluvial deposits.

The vertical succession of depositional environments reflects the evolution of the drainage systems in response to rifting: (1) initial local drainages and erosional surfaces of a depositional depression prior to rifting; (2) basin subsidence and the localization and capture of regional drainages; (3) progressive loss of stream power as fault-related uplift constricted outlets and sediment aggradation lowered gradients, (4) partial

or complete hydrographic closure of the basins, as faulting restricted outlets. Timing of these events for each basin probably depended on the relation of the regional extensional field to the orientation and distribution of Paleozoic faults and preexisting drainages. Sparse paleocurrent data in each basin as well as provenance studies suggest that initial fluvial drainages in each basin had a variety of orientations with respect to the basin shape, but they eventually oriented parallel to the basin axis in the latter stages of fluvial deposition. Fault-related uplift created highlands that produced alluvial fans sometime before the end of drainage-system evolutionary stage 3. Tectonic activity may also be reflected by 10- to 20-m-thick coarsening-upward sequences in alluvial fan deposits and by radical shifts in the locations of marginal fluvial deposits. The geometry of the bounding faults apparently produced basins of increasing area during extension. This probable size increase is reflected by progressive vertical decrease in the abundance and thickness of deep-lake laminites within cyclic lacustrine strata, as suggested by Roy Schlische and Paul Olsen in 1990, accompanied by more regionally extensive fluvial and deltaic deposits that commonly built out as large-scale terminal fans. The increase of basin area was apparently interrupted by one or more episodes of flood basalt extrusion, apparently occurring simultaneously in several basins, producing increased subsidence and resulting in thicker and more common deep-lake laminites. The final stage of sedimentation in several basins is fluvial, suggesting a decrease in subsidence or lowering of the outlet.

Climatic effects on the sedimentary record of the Newark Supergroup are pervasive at a finer scale than are the tectonic effects. The cyclic style of lake deposition common to most basins is attributed to variations of inflow and evaporation within a closed drainage, possibly due to Milankovitch periodicity forcing. This scale of lake fluctuations is also reflected in the style of deltaic deposits that intertongue with them. The cyclic climatic pattern is also visible as different order groupings of cycles and as large-scale (several hundreds of meters) variations in the abundance of arid climate features (playa, saline mudflat). The larger scale climatic fluctuations are also recognizable in fluvial deposits as alternations of perennial-dominated versus ephemeral-dominated streams, and in alluvial fan deposits as dominance of high-discharge versus low-discharge flash-flood fabrics. A regional gradation in climate of increasing aridity northward is also suggested by the occurrence of coals only in the southernmost basins and playa fabrics and eolian sandstones only in the northernmost basins.

Origin of the Santa Maria Basin, California

Richard G. Stanley, Samuel Y. Johnson, Ronald B. Cole, Mark A. Mason, Carl C. Swisher III, Mary Lou Cotton Thornton, Mark V. Filewicz, David R. Vork, Michele L. Tuttle, and John D. Obradovich

More than 800 million barrels of oil and 800 billion ft³ of associated gas have been produced from the onshore Santa Maria basin of central California. Initial subsidence of this petrolierous Neogene basin is recorded by the lower Miocene Lospe Formation, an 800-m-thick sequence of nonmarine and shallow-marine sedimentary rocks and interbedded tuffs. In its type area in the Casmalia Hills, the Lospe rests unconformably on Jurassic ophiolite, is conformably overlain by the lower Miocene (Saucesian and Relizian) Point Sal Formation, and is of early Miocene (Saucesian) age on the basis of palynomorphs and benthic foraminifers obtained from mudstones, and radiometric ages from two beds of nonwelded rhyolitic tuff. A $^{40}\text{Ar}/^{39}\text{Ar}$ age of 17.70 ± 0.03 Ma (mean of seven determinations on sanidine) was obtained from a 20-cm-thick tuff about 30 m above the base of the Lospe; a $^{40}\text{Ar}/^{39}\text{Ar}$ age of 17.39 ± 0.12 Ma (mean of six determinations on plagioclase) was measured on a 75-cm-thick tuff about 210 m above the base of the Lospe. Both tuffs are about the same age and may have erupted from the same volcanic source as a compositionally similar welded tuff yielding a $^{40}\text{Ar}/^{39}\text{Ar}$ age of 17.79 ± 0.10 Ma (mean of five determinations on sanidine) from the Tranquillon Volcanics (from a 1950 study by Dibblee) on Tranquillon Mountain in the westernmost Transverse Ranges, about 30 km south of the Lospe outcrops.

Alluvial fan and fan-delta facies within the basal part of the Lospe are as much as 200 m thick and consist mainly of reddish-brown and greenish-gray conglomerate and sandstone derived from nearby fault-bounded uplifts of Mesozoic sedimentary and igneous rocks. Conglomerate clast compositions and paleocurrent directions suggest that these coarse-grained facies were deposited in at least two subbasins separated by a northwest-trending paleohigh of Jurassic ophiolite.

The alluvial fan and fan-delta deposits grade upward into a 600-m-thick sequence of interbedded greenish-gray sandstone and mudstone that accumulated mainly in a subaqueous environment, most likely a lake that was intermittently connected to the ocean. Many of the sandstone beds are sheetlike, normally graded, and exhibit partial Bouma sequences, and probably were deposited by turbidity currents. The associated mudstones are bioturbated to laminated, display scattered

mud cracks that indicate infrequent desiccation, and contain sparse marine microfossils including dinocysts, suggesting occasional influxes of marine waters. Primary gypsum occurs in stromatolites and nodules in the lake deposits, and contains sulfate depleted in ^{34}S (0 to +3 per mil), suggesting that the sulfur was derived from hydrothermal springs on the floor of the lake. Lenses of nonwelded rhyolitic tuff as much as 20 m thick are interspersed throughout this sequence. The tuffs consist almost entirely of bubble-wall vitric shards and pumice, and were deposited primarily as subaqueous pyroclastic flows and high-concentration turbidites that most likely originated from subaerial or shallow-water magmatic eruptions. In places, the tuffs are underlain by debris flow deposits that contain unusually large blocks of Jurassic ophiolite as much as 50 m long and 20 m across.

The uppermost 30 m of the Lospe consists of storm-deposited, plane-laminated to bioturbated sandstone and bioturbated mudstone containing shallow-marine microfossils. These shallow-marine deposits are abruptly overlain by bathyal marine black shale of the Point Sal Formation, indicating rapid deepening from well-oxygenated shelf to oxygen-poor bathyal environments. The Saucesian-Relizian benthic foraminiferal stage boundary is about 2 m above the base of the Point Sal Formation.

The Lospe Formation provides a clear record of substantial topographic relief, active faulting, volcanism, hydrothermal activity, progressive deepening, and rapid subsidence during initial formation of the Neogene Santa Maria basin beginning about 17.7 Ma. These findings are inconsistent with an often-cited hypothesis which holds that the Santa Maria basin originated about 14 Ma as a pull-apart structure along a hypothetical right-slip fault system, the so-called "San Luis Obispo transform." Instead, our results support an alternative interpretation, based in part on paleomagnetic data, which holds that the basin originated about 17.7 Ma by local crustal extension and oblique right-slip faulting related to the beginning of clockwise rotation of the western Transverse Ranges.

Interactive Computer Display of Petroleum Exploration and Undiscovered Resource Potential of the United States

Kenneth I. Takahashi, Debra K. Higley, and Richard F. Mast

The history of petroleum exploration across the United States is displayed using a self-contained SuperCard program on a Macintosh II-series computer. Also included in the program are graphic displays of estimated undiscovered oil and gas resources for the United States.

The continental United States, including Alaska, is divided into 47 major petroleum-producing areas. Color images of the oil, gas, oil and gas, and no-production category of each square mile in these regions are displayed in 5-year, cumulative increments for the period 1900 through 1986. Included in each regional display are State and county boundaries, and other geographic reference points. The displays are analogous to a series of drill-hole maps that are animated by year of completion. Each symbol represents the producing category (oil, gas, oil and gas, or no production) of a 1-square-mile cell that has been drilled, rather than representing a single well. Each cell contains one or more wells that penetrate one or more target intervals. The display shows the earliest completion date (in 5-year increments) and the type of hydrocarbon occurrence (petroleum-producing category) for that cell. Estimates of undiscovered oil and gas resources for each area are also displayed. The displays of estimates of undiscovered oil and gas resources for the United States are shown by region and geologic province, as described in U.S. Geological Survey Open-File Report 88-373.

Our display illustrates (1) the history of resource development, (2) the maturity of exploration in petroleum-producing regions across the United States, (3) relationships between estimates of undiscovered resources and where and how existing resources have been discovered, and (4) petroleum mapping applications using commercially available software on personal computers.

Well locations, completion dates, and petroleum-producing categories were retrieved from the Well History Control System (WHCS) database of Petroleum Information Corporation and manipulated on a VAX 11/780 by a series of FORTRAN utilities. These programs divide regions of the United States into 1-square-mile areas and tabulate both the earliest well completion date and category of petroleum occurrence within each grid cell. By this method, the data on 1.7 million wells are summarized in approximately 430,000 cells that have been drilled across the United States.

Based on the production categories for included wells, each cell is assigned a code for oil, gas, oil and gas, or no-production (dry) category. For example, if no wells within a cell produce hydrocarbons, then a dry cell symbol is posted. A cell containing oil, gas, and no-production wells is assigned an oil and gas symbol. The year of earliest well completion is used to show when each cell was first drilled, and maps are displayed and animated relative to completion dates. Thus in cells that contain multiple plays or numerous drill holes, the earliest completion date may not correspond with results of subsequent exploration. For example, a cell that contained early nonproductive wells and later oil wells

would have an oil symbol color, but the date would represent the early, dry exploration.

File structure in SuperCard consists of a window containing an index map of the U.S. and separate windows for each petroleum region. Maps of regions are accessed by clicking with the mouse on that part of the U.S. index map that contains the region of interest. The map sequence is animated by clicking on the region's exploration history button. Alternately, cumulative exploration for each separate 5-year increment can be displayed by clicking on the button with that year interval. For example, pressing the "45-49" button will display exploration from 1900 through 1949. The resource estimate data were drawn from published reports and linked to the exploration history areas by geographic region.

Hardware requirements for this program are a Macintosh computer with color graphics capability, 8 megabytes of memory, and a minimum 20 megabyte hard disk.

NERSL—National Energy Research Seismic Library

David J. Taylor and Frederick N. Zihlman

The U.S. Geological Survey has been collecting multichannel seismic reflection data since 1973 in support of its missions and programs. The data, residing at locations in Denver, Colo., and Menlo Park, Calif., on standard nine-track magnetic tape, are becoming increasingly difficult to store and maintain properly. In an effort to decrease storage costs, protect data from deterioration, and provide a more convenient method of distributing seismic reflection data, the U.S. Geological Survey has established the National Energy Research Seismic Library (NERSL) in Denver. The NERSL catalogs, compacts, and distributes on Compact Disk—Read Only Memory (CD-ROM) publicly available multichannel seismic reflection data held and acquired by the U.S. Geological Survey.

The first of several NERSL products is a pilot CD-ROM containing processed seismic data in digital form which can be read by low-cost DOS-based microcomputers. The CD-ROM also contains navigation or location data for the various seismic lines, acquisition and processing information, and software to display the data and their location in either preview or detailed mode. The software can also be used to scale the data, adjust the colors assigned to trace amplitudes, and plot a screen image on a nine-pin dot matrix printer. In addition the software will allow users to retrieve the digital seismic reflection data in standard Society of

Exploration Geophysicists (SEG) format for downloading to more sophisticated processing systems. Seismic reflection data contained in this first pilot CD-ROM represent nine lines from the Georges Bank basin off the northeastern U.S. coast, six lines from the southern San Juan Basin in the area of Church Rock, N.Mex., and one line from the northern Powder River basin in the area of Broadus, Mont.

A second NERSL CD-ROM contains 29 seismic lines from the National Petroleum Reserve Alaska (NPRA) and a data base holding NPRA shotpoint locations in latitude and longitude, line intersection data, subsurface velocity information, and well information. A run-time version of "Paradox," a commercial data-base manager from Borland International, is present on the second NERSL CD-ROM and can be used to query the data base. Over the next 5 years, the aim of the NERSL is to broaden the software and data-base capability and reproduce current and future U.S. Geological Survey collections of publicly available digital seismic reflection data on CD-ROM.

Preliminary 1:100,000-Scale Geologic Map of Santa Maria 30' x 60' Quadrangle, Central Coastal California—Progress Toward a Digital Compilation

Marilyn E. Tennyson

A geologic map encompassing most of the onshore Santa Maria basin as well as adjoining parts of the southern California Coast Ranges and western Transverse Ranges is being compiled in support of a framework basin study of the Santa Maria province and as part of the cooperative Southern California Areal Mapping Project of the U.S. Geological Survey and the California Division of Mines and Geology. As the first step, in order to resolve differences between maps by different authors and pinpoint spots where additional field work is needed, published geologic maps of various vintages and scales, along with some unpublished new mapping, were photo-reduced and traced to make a preliminary composite. For part of the central Santa Maria basin, the only geologic map available is on a half-century-old photographic base; its contacts were transferred to a 1:24,000 topographic base by hand tracing before reduction. Some imprecision is inevitable using these methods, because of unstable base materials, differences in projection between some of the component maps and the 1:100,000 base map, and photographic distortion. In order to reduce such errors, tracings of the component maps are being scanned and imported into ARC/INFO, a commercial GIS software package.

ALACARTE, a menu interface for ARC/INFO developed at the U.S. Geological Survey, is being used to edit and tag linework, and to tag and label polygons with formation symbols. A plot of the partially completed digital version will be displayed. The scale is large enough to allow depiction of individual formations, but small enough to display regional structure. Recent revisions in age and correlation of stratigraphic units are incorporated in the map explanation.

The map centers on the Santa Maria basin, which is floored by rocks of the Franciscan Complex, Coast Range ophiolite, and Great Valley sequence. Around the margins of the basin, great thicknesses of Mesozoic and Paleogene mostly marine sedimentary rocks are present beneath upper Oligocene to lower Miocene nearshore sandstone and bathyal mudstone. In the central part of the basin, lower Miocene nonmarine conglomerate and sandstone shed from uplifted blocks along basin-forming faults are present locally, resting unconformably on the Mesozoic rocks. Siliceous, organic-rich basinal mudrocks of middle Miocene to early Pliocene age blanket much of the region. Uppermost Miocene to Quaternary marine and nonmarine clastic rocks record filling of the basin and emergence of folded and faulted blocks. Petroleum generated from the Miocene basin-filling mudrocks is found in both sandstone and fractured reservoirs, trapped in Pliocene-Quaternary faulted anticlines and stratigraphic traps.

Very young, large folds—two regional anticlines and flanking synclines—occupy the central part of the basin. The northern anticlinal trend (Casmalia-Orcutt) is separated from the Santa Maria Valley syncline to the north by a system of north-verging reverse faults. Another major north-verging reverse fault may lie in Los Alamos Valley, separating the southern anticline (Lompoc-Purisima) from the Los Alamos-San Antonio syncline; subsurface documentation will be required to confirm its existence. The geometry, offset history, and earthquake potential of most of the numerous faults that slice through the region are poorly known, and there are significant and as-yet unresolved differences between traces of major fold axes and faults as mapped by different workers.

The compilation incorporates 1:24,000-scale mapping recently completed by J.G. Vedder and others (1991; U.S. Geological Survey OF 91-109, and unpub. data) along and southwest of the Sur-Nacimiento fault. This mapping shows that the East Huasna fault extends southeastward at least as far as the Sisquoc River and that the Suey fault, shown on State geologic maps, is not a throughgoing major structure. The West Huasna fault, which extends into the map area from the north, is the boundary between an apparent late early Miocene paleohigh on the west and a bathyal low on the east. More mapping and subsurface studies along the southeasterly

projection of the West Huasna fault are needed (1) to establish whether it is continuous with the Little Pine-Foxen Canyon fault system to the southeast and (2) to evaluate possible strike-slip offset along the fault.

Multifaceted Studies of a Lacustrine Source Rock—The Paleogene Green River Formation, Colorado, Utah, and Wyoming

Michele L. Tuttle, Walter E. Dean, Mark Stanton, James Collister, Wendy Harrison, Thomas D. Fouch, Janet Pitman, Trond Hanesand, and Nils Telnaes

Geologic and geochemical studies of petroleum source rocks formed in lakes are fewer in number and, historically, less detailed than studies of source rocks formed in marine environments. Lacustrine sediments are less studied partly because of the large variability in physical, chemical, and biological processes within and among lakes. This variability limits the ability to construct depositional or diagenetic models that can be used to interpret study results from lacustrine units other than those originally modeled. However, we have found certain lithofacies of the lacustrine Paleogene Green River Formation to be well suited for source-rock studies because lithologic variability was minimal during hundreds of thousands to millions of years of deposition in the large Green River lakes. Our goal is to investigate processes active during deposition and diagenesis of the open-water facies of the Green River and to evaluate variability in processes among depositional basins and lake phases.

The Green River formed in lakes that existed for 10–23 m.y. in three Laramide fault-bounded basins that collectively covered more than 62,000 km². Ancient Lake Uinta occupied the Uinta Basin of Utah and the Piceance basin of Colorado, and ancient Lake Gosiute occupied the greater Green River basin of Wyoming. Part of the Green River is an excellent source rock, but in most areas the formation is not buried deep enough to thermochemically mature the kerogen. An exception is in the western portion of the Uinta Basin, Utah, where the lower part of the Green River is within the oil-generation window and has produced significant amounts of oil.

Geochemical and biogeochemical studies used material cored from a 6-m.y. interval (latest early Eocene to middle Eocene) of the Green River that was deposited within the three lacustrine depocenters. The rocks within this interval are still immature with respect to petroleum generation. In order to better integrate results from each

study and to increase the applicability of these results to lacustrine source rocks in general, many of the analyses were performed on the same samples. Our studies span a wide range of disciplines—inorganic and organic chemistry; stable isotopy ($^{34}\text{S}/^{32}\text{S}$), petrography, and trace-element content of sulfide minerals; stable isotopy of organic matter ($^{13}\text{C}/^{12}\text{C}$, $^{15}\text{N}/^{14}\text{N}$, $^{34}\text{S}/^{32}\text{S}$); evaluation of a modern lake as a geochemical analog for the ancient Green River Lakes Uinta and Gosiute; and an experimental study on iron diagenesis in saline, high-pH environments similar to those within the Green River lakes. Results and preliminary interpretations of these studies are appearing in U.S. Geological Survey Bulletin 1973. Work in progress addresses major- and trace-element chemistry and stable isotopy of carbonate minerals ($^{13}\text{C}/^{12}\text{C}$, $^{18}\text{O}/^{16}\text{O}$), sedimentology of core material, and composition of the bitumen and kerogen of the Green River Formation.

Results of these studies have identified chemical and biological processes active within each lake depocenter and variably influenced by climatic and tectonic cycles having observed durations from ≈0.1 to 5 m.y. Primary productivity (that of algae) is linked to these cycles because the cycles, in part, affected the availability of nutrients. Inflow was the source of sulfate and probably phosphate, but nitrogen was replenished by recycling through a complex set of inorganically and biologically mediated reactions. During fresh- and brackish-water phases, nutrients were abundant and productivity was high in both lakes. The abundant organic matter produced anoxic conditions within the sediment where anaerobic bacterial processes formed sulfide and carbonate minerals. During lake lowstands, Lake Uinta was sufficiently deep to remain stratified. Euxinic (H_2S -bearing) bottom water conditions were established as bacteriogenic H_2S diffused out of the sediment where extremely high porewater pH kinetically inhibited formation of iron sulfides. The extensive bacterial activity in Lake Uinta during this time, together with the very long stability of lake stratification, caused an evolution of the isotopic composition of both the sulfur and carbon reservoirs—in the case of sulfur, to unprecedented ^{34}S enrichment. During compaction, saline waters were expelled, carrying solutes into overlying beds where additional sulfide and saline carbonate minerals formed. In contrast to Lake Uinta, Lake Gosiute was only intermittently stratified during lowstands due to frequent mixing of the shallow water column. Organic-matter production and preservation decreased under these conditions but were sufficient to support some anaerobic bacterial activity during early diagenesis. Again, high porewater pH inhibited iron sulfidization, but because the water column frequently mixed, euxinic conditions were ephemeral and isotopic evolution much less dramatic than in Lake Uinta.

The interpretive results of these studies have increased our understanding of, and appreciation for, the complex geochemical processes affecting the Green River lakes. Similarities between Lakes Uinta and Gosiute have been proposed in previous studies and have often been used to justify extrapolations of study results from one lake to the other. We have shown that, although geochemical and biological processes within the two lakes were similar, depositional and diagenetic conditions were significantly different, and that the differences affected the hydrocarbon-producing capability of these lacustrine source rocks.

Ground-Truthing the Distal Mississippi Fan with SeaMARC Images and Cores—What Happens at the End of the Pipe

D.C. Twichell, W.C. Schwab, C.H. Nelson, H.J. Lee, N.H. Kenyon, T.F. O'Brien, and W. Danforth

In detailed high-resolution sidescan sonar studies of modern submarine fans, the channel systems have been the primary focus of attention. In studies of ancient submarine fans, the deposits at the ends of channels have received considerable attention; but the deposits at the ends of modern channels have heretofore received little study. The deposits and styles of deposition at the ends of channels on modern fan systems have been the direct subject of a SeaMARC I sidescan sonar and coring program conducted on the distal Mississippi Fan.

In previous work, the entire Mississippi Fan was imaged by the GLORIA sidescan sonar system. These data enabled us to see the surface of the Mississippi Fan as a series of lobe-shaped deposits. Using the GLORIA image as a guide, we included in the SeaMARC I survey area part of the meandering main leveed channel that originates in the Mississippi Canyon and a smaller, slightly sinuous channel that extends from the main channel for 120 km across one of the lobe-shaped deposits to its distal edge, where the channel splay into a series of even smaller channels. These smaller channels have less than 2 m relief and terminate in areas of high acoustic backscatter. The channels, exclusive of the main channel, are less than 300 m wide; at the distal edge of the lobe, most channels are less than 100 m wide. The high-backscatter areas around the channels are elongate and have crenulated edges that have abrupt rather than gradational transitions to the surrounding deposits. Relative backscatter intensity and crosscutting relations of the different channels and high-backscatter areas suggest that our survey area is composed of a series of even smaller depositional areas.

Cores from the survey area recovered three principal distinctive sedimentary facies. The first of these facies was gray mud with darker bands. This mud facies corresponded with areas of low acoustic backscatter on the SeaMARC images. The second facies was a graded clastic sand that comprised medium to fine sand at the base of the beds and showed no visible internal structures. These beds were mostly 30–50 cm thick. The third facies was termed a chaotic sand. These chaotic sand beds were mostly 30–100 cm thick, composed of clastic sandy silt with interspersed clay clasts; they displayed distorted bedding and contained wood fragments in their upper parts. The distribution of the two sandy facies coincided with the areas of high acoustic backscatter on the SeaMARC images, but whether distribution of these two facies is systematic within the high-backscatter areas is not yet determined. Depth to the first sand layer varies roughly with backscatter strength on the sonar images. Relatively high backscatter areas appear to be relatively younger parts of the lobe inferred from the SeaMARC images, where the sandy facies are less deeply buried by muds.

The SeaMARC images and coring results suggest that channelized flow rather than sheet flow was the dominant mechanism of transport of sandy sediments away from the main leveed channel on the Mississippi Fan. The presence of sand at the distal ends of the small channels indicates an efficient transport process across the outer part of the fan, and the abrupt edges of the sand deposits imply an abrupt transition from transport to deposition of the sands. The two types of sand facies suggest two mechanisms of sand transport. The graded beds are presumably transported by turbidity currents, and the chaotic sands as debris flows. The resulting facies at the ends of the channels appears to be a series of discontinuous lenses of sand separated by muds rather than a continuous sheet of sand as is inferred on ancient fans. This picture of the end of a channel system on a modern fan may be a valuable analog in the study of ancient as well as other modern fan systems.

Major Frontier Exploration Plays in Petroleum Basins of the U.S.S.R.

Gregory F. Ulmishek

About 2 dozen sedimentary basins produce oil and gas in the U.S.S.R. (fig. 1). Several currently unproductive regions, many of them offshore, possess good potential for significant discoveries. Major exploration activity is concentrated at present in the West Siberian, Timan-Pechora, and North Caspian basins. These three basins and offshore areas of the North

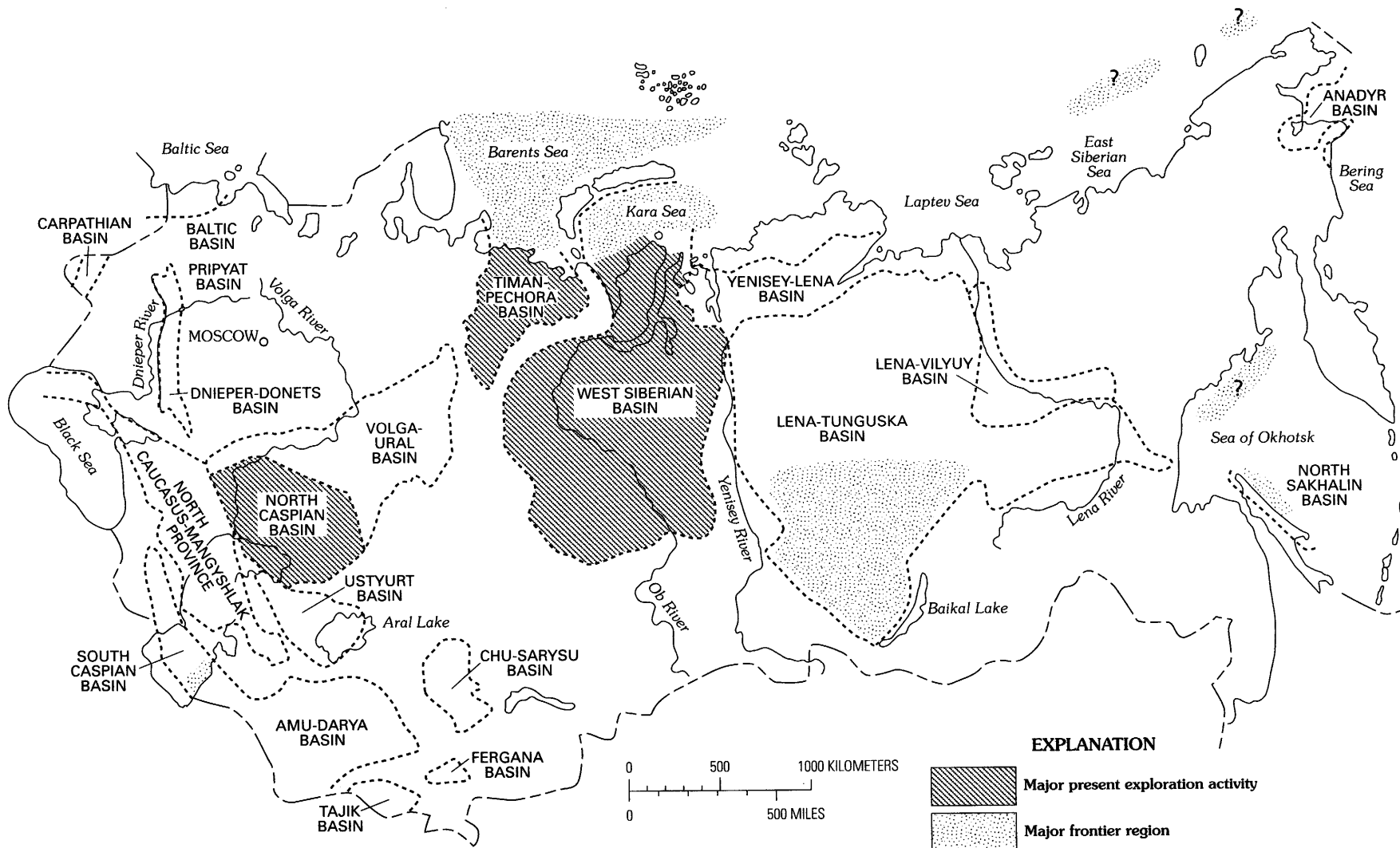


Figure 1 (Ulmishek). Petroleum basins of the U.S.S.R.

Sakhalin and South Caspian basins currently attract most of the attention of international oil companies.

In the oil-productive Middle Ob region of the West Siberian basin, most of the large structural traps in Neocomian rocks (main basin producer) have already been discovered. Major exploration efforts are directed now toward stratigraphic traps in the Neocomian deltaic section and to structural and stratigraphic traps in underlying Jurassic continental clastics. The efficiency of exploration in these deeper plays is significantly lower. In the gas-prone northern part of the basin, recent drilling offshore in the southern Kara Sea resulted in huge gas discoveries. However, the economic viability of these discoveries is very doubtful.

The approach to exploration in the North Caspian basin is still strongly influenced by supergiant discoveries in the Tengiz (oil) and Karachaganak (gas condensate) fields. However, no additional significant discoveries have been made in more than 10 years. Carbonate platforms and associated reefs remain the main play, but poor seismic resolution hampers exploration. Clastic wedges (clinoforms) on the basin's margins are the secondary exploration objective. Better understanding of trap distribution and geochemical modeling are needed for success.

The last 10 years of exploration in the Timan-Pechora basin were moderately successful. Although no giants were found, many medium-size fields were reportedly discovered. Two major exploration plays are Upper Devonian reefs and drape structures over them in the Vuktyl-Dzhebol intrashelf basin, and Upper Silurian through Lower Permian carbonates in structural traps in the previously unexplored northeastern area of the basin. An oil discovery in the Prirazlomnaya field offshore sparked much interest, but the discovery itself is noncommercial.

The Barents Sea may become an important hydrocarbon-producing province in the future. The giant (100–140 TCF) Shtokman discovery is undergoing a feasibility study. Several other discoveries, although much smaller, support a high resource assessment. However, Upper Triassic and Jurassic prospects are obviously gas prone, and the potential of deeper Paleozoic reservoirs for oil is uncertain.

An important oil and gas discovery in the Yurubchen field on the southwest of the Lena-Tunguska basin (East Siberia) identified a new play with possibly significant exploration potential. The hydrocarbons are in Riphean vuggy carbonates, and the geology indicates that the source rocks are also in the Riphean. Previous discoveries were mostly in younger rocks of the Nepa-Botuoba arch, on which hydrocarbon-source rocks are practically absent.

The offshore part of the North Sakhalin basin recently attracted much interest from western oil

companies. This offshore area is very lightly explored although several rather sizable (150–400 million barrels) discoveries have been made. In addition to the main exploration play in Miocene-Pliocene deltaic sandstones of the paleo-Amur River, the area has a good potential for significant oil reserves in fractured diatomaceous shales of Monterey Formation type.

The South Caspian basin is the oldest oil producer in the U.S.S.R. However, the geology of the basin, and especially its offshore part, is still poorly understood. Water is deep (to 1,000 m) in the unexplored central part of the southern Caspian Sea, but the wide eastern shelf is also almost undrilled. More data on distribution of source rocks and reservoir rocks are needed for prospecting on the shelf.

Many other, more maturely explored basins of the U.S.S.R. still possess a significant undiscovered oil and gas potential. Some frontier basins in the Arctic and Pacific Oceans are very poorly known, but may become interesting exploration targets.

The Coal Resource Evaluation and Assessment Project (COALREAP) in Pakistan—Energy for the Future

Peter D. Warwick, John R. SanFilipo,
Roger E. Thomas, and James E. Fassett

In August 1985, the U.S. Agency for International Development, as part of its long-range "Energy Planning and Development Project" in Pakistan, contracted with the USGS to assist the Geological Survey of Pakistan (GSP) in a multidisciplinary program to assess Pakistan's Tertiary coal resources (fig. 1), to train GSP geologists in various aspects of geology, and to improve the GSP's physical facilities. Investigations were carried out through 1989 to map and assess the quantity and quality of the coal resources of southern Sindh at 1:50,000 scale. Drilling in the Lakhra and Sonda coal fields by a private contractor and the GSP totaled 71 holes.

Results indicate that presently known and mined coal fields in southern Sindh are not isolated coal basins; rather, much of southern Sindh, including the Thar Desert, appears to be continuously underlain by coal-bearing rocks. Coal resources of 1,080 million t (metric tons) have been estimated for seven out of nine identified coal zones in those parts of the Lakhra area where coal-bed thicknesses range from a few centimeters to 5 m. In the Sonda West area, 3,700 million t of coal have been identified, the thickest coal bed being 6.3 m. In the Sonda East area, coal-bed thickness is as much as 2.4 m and coal resources for 10 zones have been estimated at 1,500 million t. The apparent rank of the coal in these

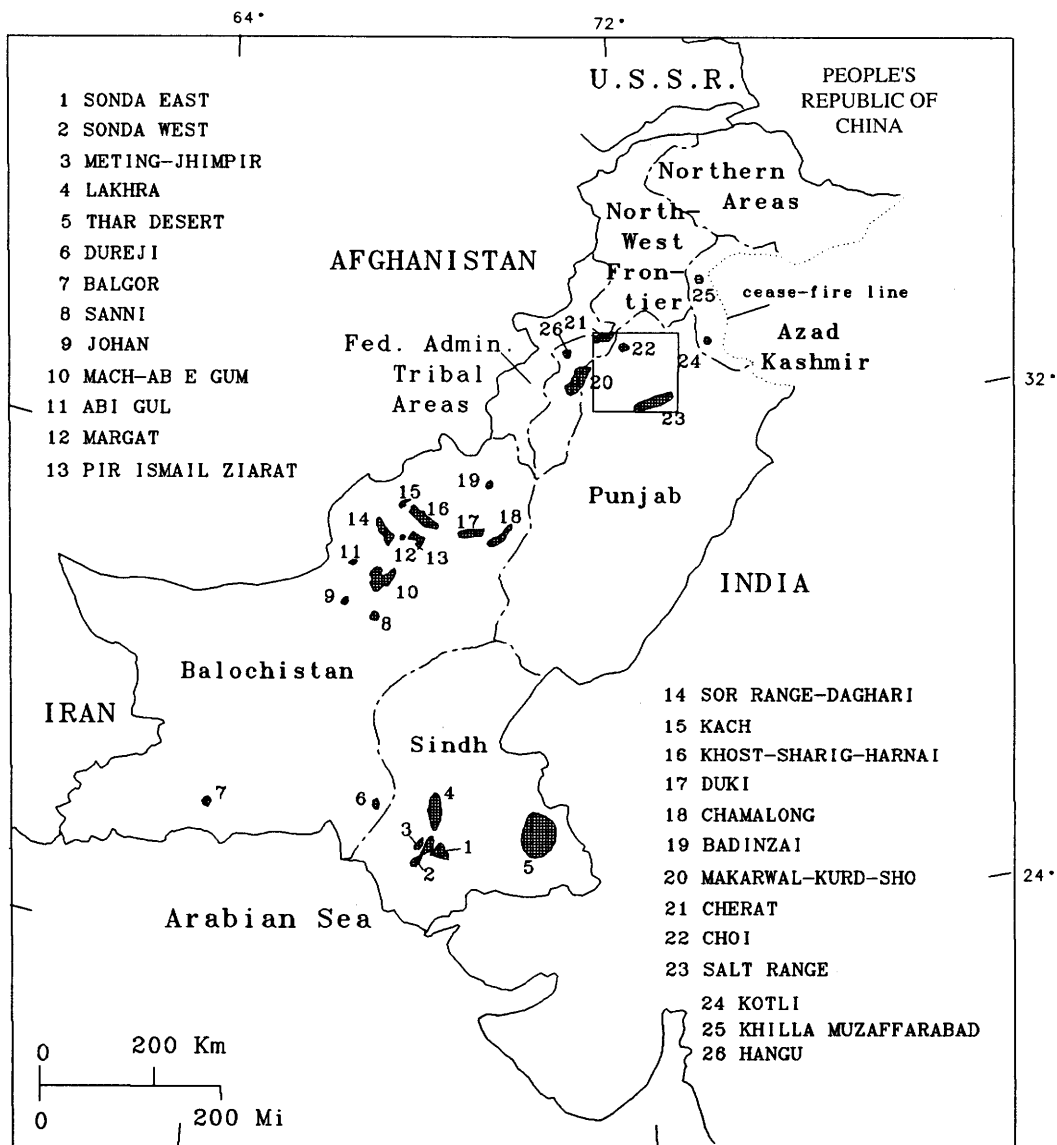


Figure 1 (Warwick and others). Location of Pakistan coal fields and occurrences. Box shows Punjab Regional Framework area.

fields ranges from lignite to subbituminous. Additional drilling and field work, mainly to identify coal reserves for mine development, are scheduled for these areas.

More than 400 core and mine samples were collected in south Sindh for proximate and ultimate analyses and determinations of major, minor, and trace elements. Analytical results on an as-received basis indicate that sampled coal beds contain on the average 31.3 percent moisture, 17.3 percent ash, 4.5 percent sulfur, 23.2 percent fixed carbon, 27.6 percent volatile matter, and 34.9 percent oxygen. Calculated heating potentials expressed as averaged calorific values are: Lakhra coal samples 3,660 Kcal/kg, Sonda West samples 4,020 Kcal/kg, and Sonda East samples 3,720 Kcal/kg.

A second phase of COALREAP, begun in FY 88 with surface exploration in the Salt Range coal field, Punjab Province, revealed an average coal bed thickness in the Salt Range area of 0.5 m and provided a preliminary coal-resource estimate of 235 million t. Analytical results on an as-received basis indicate that coal beds contain on the average 9.0 percent moisture, 24.2 percent ash, 5.3 percent sulfur, 33.5 percent fixed carbon, 33.3 percent volatile matter, and 16.1 percent oxygen. Calculated heating potential expressed as averaged calorific values is 4,970 Kcal/kg; apparent rank is bituminous. Similar resource exploration projects, including regional structural and biostratigraphic studies, are continuing in the other coal fields of Punjab, North-West Frontier, Sindh, and Balochistan Provinces.

To supplement coal exploration work in the Salt Range-Potwar Plateau area, a regional framework study was undertaken in 1988. This program is designed to provide training to GSP geologists and technicians working with USGS counterparts, and when expanded to other regions, will serve as a guide for the 1:250,000-scale evaluation of the geologic framework of Pakistan's coal fields.

COALREAP is scheduled for completion in 1992. Detailed descriptions of project work and results are included in 33 administrative reports, many of which have been released as USGS Open-File Reports or published in scientific journals.

Diagenesis in a Bottle—Experimental Strategies for Studying Thermal Maturity in Clays and Organic Matter

Gene Whitney and Michael D. Lewan

Our experimental studies of clay diagenesis and oil generation demonstrate that it is possible to understand major aspects of complex diagenetic reactions by performing relatively simple experiments. It is difficult to understand the details of these diagenetic reactions in natural systems because the reactions (1) rarely reach equilibrium, (2) are often kinetically controlled and tend to be slow because of low temperatures, (3) are often irreversible, (4) usually involve a complex assemblage of heterogeneous fluids and fine-grained solids, and (5) proceed in an open chemical system. In addition, natural systems exhibit variations in lithofacies or organic facies, and samples representing an entire reaction series of interest are usually difficult or impossible to obtain. In fact, reactions used to monitor thermal maturity of sediments may actually be groups or series of fundamental reactions which cannot be thoroughly understood except through experimentation.

Our general approach to experimental investigation of these reactions is: (1) identify a critical diagenetic reaction (or set of reactions) in nature, (2) devise experiments to test and measure the effects of key variables in the reaction, (3) conduct experiments over a range of temperatures and times using appropriate starting materials, (4) interpret reaction mechanisms and (or) calculate reaction rates and determine rate laws, and (5) validate the interpretations of experimental data by comparing experimental results with natural diagenetic settings. Using this approach, we have studied the illitization reaction (conversion of smectite to illite via an interstratified illite/smectite (I/S) intermediate phase) and oil generation.

The illitization reaction has been used as a thermal maturity indicator, but our confidence in this reaction as

a geothermometer is diminished by some observed exceptions to empirical trends. Our experiments have shown that illitization is not a single reaction, but is in fact a complex series of dissolution and precipitation processes. The reaction consists of (at least) two separate stages that proceed by different mechanisms. The rate and extent of these reaction processes are predictably controlled primarily by temperature and time, but solution chemistry, chemical composition of the starting smectite, fluid:solid ratio, and texture also affect the overall reaction significantly. The two stages of illitization have different rates of isotopic exchange and different rates of solute release, thus affecting mass balance in shales during the course of diagenetic alteration.

Kinetic models derived from natural data do not adequately describe or predict the timing of oil generation in sedimentary basins. Our experiments show that the rate and extent of oil generation from thermally decomposing organic matter cannot be described by one universal set of kinetic parameters or by direct correlation with a vitrinite reflectance scale. Bond types and the amount of sulfur bonding in organic matter are critical in determining the rate and extent of oil generation. Experiments have also demonstrated that pressure and water salinity may be important factors in oil generation.

Oil generation and illitization reactions are both scientifically and economically important, and our future experimental work will be aimed at understanding and quantifying the interaction of clay minerals and organic matter during diagenesis.

Late Paleocene and Early Eocene Terrestrial and Marine Environments, Lakhra Coal Field, Sindh Province, Pakistan

Christopher Wnuk, Elisabeth M. Brouwers, and Norman Frederiksen

The upper Paleocene sedimentary rocks of south Sindh are divided into four units. The coal-bearing upper part of the Bara Formation (>250 m) is stratigraphically lowest, followed by the Lakhra Formation (194 m), the coal-bearing Sohnari Formation (58 m), and the basal part of the Meting Limestone and Shale Member of the Laki Formation (unmeasured). The Bara Formation consists of as many as 18 cycles of facies successions. Well-sorted, fine- to medium-grained quartz arenites occur at cycle bases. These sandstones contain planar-tangential crossbeds, some of which are as much as 15 m high; these sandstones exhibit unmistakable evidence of tidal influence, specifically, sigmoidal tidal bundles with

clay couplets, graded crossbed laminae, and bidirectional crossbedding. All these marine sand bodies are in sharp or erosive contact with the terrestrial facies of the underlying cycle. The sediments of the basal facies are interpreted as sand waves and sand ridges that accumulated on tide-dominated inner shelf environments. The clean basal sandstones grade upward into estuarine and intertidal dirty sandstones, siltstones, and claystones containing wavy, flaser, and lenticular bedding. Coastal peat swamps prograded over and rooted through the intertidal sediments. In places, storm beds consisting of poorly sorted, dirty, calcareous sandstones and arenaceous limestones containing graded intraformational rip-up clasts and shell fragments are interbedded with the estuarine deposits. Abundant pyrite and carbonaceous debris suggest that the estuarine sediments were anoxic. That stunted ostracode faunas occur suggests that the sediment-water interface was dysaerobic at times. The coals formed in a marginal marine environment, which is indicated by mangrove pollen and dinoflagellates in beds adjacent to the coals, the occurrence of mangrove pollen in some coal samples, the high sulfur content of most coal beds, and the abundance of current-rippled quartz-arenite partings in the coal beds. The distribution of coal beds within cycles was controlled by the localized compaction and dewatering of the estuarine and intertidal sediments. Consequently, individual coal beds are lenticular and discontinuous even though coal zones are persistent.

Patterns of increasing ostracode species diversity and specimen abundance show that the Bara Formation becomes increasingly marine upsection toward its gradational contact with the Lakhra Formation. The ostracode assemblages indicate that the uppermost part of the Bara and all of the Lakhra Formation were deposited in waters of normal marine salinity.

The Lakhra Formation is mostly composed of beds of intensely bioturbated glauconitic sandstone, and less bioturbated, wavy, lenticular, and flatbedded siltstone and claystone. Cyclicity in ostracode abundance and diversity suggests that the cyclic shoaling-upward patterns of the Bara persist into the Lakhra. In contrast to the Bara, the Lakhra contains abundant shell fragments and glauconite and sparse carbonaceous debris; storm beds are abundant. Argillaceous foraminiferal limestone and cleaner, skeletal limestone appear in the upper part of the unit and compose about 20 percent of the total section, though geophysical logs indicate that the Lakhra may locally consist almost entirely of limestone.

An increase in ostracode diversity and an increase in the proportion of delicately ornamented taxa imply that the depth of the water in which the sediments were deposited became greater upward within the Lakhra. Species diversity and abundance decrease near the top of the Lakhra as it grades into the more terrestrial Bara-like

Sohnari Formation. The Sohnari contains one coal zone, and sedimentation patterns become Lakhra-like again above the highest coal. The Sohnari fauna and flora contain alternating marginal-marine and shallow-marine assemblages, with several cycles indicated by fluctuations in ostracode abundance and diversity.

The abrupt change from predominantly clastic sedimentation of the Bara, Lakhra, and Sohnari to the predominantly carbonate sedimentation of the Meting Limestone suggests an unconformity between the Sohnari and the Meting Limestone. Paleontological evidence suggests that the Paleocene-Eocene boundary occurs within the basal Meting, somewhere above the Sohnari-Meting contact.

Energy Research on Indian Lands

R.S. Zech, H.H. Arndt, L.H. Biewick, J.K. Hardie, R.C. Johnson, J.L. Ridgley, Courteney Williamson, and Robyn Wright-Dunbar

The U.S. Geological Survey conducts energy-related research on Indian lands in cooperation with Tribal governments and the Bureau of Indian Affairs. These studies are conducted in areas that range from small and site specific to large regions containing several Reservations. The studies may include methods as diverse as the airborne measurement of magnetics, drilling, and laboratory measurement of vitrinite reflectance. Research projects on the Ute Mountain Ute, Wind River, Fort Peck, and Southern Ute Reservations are examples of investigations during the last 2 years that are completed or are in progress.

Research on hydrocarbon reservoirs within the Ute Mountain Ute and Southern Ute Reservations (Colorado and New Mexico) focuses on the Upper Cretaceous Point Lookout Sandstone. This investigation has two parts: (1) description of sandstone geometry and depositional environments based on outcrop study, and (2) petrographic reservoir characterization from core samples. Outcrop sections in the area between Pagosa Springs and the mouth of Mancos Canyon, south of Cortez, Colo., show a change from thick deposits of a linear strandplain to thinner deposits of a delta. Studies of two drill cores obtained near the western boundary of the Southern Ute Reservation measured the porosity and permeability of sandstones and correlated these parameters to depositional environments and electric logs. These studies of the Point Lookout provide the basic data for characterizing the reservoir in this area and provide a model for other regressive sandstone reservoirs of the Western Interior seaway. The study should be completed in 1992.

The assessment of the coal resource of the Fort Peck Reservation, Montana, began with collection of data from drilling, measured sections, and logging more than 500 seismograph shot holes and water wells. From these data, isopach, structure, occurrence, and overburden maps were generated for each of the 15 potentially mineable coal beds identified in the area. Coal samples collected across the Reservation were analyzed, and thickness and extent of coal were entered into the National Coal Resources Data System. Surficial and subsurface mapping of rock units was conducted, and illustrative products including cross sections, geologic maps, structure maps, and isopach maps were generated. Coal resources were then calculated. In addition to providing an improved understanding of the geology and coal resources of the area, this study identified gravel deposits, aquifers, and possible hydrocarbon reservoirs.

Assessment of oil, gas, and coal-bed methane resources of the Wind River Reservation, Wyoming, began in 1990 and will be completed in 1993. Oil and gas assessment here consists of several procedures: (1) structure-contour, lithologic, and isopach maps are constructed for productive intervals; (2) thermal maturity and source-rock studies indicate areas where hydrocarbons have been generated and help define possible migration pathways; (3) gravity and magnetic studies determine the structure; and (4) detailed surface and subsurface studies establish the depositional facies of productive beds and help integrate other aspects of the

investigation. Thus far the marginal lacustrine units in the Paleocene Fort Union Formation appear to have the greatest potential for undiscovered hydrocarbons. To evaluate coalbed methane resources, coal-rank maps, coal-isopach maps, and structure-contour maps are being constructed. In addition, a drilling program to determine the methane content of coals at shallow depth (< 1,000 ft) was carried out during 1990 and 1991. Significant quantities of methane were discovered in shallow Cretaceous coal over a large area in the southern and central parts of the Reservation.

The Southern Ute Dakota project of southwestern Colorado has focused on the structural, sedimentologic, and depositional history of the Upper Cretaceous Dakota Sandstone, a major gas producer. The Dakota was divided into six genetic packages, each related to major or minor transgression or regression. Sandstone geometry and depositional systems for each genetic package were defined and compared to local and regional structure. The sandstone bodies have a pronounced NW-NE orientation coincident with the regional structural framework, suggesting subtle structural control on location and thickness of fluvial and coastal marine sandstone bodies. Gas production is from distributary channel, deltaic, and shoal sandstones and appears to be controlled more by depositional facies than by structure. This study was recently completed, and the results will be published as a U.S. Geological Survey Professional Paper.

AUTHOR INDEX

A

Ahlbrandt, T.S., USGS, Denver.....	1
Alam, A.M.N., Geological Survey of Bangladesh, Dhaka, Bangladesh	39
Ambroziak, R.A., USGS, Reston	57
Armstrong, A.K., New Mexico Bureau of Mines and Mineral Resources, Socorro, NM 87801	42
Arndt, H.H., USGS, Denver	82
Arthur, M.A., Department of Geosciences, The Pennsylvania State University, 503-A Deike Bldg., University Park, PA 16802	17
Attanasi, E.D., USGS, Reston	68

B

Ball, M.M., USGS, Denver	2
Barton, C.C., USGS, Denver	3
Beard, L.S., USGS, Flagstaff	47
Beyer, L.A., USGS, Menlo Park	3
Biewick, L.R.H., USGS, Denver	5, 82
Bird, K.J., USGS, Menlo Park	7, 8, 51
Blake, Dorsey, USGS, Denver	5
Blank, H.R., USGS, Denver	8
Bogino, Vladamir, Petroleum Research Institute, Minsk, U.S.S.R.....	2
Bohannon, R.G., USGS, Menlo Park.....	11
Bradley, D.C., USGS, Anchorage	11
Bredehoeft, J.D., USGS, Menlo Park	13
Brouwers, E.M., USGS, Denver	81
Burruss, R.C., USGS, Denver	68

C

Carter, M.D., USGS, Reston	13
Cecil, C.B., USGS, Reston	14
Clayton, J.L., USGS, Denver.....	2, 24, 64
Cobb, J.C., Kentucky Geological Survey, Lexington, KY 40506-0107.....	13
Cobban, W.A., USGS, Denver	31
Cole, R.B., Department of Geological Sciences, University of Rochester, Rochester, NY 14627	73
Collett, T.S., USGS, Denver	7, 14
Collister, James, Department of Geology, Indiana University, Bloomington, IN 47405	76
Cook, H.E., USGS, Menlo Park	65
Crovelli, R.A., USGS, Denver	21
Crysdale, B.L., USGS, Denver	15
Cunningham, K.I., USGS, Denver	16

D

Dalrymple, Brent, USGS, Reston	36
Danforth, W., USGS, Woods Hole	77
Daws, T.A., USGS, Denver	2
Dean, W.E., USGS, Denver	17, 65, 76
Dillon, W.P., USGS, Woods Hole	18, 26
Dolton, G.L., USGS, Denver	2, 21
Drew, L.J., USGS, Reston	22
Dubiel, R.F., USGS, Denver	24

E

Edgar, N.T., USGS, Reston	24
Ellis, M.S., USGS, Denver	5, 66

F

Fassett, J.E., USGS, Reston	79
Fedorko, Nick III, West Virginia Geologic and Economic Survey, Morgantown, WV 26507-0879	13
Fehlhaber, Kristen, USGS, Woods Hole	18, 26
Filewicz, M.V., Unocal Corp., P.O. Box 6176, Ventura, CA 93006	73
Finkelman, R.B., USGS, Reston	27
Fishman, N.S., USGS, Denver	28
Fitzpatrick, J.J., USGS, Denver	29
Flores, R.M., USGS, Denver	5, 64, 66
Fouch, T.D., USGS, Denver	13, 29, 31, 54, 76
Franczyk, K.J., USGS, Denver	31
Frederiksen, Norman, USGS, Reston	81
Furer, L.C., Indiana Geological Survey, 611 North Walnut Grove Ave., Bloomington, IN 47405	44

G

Gardner, N.K., USGS, Reston	13
Gay, F.E., USGS, Denver	57
Geist, E.L., USGS, Menlo Park	11
Golmshtok, A.J., Institute Oceanology, U.S.S.R. Academy of Sciences, Gelendzhik, U.S.S.R.	37
Good, S.C., Department of Geological Sciences, University of Colorado, Boulder, CO 80309	24
Grow, J.A., USGS, Denver	8, 60, 65

H

Halley, R.B., USGS, St. Petersburg, FL.....	31
Hanesand, Trond, Norsk Hydro a.s. Research Centre Petroleum Geochemistry, Bergen, Norway	76
Hardie, J.K., USGS, Denver	82
Harrison, Wendy, Department of Geology and Geological Engineering, Colorado School of Mines, Golden, CO 80401.	76
Hatch, J.R., USGS, Denver.....	33, 68
Hester, T.C., USGS, Denver	33
Hettinger, R.D., USGS, Denver	34
Higley, D.K., USGS, Denver	73
Hinkley, T.K., USGS, Denver.....	29
Holdsworth, G., NHRI, Saskatoon, Saskatchewan	29
Holmes, C.W., USGS, Denver	36
Howell, D.G., USGS, Menlo Park	8, 36
Huffman, A.C., Jr., USGS, Denver	65
Hutchinson, D.R., USGS, Woods Hole.....	37

I

Isaacs, C.M., USGS, Menlo Park	39, 41
--------------------------------------	--------

J

Johnson, R.C., USGS, Denver	31, 82
Johnson, S.Y., USGS, Denver	39, 65, 73
Johnsson, M.J., USGS, Menlo Park	8

K

Kaiser, W.R., Texas Bureau of Economic Geology, University of Texas at Austin, Austin, TX 78713.....	27
Karl, S.M., USGS, Anchorage	51
Keighin, C.W., USGS, Denver	41
Keller, M.A., USGS, Menlo Park	41
Keller, Michael, Ministry of Geology, Moscow, U.S.S.R.	2
Kelley, J.S., USGS, Anchorage	42
Kenyon, N.H., Institute of Oceanographic Sciences, Wormley, U.K.	77
Kidd, W.S.F., Department of Geological Sciences, SUNY, Albany, NY 12222	11
Kirschbaum, M.A., USGS, Denver	43
Klitgord, K.D., USGS, Woods Hole	37
Kolata, D.R., Illinois State Geological Survey, 615 E. Peabody Dr., Champaign, IL 61821	44
Krohn, K.K., USGS, Reston	44

L

Landis, G.P., USGS, Denver	29
Law, B.E., USGS, Denver	64
Lee, H.J., USGS, Menlo Park	77
Lee, M.W., USGS, Denver	18, 26, 37
Lerch, H.E., USGS, Reston	45
Lewan, M.D., USGS, Denver	46, 81
Lillis, P.G., USGS, Denver	2
Lore, G.L., Minerals Management Service, New Orleans, LA 70123	22
Lund, Karen, USGS, Denver	47, 60
Luppens, J.A., Phillips Coal Co., 2929 N. Central Expressway, Richardson, TX 75080	27

M

Magoon, L.B., USGS, Menlo Park	8
Mason, M.A., 1215 Roosevelt Ave., Richmond, CA 94801	73
Mast, R.F., USGS, Denver	2, 18, 21, 73
Masters, C.D., USGS, Reston	47
McCabe, P.J., USGS, Denver	34, 43, 50, 67
Meyer, R.F., USGS, Reston	15
M'Gonigle, John, USGS, Denver	36
Michalski, T.C., USGS, Denver	64
Miller, W.G., USGS, Reston	44, 50
Molenaar, C.M., USGS, Denver	31
Molnia, C.L., USGS, Denver	5, 44
Moore, T.A., USGS, Reston	45
Moore, T.C., University of Michigan, Ann Arbor, MI 48190	37
Moore, T.E., USGS, Menlo Park	51
Mull, C.G., Alaska Division of Geological and Geophysical Surveys, Fairbanks, AK 99709	51

N

Nelson, C.H., USGS, Menlo Park	77
Nelson, W.J., Illinois State Geological Survey, 615 E. Peabody Dr., Champaign, IL 61821	44
Nichols, D.J., USGS, Denver	66
Noger, M.C., Kentucky Geological Survey, Lexington, KY	44
Normark, W.R., USGS, Menlo Park	52
Nuccio, V.F., USGS, Denver	54

O

Obradovich, J.D., USGS, Denver	73
O'Brien, T.F., USGS, Woods Hole	77
Orem, W.H., USGS, Reston	45

P

Palacas, J.G., USGS, Denver	58
Pantea, M.P., USGS, Denver	57
Pawlewicz, Mark, USGS, Denver	58
Perry, W.J., Jr., USGS, Denver	47, 60, 66
Peterson, Fred, USGS, Denver	59
Pitman, J.K., USGS, Denver	29, 76
Pollastro, R.M., USGS, Denver	59
Potter, C.J., USGS, Denver	60, 65
Poznaikovitch, Zinovy, Petroleum Research Institute, Minsk, U.S.S.R.	2
Price, Leigh, USGS, Denver	63

R

Rice, D.D., USGS, Denver	64
Richards, D.L., USGS, Denver	64
Ridgley, J.L., USGS, Denver	65, 82

Robbins, S.L., USGS, Denver	65
Roberts, L.N.R., USGS, Denver.....	43
Roberts, S.B., USGS, Denver	66
Robinson, J.W., Dept. of Geology and Geological Engineering, Colorado School of Mines, Golden, CO	67
Root, D.H., USGS, Reston	68
Ryder, R.T., USGS, Reston.....	68
Rye, R.O., USGS, Denver	29

S

SanFilipo, J.R., USGS, Reston	79
Sargent, M.L., Illinois State Geological Survey, 615 E. Peabody Dr., Champaign, IL 61821	44
Schenk, C.J., USGS, Denver.....	15, 24, 41, 59, 69, 70
Schmoker, J.W., USGS, Denver.....	33, 54, 70, 71
Scholz, C.A., Duke University Marine Lab, Beaufort, NC 28516	37
Schwab, W.C., USGS, Woods Hole	77
Sites, R.S., Virginia Division of Mineral Resources, Charlottesville, VA 22903.....	13
Smoot, J.P., USGS, Denver.....	72
Snee, L.W., USGS, Denver	47
Stanley, R.G., USGS, Menlo Park.....	41, 73
Stanton, Mark, USGS, Denver	76
Stanton, R.W., USGS, Reston	64
Stricker, G.D., USGS, Denver.....	66
Swisher, C.C. III, Geochronology Center at the Institute for Human Origins, 2453 Ridge Road, Berkeley, CA 94709.	73
Sykes, Richard, DSIR, Geology and Geophysics, Lower Hutt, New Zealand.....	5

T

Takahashi, K.I., USGS, Denver.....	16, 73
Taylor, D.J., USGS, Denver.....	74
Telnaes, Nils, Norsk Hydro a.s. Research Centre Petroleum Geochemistry, Bergen, Norway	76
Tennyson, M.E., USGS, Denver.....	75
Tewalt, S.J., USGS, Reston	27, 44
Thomas, R.E., USGS, Reston	79
Thornton, M.L.C., Unocal Corp., P.O. Box 6176, Ventura, CA 93006.....	73
Treworgy, J.D., Illinois State Geological Survey, 615 E. Peabody Dr., Champaign, IL 61821	44
Turner, C.E., USGS, Denver	28
Tuttle, M.L., USGS, Denver	73, 76
Twichell, D.C., USGS, Woods Hole	77

U-V

Ulmishek, Gregory, USGS, Denver.....	2, 77
Vork, D.R., Unocal Corp., P.O. Box 6176, Ventura, CA 93006.....	73

W

Wallace, W.K., Department of Geology and Geophysics, University of Alaska, Fairbanks, AK 99775.....	51
Warden, Augusta, USGS, Denver.....	2
Warwick, P.D., USGS, Reston.....	79
Wesley, J.B., USGS, Denver, and Colorado School of Mines, Golden, CO	13
Whitaker, S.T., Illinois State Geological Survey, 615 E. Peabody Dr., Champaign, IL 61821.....	44
Whitney, Gene, USGS, Denver	81
Wilber, R.J., Sea Education Association, Woods Hole, MA 02543.....	31
Williamson, Courteney, USGS, Denver	82
Wnuk, Christopher, USGS, Reston	81
Wright-Dunbar, Robyn, USGS, Denver	82
Wrucke, C.T., USGS, Menlo Park	42

Z

Zech, R.S., USGS, Denver	82
Zihlman, F.N., USGS, Denver.....	74

ORGANIZATION OF THE U.S. GEOLOGICAL SURVEY

Office	Name	Telephone	City
Office of the Director			
Director	Dallas L. Peck	703/648-7411	Reston
Associate Director	Doyle G. Frederick	703/648-7412	Reston
Assistant Director for Research	Steven E. Ragone	703/648-4450	Reston
Assistant Director for Engineering Geology	James F. Devine	703/648-4423	Reston
Assistant Director for Administration	Jack J. Stassi	703/648-7200	Reston
Assistant Director for Programs	Peter F. Bermel	703/648-4430	Reston
Assistant Director for Intergovernmental Affairs	John J. Dragonetti	703/648-4427	Reston
Chief, Public Affairs Office	Donovan B. Kelly	703/648-4459	Reston
Assistant Director for Information Systems	James E. Biesecker	703/648-7108	Reston
National Mapping Division			
Chief	Allen H. Watkins	703/648-5748	Reston
Geologic Division			
Chief Geologist	Benjamin A. Morgan	703/648-6600	Reston
Water Resources Division			
Chief Hydrologist	Philip Cohen	703/648-5215	Reston
Information Systems Division			
Assistant Director	James E. Biesecker	703/648-7108	Reston
Administrative Division			
Assistant Director	Jack J. Stassi	703/648-7200	Reston

ORGANIZATION OF THE GEOLOGIC DIVISION

Office of the Chief Geologist			
Chief Geologist	Benjamin A. Morgan	703/648-6600	Reston
Associate Chief Geologist	William R. Greenwood	703/648-6601	Reston
Assistant Chief Geologist for Program	David P. Russ	703/648-6640	Reston
Assistant Chief Geologist, Eastern Region	Vacant	703/648-6660	Reston
Assistant Chief Geologist, Central Region	Harry A. Tourtelot	303/236-5438	Denver
Assistant Chief Geologist, Western Region	William R. Normark	415/329-5101	Menlo Park
Office of Mineral Resources			
Chief	Glenn H. Allcott	703/648-6100	Reston
Chief, Branch of Alaskan Geology	Willis H. White	907/786-7403	Anchorage
Chief, Branch of Eastern Mineral Resources	Klaus J. Schulz	703/648-6327	Reston
Chief, Branch of Central Mineral Resources	David A. Lindsey	303/236-5568	Denver
Chief, Branch of Western Mineral Resources	William C. Bagby	415/329-5400	Menlo Park
Chief, Branch of Geochemistry	David B. Smith	303/236-1800	Denver
Chief, Branch of Resource Analysis	William D. Menzie	703/648-6125	Reston
Chief, Branch of Geophysics	David L. Campbell	303/236-1212	Denver
Office of Energy and Marine Geology			
Chief	Gary W. Hill	703/648-6472	Reston
Chief, Branch of Petroleum Geology	Thomas S. Ahlbrandt	303/236-5711	Denver
Chief, Branch of Coal Geology	Harold J. Gluskoter	703/648-6401	Reston
Chief, Branch of Sedimentary Processes	Walter E. Dean	303/236-1644	Denver
Chief, Branch of Pacific Marine Geology	David A. Cacchione	415/329-3184	Menlo Park
Chief, Branch of Atlantic Marine Geology	Bradford Butman	617/837-4211	Woods Hole
Chief, Center for Coastal Geology and Regional Marine Studies	Abby Sallenger	813/893-3100 ext. 3002	St. Petersburg

Office of Regional Geology

Chief	Mitchell W. Reynolds	703/648-6960	Reston
Chief, Branch of Eastern Regional Geology	Wayne L. Newell	703/648-6900	Reston
Chief, Branch of Central Regional Geology	David L. Schleicher	303/236-1258	Denver
Chief, Branch of Western Regional Geology	John (Jack) W. Hillhouse	415/329-4909	Menlo Park
Chief, Branch of Isotope Geology	Carl E. Hedge	303/236-7880	Denver
Chief, Branch of Astrogeology	Philip Davis	602/527-7201	Flagstaff
Chief, Branch of Paleontology and Stratigraphy	John Pojeta, Jr.	703/648-5288	Reston

Office of Earthquakes, Volcanoes, and Engineering

Chief	Robert L. Wesson	703/648-6714	Reston
Chief, Branch of Engineering Seismology and Geology	Thomas L. Holzer	415/329-5613	Menlo Park
Chief, Branch of Global Seismology and Geomagnetism	John Filson	703/648-6785	Reston
Chief, Branch of Seismology	Allan Lindh	415/329-4778	Menlo Park
Chief, Branch of Geologic Risk Assessment	Kaye M. Shedlock	303/236-1585	Denver
Chief, Branch of Tectonophysics	William H. Prescott	415/329-4810	Menlo Park
Chief, Branch of Igneous and Geothermal Processes	Peter W. Lipman	415/329-5228	Menlo Park
Chief, Branch of Lithospheric Processes	Bruce Hemingway	703/648-6740	Reston

Office of Scientific Publications

Chief	John M. Aaron	703/648-6077	Reston
Chief, Branch of Eastern Technical Reports	Herbert A. Wolford	703/648-6147	Reston
Chief, Branch of Central Technical Reports	Lawrence F. Rooney	303/236-5457	Denver
Chief, Branch of Western Technical Reports	James B. Pinkerton	415/329-5043	Menlo Park
Chief, Library and Information Services	Barbara A. Chappell	703/648-4305	Reston
Chief, Branch of Visual Services	John R. Keith	703/648-4357	Reston

Office of International Geology

Chief	A. Thomas Ovenshine	703/648-6047	Reston
Associate Chief for OIG and Deputy Chief for European Geology	Richard Krushensky	703/648-6060	Reston
Deputy Chief for Asian and Pacific Geology	Jack H. Medlin	703/648-6062	Reston
Deputy Chief for Latin American Geology	Darrell Herd	703/648-6012	Reston
Deputy Chief for Middle Eastern and African Geology	Frederick O. Simon	703/648-6055	Reston
Deputy Chief for Polar Programs	Bruce Molnia	703/648-4120	Reston
Deputy Chief for Soviet Programs	Paul Hearn	703/648-6287	Reston

Addresses

U.S. Geological Survey Reston, VA 22092	U.S. Geological Survey Box 25046 Denver Federal Center Denver, CO 80225	U.S. Geological Survey 345 Middlefield Road Menlo Park, CA 94025
U.S. Geological Survey Branch of Alaskan Geology 4200 University Drive Anchorage, AK 99508-4667	U.S. Geological Survey 2255 North Gemini Drive Flagstaff, AZ 86001	U.S. Geological Survey Quissett Campus, Building B Woods Hole, MA 02543
U.S. Geological Survey Hawaiian Volcano Observatory Hawaii National Park HI 96718	U.S. Geological Survey David A. Johnston Cascades Volcano Observatory 5400 MacArthur Boulevard Vancouver, WA 98661	

This book was prepared in USGS Central region, Denver, CO

Typesetting by Shelly A. Fields

Final illustration preparation by Marl L. Kauffmann

Cover design by Robert K. Wells

